NASA TN D-425

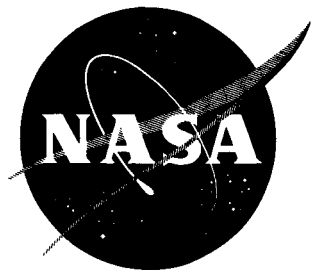

TECHNICAL NOTE
D-425

TRIM DRAG AT SUPERSONIC SPEEDS OF VARIOUS DELTA-PLANFORM CONFIGURATIONS

By M. E. Graham and B. M. Ryan

Douglas Aircraft Company, Inc.
Santa Monica, Calif.

NATIONAL AERONAUTICS AND SPACE ADMINISTRATION

WASHINGTON

June 1960

TABLE OF CONTENTS

NATIONAL AERONAUTICS AND SPACE ADMINISTRATION

TECHNICAL NOTE D-425

TRIM DRAG AT SUPERSONIC SPEEDS OF VARIOUS DELTA-PLANFORM CONFIGURATIONS*

By M. E. Graham and B. M. Ryan

SUMMARY

The drag due to lift and the maximum lift-to-drag ratio at supersonic speeds of zero-thickness, trimmed, statically stable (1) delta-wing-plus-tail, (2) delta-wing-plus-canard, and (3) delta-wing-alone configurations are studied with the aid of linear theory. These configurations do not include a body.

In general it is found that the drag due to lift decreases and the maximum lift-to-drag ratio increases as the aspect ratio increases, the vertical gap increases, the "tail length" increases and the static margin decreases; also suitable camber and twist decrease the drag. However, calculations for wing-with-flap configurations indicate that if full leading-edge thrust exists there is a range of aspect ratio in which decreasing the aspect ratio decreases the drag due to lift. Also if leading-edge thrust exists, or if the surfaces are twisted and cambered there can sometimes be less drag due to lift at a small positive static margin than at zero static margin. The optimum trim-surface area (trim area to give highest $(L/D)_{max}$) depends in general upon the static margin, the tail length, and the net interference between the surfaces (which may itself depend upon the trim-surface area.) A limited investigation of flat sonic-edge wings and trim surfaces indicates that if there is no net interference large trim surfaces are desirable, if there is much interference small trim surfaces are desirable at least

* Orginally prepared as Report SM-23635, Douglas Aircraft Company, Inc., and reprinted in original form by NASA, by agreement with Douglas Aircraft Company, Inc., to increase availability.

if the static margin is not too large. For example, large flaps are desirable, large tails or canards if the gap is large, small tails and canards if the gap is small and the static margin not too large.

There is little difference between wing-canard and wing-tail configurations at cruise conditions if the gap is not too small. If the gap is small, the lift-drag ratio of the wing-canard configuration becomes poorer than that of the corresponding wing-tail configuration unless the wing of the canard configuration is suitably twisted. At moderate static margins there is little difference between trimmed flat wing-flap configurations and flat wing-plus-tail or wing-plus-canard configurations with not too small gaps. At large static margins the lift-drag ratio of the wing-flap configuration is poor compared to the wing-tail or wing-canard configurations of not too small gap unless the wing is suitably cambered and twisted.

From this investigation it appears that the choice of a type of trim surface (tail, canard or flap) will depend primarily upon considerations other than supersonic cruise performance. The major influence upon the cruise lift-drag ratio will then be these other considerations rather than the direct optimization of the configuration to give the highest $(L/D)_{MAX}$ for the supersonic condition.

I. INTRODUCTION

The purpose of this report is to present supersonic trim-drag* calculations in such a form that wing-plus-tail, wing-plus-canard and wing-alone configurations may be easily compared, and in such a form that the static margin is immediately available. First, general equations for the lift coefficient, moment coefficient, and drag coefficient due to lift are presented. Then $C_{D_i}/\beta C_L^2$ for flat trimmed configurations is expressed as a function of the first and second powers of $(\partial C_M/\partial C_L)_\delta \div (\partial C_M/\partial \delta)_{C_L}$, the static longitudinal stability derivative (negative static margin) divided by a derivative similar to the "elevator power." Here the "elevator" or trim surface is an all-movable tail or canard or a full-span flap at the wing trailing edge. The coefficients in this drag equation depend upon the lift-curve slope of the wing alone, the lift-curve slope of the tail or canard or flap alone, and also upon certain average values of $d\epsilon/d\alpha$ in cases where there is wing-tail (or wing-canard) interference. In this form the equation applies to quite general planform shapes. However, the lift-curve slopes, trim surface effectiveness, and the average values of $d\epsilon/d\alpha$ can be evaluated only if a specific configuration geometry has been picked. For the calculations, delta wings and tails or canards, and trapezoidal constant chord flaps have been assumed, and $d\epsilon/d\alpha$ has been evaluated at the Trefftz plane.

The trim drag of certain cambered and twisted configurations has also been found; specifically, configurations put together from the optimally twisted and cambered sonic-delta wings of Germain; and also a configuration consisting of a sonic-delta wing with twisted tip panels plus a canard. $C_{D_i}/\beta C_L^2$ again depends on first and second powers of $(\partial C_M/\partial C_L)_\delta$, but the equations have not always been expressed explicitly in this form.

The basic equations depend upon linear theory. The induced loads on the rear surface are calculated essentially by the methods and from equations of Ref. 1. The results of this report differ from those of Ref. 1 and 2 in that here (a) the static margin has been introduced,

---

* As used in this report, the term "trim drag" means the drag due to lift of a configuration which is in trim. It does not mean an increment of drag which is to be added to an untrimmed configuration when it is brought into trim.

(b) the "gap," vertical distance between rear surface and vortex sheet, has been taken as an independent parameter rather than as a function of α in computing any derivatives with respect to α, (c) certain twisted and/or cambered configurations have been studied, (d) leading-edge suction has been included in some configurations with subsonic leading-edges, and (e) $C_{D_i}/\beta C_L^2$ has been computed for a greater range of aspect ratio and gap ratio.

Wing-plus-tail and wing-plus-canard configurations have been compared solely on the basis of supersonic trim drag and zero-thickness maximum lift-to-drag ratios. No attempt has been made to evaluate their relative merits taking into account other matters, such as subsonic performance and stability, and landing and take-off.

II. NOTATION

AR	aspect ratio
b_T	maximum span of the tail
b_W	maximum span of the wing
$\bar{c}$	length of mean aerodynamic chord of the wing (2/3 c for delta wing)
c	root chord of the wing
c_2	chord of trailing-edge flap (constant across span)
C_{D_i}	coefficient of induced drag (drag due to lift) of the total configuration
C_{D_o}	coefficient of induced drag due to twist and camber only
$C_{D_{o_W}}, C_{D_{o_T}}$	coefficients of induced drag due to twist and camber only on the wing or trim surfaces respectively
C_{D_T}, C_{L_T}	coefficients of induced drag and lift of the trim surface based on trim-surface planform area
C_{D_W}, C_{L_W}	coefficients of induced drag and lift of the wing based on wing planform area
C_L	lift coefficient of total configuration
C_{L_α}	$\partial C_L/\partial\alpha$ lift-curve slope of total configuration due to α deflection
$(C_{L_\alpha})_T$	lift-curve slope of trim surface in the free stream based on trim-surface area
$(C_{L_\alpha})_W$	lift-curve slope of wing in the free stream based on wing area
C_{L_δ}	$\partial C_L/\partial\delta$ lift-curve slope of total configuration due to δ deflection
C_{L_o}	lift coefficient due to any twist and camber of the surfaces
$C_{L_{o_W}}, C_{L_{o_T}}$	lift coefficients due to twist and camber only of the wing or trim surfaces respectively
C_M	moment coefficient of total configuration about center of gravity, positive for pitch-up

$\frac{d\epsilon}{d\alpha}$	downwash angle per unit of deflection of the forward surface
e	distance from leading edge of flap to center of pressure due to δ deflection (when $m \geq 1$, the center of pressure due to δ deflection is the centroid of area of the flap)
G	vertical gap between the rear surface and the vortex sheet shed from the forward surface measured in units of wing span
k_{TOW}	average value of $d\epsilon/d\alpha$ induced by trim surface on wing
k_{WOT}	average value of $d\epsilon/d\alpha$ induced by wing on trim surface
l	distance from centroid of wing area to centroid of trim surface ("tail length")
l_α, l_δ, l_o	local lift at (x,y) produced by α, δ, twist plus camber, respectively
L_α, L_δ, L_o	total lift produced by α, δ, twist plus camber, respectively
$(L/D)_{MAX}$	maximum lift-to-drag ratio
m	$\beta \tan \omega$ (for delta planforms, $\tan\omega = AR/4$)
$m.a.c.$	mean aerodynamic chord
$\bar{p}$	non-dimensional distance from the center of pressure of Germain's twisted-cambered wing to the centroid of the wing area
q	dynamic pressure
R	$\frac{-\partial C_M/\partial C_L}{-\beta(\partial C_M/\partial \delta)_{C_L}}$
s_p	ratio of area of two twisted wing tip panels to area of wing
S_p	area of two twisted wing tip panels
s_T	ratio of trim-surface area to wing area
S_T	trim-surface area
S_w	wing area (see note at end of notation)
U	free stream velocity
x, y	streamwise and spanwise rectangular coordinates

x_α, x_δ, x_o	distance from C.G. of configuration to "center" of l_α , l_δ , l_o load distributions respectively
x_{oT}	distance from C.G. to center of load due to twist and camber of the trim surface
x_{ow}	distance from C.G. to center of load due to twist and camber of the wing
x_T	center of direct load on trim surface measured from the centroid of the trim surface
x_{TOW}	center of load induced by trim surface on the wing measured from the centroid of the wing
x_{WOT}	center of load induced by the wing on trim surface measured from the centroid of the trim surface
α	angle of attack of wing with respect to free stream
$\bar{\alpha}$	$\alpha/\beta C_L$
α_o	additional angle of attack distribution corresponding to any local twist and camber
$\bar{\alpha}_o$	$\alpha_o/\beta C_L$
β	$\sqrt{M^2-1}$ where M = Mach number
δ	angle of attack of trim surface with respect to wing
$\bar{\delta}$	$\delta/\beta C_L$
ω	angle between free-stream direction and leading edge of wing, tail or canard
$\frac{\partial C_M}{\partial C_L}$	or $(\partial C_M/\partial C_L)_\delta$ stick-fixed static longitudinal stability derivative
$\left(\frac{\partial C_M}{\partial \delta}\right)_{C_L}$	moment coefficient per unit deflection of the trim surface at constant C_L ("power" of trim surface)

Lift and drag coefficients and derivatives are based on wing area except as otherwise noted. For wing-flap configurations the wing area can be defined to include the flap area (wing-with-flap configuration) or alternatively to exclude the flap area (wing-plus-flap configuration). In general, the former definition of wing area is used. Any exceptions are noted. Moment coefficients and derivatives are based on wing area and wing m.a.c. Angles are measured in radians. Distances b_T, b_W, c, $\bar{c}$, and c_2 are actual dimensions. The gap G is measured in units of wing span (b_W). All other distances are measured in units of wing m.a.c. ($\bar{c}$). Subscripts W and T refer to the wing and trim surfaces, respectively.

III. ANALYSIS

A. Configurations

The configurations studied in this report consist of a delta planform wing at an angle of attack α with respect to the free stream plus a trimming surface at an angle δ with respect to the wing:

(1) Wing plus tail, both of delta planform. ("Tail" will be used to denote separate trim surface aft of wing.)
   (a) Flat wing plus flat tail.
   (b) Wing with twist and camber distribution such that the drag would be a minimum for a specified lift if the wing were alone in the free stream. Tail with same distribution of twist and camber but different magnitude.

(2) Wing plus canard, both of delta planform. ("Canard" will be used to denote separate trim surface forward of the wing.)
   (a) Flat wing plus flat canard.
   (b) Same as Config. 1-b except that it is a wing-plus-canard configuration.
   (c) Flat wing with twisted tip panels plus flat canard.

(3) Wing alone
   (a) Flat wing with full-span flap of constant chord at wing trailing edge. ("Flap" will be used to denote trim surface which is a part of the wing. The wing area includes the flap area unless otherwise noted.)
   (b) Wing with twist and camber such that the drag is minimum for a specified lift and specified moment. No special trimming surface.

The configurations are illustrated in Fig. 1. Detailed calculations are made for Configs. 1-a, 2-a, 2-c, 3-a. The drag calculations for 1-b, 2-b and 3-b may be looked upon as lower bounds for the drag of wing-plus-tail (or wing-plus-canard) configurations and wing-with-flap configurations. They are unrealistic in the sense that the twist and camber, for the purpose of these calculations, are changed continuously as a function of the Mach number, lift coefficient and C.G. position.

Furthermore in 1-b and 2-b wing-tail (or wing-canard) interference is assumed negligible.

B. Basic Equations

Lift coefficient: Within linearized theory, the lift coefficient of the configuration wing plus trim surface is

$$C_L = C_{L_\alpha}\alpha + C_{L_\delta}\delta + C_{L_o} \tag{1}$$

C_{L_α}, C_{L_δ} and C_{L_o} are defined as follows:

$$C_{L_\alpha} = \frac{\partial C_L}{\partial \alpha} = \frac{1}{\alpha}\iint_{\substack{\text{wing plus}\\ \text{trim surface}}} \frac{\ell_\alpha(x,y)\,dx\,dy}{q\,S_w} \tag{2}$$

$$C_{L_\delta} = \frac{\partial C_L}{\partial \delta} = \frac{1}{\delta}\iint_{\substack{\text{wing plus}\\ \text{trim surface}}} \frac{\ell_\delta(x,y)\,dx\,dy}{q\,S_w} \tag{3}$$

$$C_{L_o} = \iint_{\substack{\text{wing plus}\\ \text{trim surface}}} \frac{\ell_o(x,y)\,dx\,dy}{q\,S_w} \tag{4}$$

where ℓ_α, ℓ_δ and ℓ_o are the local lifts produced directly and indirectly by the angle of attack α, the trim deflection δ and the twist plus camber respectively. The superposition procedures used to obtain ℓ_α, ℓ_δ and ℓ_o are described in Appendix A. C_{L_α}, C_{L_δ} and C_{L_o} depend only upon the geometry of the configuration and upon the Mach number. Note that they, and hence C_L, are based upon the wing area S_w.

The lift derivatives of the various configurations are given by:

$$C_{L_\alpha} = (C_{L_\alpha})_W + s_T (C_{L_\alpha})_T (1 - k_{WOT}) \qquad \text{wing plus tail} \tag{5a}$$

$$C_{L_\alpha} = (C_{L_\alpha})_W (1 - k_{TOW}) + s_T (C_{L_\alpha})_T \qquad \text{wing plus canard} \tag{5b}$$

$$C_{L_\alpha} = (C_{L_\alpha})_W \qquad \text{wing alone (with or without flap)} \tag{5c}$$

and

$$C_{L_\delta} = s_T (C_{L_\alpha})_T \qquad \text{wing plus tail} \qquad (6a)$$

$$C_{L_\delta} = (C_{L_\alpha})_W (-k_{TOW}) + s_T (C_{L_\alpha})_T \qquad \text{wing plus canard} \qquad (6b)$$

$$C_{L_\delta} = s_T (C_{L_\alpha})_T \qquad \text{wing with flap} \qquad (6c)$$

$(C_{L_\alpha})_W$ is the lift curve slope which the wing would have if it were alone in the free stream. Similarly $(C_{L_\alpha})_T$ is the lift curve slope which the trim surface (tail, canard or flap) would have if it were alone in the free stream. $(C_{L_\alpha})_T$ is based on the area of the trim surface and s_T is the ratio of that area to the wing area. (For the wing with flap, the wing area includes the flap area.) k_{WOT} is an average value of the downwash angle induced on the tail by a unit deflection of the wing. Similarly k_{TOW} is an average value of the downwash angle induced on the wing by a unit deflection of the canard. Values of the lift curve slopes and of k_{WOT} and k_{TOW} are given in Appendices A and B for delta-planform configurations. (Certain assumptions about the downwash field underlie the calculations of k_{WOT} and k_{TOW}.)

Moment coefficient: The moment coefficient of the wing-plus-trim-surface configuration is

$$C_M = -x_\alpha C_{L_\alpha} \alpha - x_\delta C_{L_\delta} \delta - x_o C_{L_o} \qquad (7)$$

C_M will be based on the wing area and on the mean aerodynamic chord, $\bar{c}$, of the wing. (For the delta wing the m.a.c. is 2/3 the maximum chord.) x_α, x_δ, and x_o are the distances (Fig. 1) from the C.G. of the configuration to the "center" of the l_α, l_δ, and l_o load distributions respectively. These lengths are measured in units of the m.a.c. They depend only upon the C.G. position, the geometry of the configuration, and the Mach number. The difference between any two of them depends only upon the geometry and Mach number. $x_\delta - x_\alpha$ and $x_o - x_\alpha$ are evaluated in Appendix A.

Stability parameter: The stick fixed static longitudinal stability derivative, or static margin, is

$$\frac{\partial C_M}{\partial C_L} = \frac{(\partial C_M / \partial \alpha)_\delta}{(\partial C_L / \partial \alpha)_\delta} = - \bar{x}_\alpha \tag{8}$$

the partial differentiations carried out with δ held constant. When $\partial C_M / \partial C_L = 0$, the configuration is neutrally stable and the C.G. is at the "center" of the ℓ_α load distribution. For $\partial C_M / \partial C_L < 0$, the configuration is stable.

Drag due to lift: The coefficient of induced drag due to lift (based on the wing area) is

$$C_{D_i} = \alpha \underset{\substack{\text{wing plus} \\ \text{trim surface}}}{\iint} \frac{\ell_\alpha + \ell_\delta + \ell_o}{q S_w} dx\, dy + \delta \underset{\substack{\text{trim} \\ \text{surface}}}{\iint} \frac{\ell_\alpha + \ell_\delta + \ell_o}{q S_w} dx\, dy + \underset{\substack{\text{twisted and} \\ \text{cambered surfaces}}}{\iint} \frac{\alpha_o (\ell_\alpha + \ell_\delta + \ell_o)}{q S_w} dx\, dy \tag{9}$$

where $\alpha_o = \alpha_o(x, y)$ is the additional angle of attack distribution corresponding to any local twist and camber. With the aid of Eqs. 2 through 6, Eq. 9 becomes

$$C_{D_i} = \alpha \left[C_{L_\alpha} \alpha + C_{L_\delta} \delta + C_{L_o} \right] + \delta \left[s_T \left(C_{l_\alpha} \right)_T \delta + \underset{\substack{\text{trim} \\ \text{surface}}}{\iint} \frac{\ell_\alpha + \ell_o}{q S_w} dx\, dy \right] + \underset{\substack{\text{twisted and} \\ \text{cambered surfaces}}}{\iint} \frac{\alpha_o (\ell_\alpha + \ell_\delta)}{q S_w} dx\, dy + C_{D_o} \tag{10}$$

where C_{D_o} is the drag coefficient due to camber plus twist, i.e., the drag coefficient due to the load distribution when α and δ are zero. Note that the first bracket is simply C_L.

It is convenient to introduce the notation $\bar{\alpha} = \alpha/\beta C_L$, $\bar{\delta} = \delta/\beta C_L$ $\bar{\alpha}_o = \alpha_o/\beta C_L$. Then Eq. 10, with the aid of Eqs. 5 and 6, can be rearranged as follows: For the wing plus tail (or wing plus canard), Config. 1 or 2,

$$\frac{C_{D_i}}{\beta C_L^2} = \beta (C_{L\alpha})_w \left[\bar{\alpha} - k_{TOW}(\bar{\alpha} + \bar{\delta})\right] \bar{\alpha}$$

$$+ S_T \beta (C_{L\alpha})_T \left[\bar{\alpha} + \bar{\delta} - k_{WOT}\bar{\alpha}\right](\bar{\alpha} + \bar{\delta}) + \frac{C_{D_0}}{\beta C_L^2} \qquad \text{(11a)}$$

$$+ \underset{\substack{\text{twisted and}\\ \text{cambered surfaces}}}{\iint} \bar{\alpha}_o \frac{(l_\alpha + l_\delta)}{q S_w C_L} dx\, dy + \bar{\delta} \underset{\substack{\text{trim}\\ \text{surface}}}{\iint} \frac{l_o\, dx\, dy}{q S_w C_L} + \frac{C_{L_0}}{C_L} \bar{\alpha}$$

(In applying Eq. 11a to Config. 1, put $k_{TOW} = 0$, and when applying it to Config. 2, put $k_{WOT} = 0$.) The first term is the drag (or, more strictly, the contribution to $C_{D_i}/\beta C_L^2$) produced on the wing with no twist or camber, the second term is the drag on the trim surface with no twist or camber, and the remaining four terms give the additional drag that arises if the surfaces are twisted and cambered.

For the wing-alone case, Config. 3,

$$\frac{C_{D_i}}{\beta C_L^2} = \beta (C_{L\alpha})_w \bar{\alpha}^2 (1 - S_T) + (\bar{\alpha} + \bar{\delta})\left[\beta (C_{L\alpha})_w \bar{\alpha} + \beta (C_{L\alpha})_T \bar{\delta}\right] S_T \qquad \text{(11b)}$$

$$+ \frac{C_{D_0}}{\beta C_L^2} + \underset{\substack{\text{twisted}\\ \text{and cambered}\\ \text{surfaces}}}{\iint} \bar{\alpha}_o \frac{(l_\alpha + l_\delta)}{q S_w C_L} dx\, dy + \bar{\delta} \underset{\text{flap}}{\iint} \frac{l_o\, dx\, dy}{q S_w C_L} + \frac{C_{L_0}}{C_L} \bar{\alpha}$$

where the first term is the drag on the part of the wing forward of the flap and the second term is the drag on the flap, both surfaces assumed to be untwisted and uncambered. The remaining four terms give the additional drag that arises if the surfaces are twisted or cambered.

If the trim surface is undeflected with respect to the wing ($\delta = 0$) and if the surfaces are flat ($\ell_o = 0$, hence $C_{D_o} = 0$ and $C_{L_o} = 0$), then, from Eqs. 10 or 11, the induced drag parameter is simply

$$\frac{C_{D_i}}{\beta C_L^2} = \bar{\alpha} \quad \text{for } \delta = 0, \qquad \text{flat surfaces} \tag{12}$$

for all three configurations.

Trim condition: If the configuration is in trim, then $C_M = 0$. The angles α and δ are then determined as a function of $\partial C_M / \partial C_L$ from Eqs. 1, 7, 8 with $C_M = 0$. The result is

$$\bar{\alpha} = \frac{1 - C_{L_o}/C_L}{\beta C_{L_\alpha}} + \left(\frac{x_o - x_\alpha}{x_\delta - x_\alpha}\right) \frac{C_{L_o}/C_L}{\beta C_{L_\alpha}} - \frac{\partial C_M / \partial C_L}{(x_\delta - x_\alpha)\beta C_{L_\alpha}} \tag{13}$$

$$\bar{\delta} = -\left(\frac{x_o - x_\alpha}{x_\delta - x_\alpha}\right) \frac{C_{L_o}/C_L}{\beta C_{L_\delta}} + \frac{\partial C_M / \partial C_L}{(x_\delta - x_\alpha)\beta C_{L_\delta}} \tag{14}$$

Drag due to lift of flat configurations in trim: For these configurations the terms of Eqs. 11a, -b, due to twist and camber are zero and C_{L_o} in Eqs. 13 and 14 is zero. Inserting the trim values of α and δ in Eq. 11a then gives for the wing-plus-tail (or wing-plus-canard) configuration

$$\frac{C_{D_i}}{\beta C_L^2} = \frac{1}{\beta C_{L_\alpha}} \left\{ 1 + \left[k_{WOT} S_T \beta (C_{L_\alpha})_T - k_{TOW} \beta (C_{L_\alpha})_W \right] R + S_T \beta (C_{L_\alpha})_T \beta (C_{L_\alpha})_W R^2 \right\} \tag{15a}$$

WITH $R = \dfrac{-(\partial C_M / \partial C_L)}{-\beta (\partial C_M / \partial \delta)_{C_L}}$ AND $\left(\dfrac{\partial C_M}{\partial \delta}\right)_{C_L} = -C_{L_\delta}(x_\delta - x_\alpha)$

$(\partial C_M / \partial \delta)_{C_L}$, which is obtained by holding C_L fixed but letting α vary with δ, is a derivative similar to the "elevator power", where here the "elevator" or trim surface is an all-movable tail or canard (Eq. 15a) or a wing trailing-edge flap (Eq. 15b). The

corresponding equation for the wing-with-flap configuration (from Eq. 11b) is

$$\frac{C_{Di}}{\beta C_L^2} = \frac{1}{\beta (C_{L\alpha})_W} + s_T \left[\frac{\beta (C_{L\alpha})_T}{\beta (C_{L\alpha})_W} - 1 \right] R + (1 - s_T) s_T \beta (C_{L\alpha})_T R^2 \qquad (15b)$$

with R as in Eq. 15a. In Eq. 15b the wing area is defined, in accord with current usage, to include the area of the flap. If instead one were to exclude the flap area from the wing area, then Eq. 15a would also apply to the wing-plus-flap case. k_{TOW} would be zero, and k_{WOT} would be $1-(C_{L\alpha})_W/(C_{L\alpha})_T$. (Note that s_T would then be the ratio of the flap area to the area of the wing forward of the flap.) C_{L_α} would be given by Eq. 5a.

Eq. 15 does not include any leading-edge thrust which might exist when the leading edges are subsonic ($\beta AR < 4$). The reduction in drag due to leading-edge thrust is computed in Appendix D for some special cases of flat configurations.

Drag due to lift of canard plus wing with tip panels uniformly twisted, in trim: For this configuration, the wing tip panels are deflected by the constant angle α_o with respect to the inboard portion of the wing, giving the wing an elementary twist. Eq. 11a, with the aid of Eq. 1, becomes

$$\frac{C_{Di}}{\beta C_L^2} = \bar{\alpha} + s_T \beta (C_{L\alpha})_T \bar{\delta} (\bar{\delta} + \bar{\alpha}) + A_o \bar{\alpha}_o^2 + A_\alpha \bar{\alpha}_o \bar{\alpha} + A_\delta \bar{\alpha}_o \bar{\delta} \qquad (16)$$

The first two terms of Eq. 16 are exactly equal to the first two terms of Eq. 11a with $k_{WOT} = 0$ plus the last term of Eq. 11a. The coefficients A_o, A_α and A_δ depend on the configuration geometry and Mach number and are evaluated for a special case in Appendix C. The values of α and δ for trim are given by Eq. 13 and 14 with

$$\frac{C_{L_o}}{C_L} = 4 s_p \bar{\alpha}_o \qquad (17)$$

for a delta wing with sonic or supersonic leading edges. s_p is the ratio of the area of the two panels to the area of the wing.

If one chooses α_o to minimize the drag (Eq. 16) of the configuration, then

$$(\bar{\alpha}_o)_{OPT} = B_1 + B_2 (\partial C_M / \partial C_L) \tag{18}$$

The coefficients B_1 and B_2 are functions of Mach number and the configuration geometry and are evaluated numerically for a special case in Appendix C. Note that $(\bar{\alpha}_o)_{OPT}$ varies with $\partial C_M / \partial C_L$.

Drag due to lift of configurations with varying twist and camber, in trim: Germain [3] has determined the induced drag of certain optimally twisted and cambered delta planform wings with sonic leading edges ($\beta AR = 4$). Specifically, he has determined the minimum drag for a prescribed lift, and the minimum drag when both lift and moment are specified. The results can be presented in the form

$$\left(\frac{C_{D_i}}{\beta C_L^2}\right)_{MIN} = \text{function of } \bar{P} \equiv f(\bar{P}) \tag{19}$$
$$= 0.2222 + 1.409(0.0556 - \bar{P})^2$$

where $\bar{P}$ is the non-dimensional distance from the center of pressure of the twisted-cambered wing to the centroid of the wing area. For any given value of $\bar{P}$ a specific distribution of local angle of attack is required to achieve the minimum $C_{D_i}/\beta C_L^2$. The magnitude of the angle of attack at any point depends also upon β and C_L. If lift only is prescribed, the minimum value of drag is obtained with $\bar{P} = .0556$ (measured in m.a.c. units of whatever delta surface is being considered).

For Configs. 1-b and 2-b, both the wing and the trim surface are optimally twisted and cambered for a prescribed lift, so that for

either surface alone in the free stream, Eq. 19 with $\bar{P} = .0556$ applies. That is

$$\frac{C_{D_W}}{\pi C_{L_W}^2} = f(0.0556) = 0.2222 \tag{20a}$$

$$\frac{C_{D_T}}{\pi C_{L_T}^2} = f(0.0556) = 0.2222 \tag{20b}$$

where C_{D_T} and C_{L_T} are based on the trim-surface planform area. The total load on the wing and load on the tail may be varied so that the configuration can be trimmed. One can arbitrarily choose $\alpha = 0$ AND $\delta = 0$ so that the total lift comes from the distribution of twist and camber. If one neglects the interference between the wing and the trim surface*, then the lift, moment and induced drag coefficients are

$$C_L = C_{L_o} = C_{L_{o_W}} + S_T C_{L_{o_T}} \tag{21}$$

$$C_M = C_{M_o} = -\chi_{o_W} C_{L_{o_W}} - \chi_{o_T} S_T C_{L_{o_T}} \tag{22}$$

$$C_{D_i} = C_{D_o} = C_{D_{o_W}} + S_T C_{D_{o_T}} \tag{23}$$

where χ_{o_W} and χ_{o_T} are measured from the C.G. to the centers of load on the wing and trim surfaces respectively. With the aid of Eq. 20 the drag equation may be written

$$\frac{C_{D_i}}{\pi C_L^2} = \frac{C_{D_o}}{\pi C_L^2} = f(0.0556)\left[\left(\frac{C_{L_{o_W}}}{C_L}\right)^2 + S_T\left(\frac{C_{L_{o_T}}}{C_L}\right)^2\right] \tag{24}$$

* The interference $\to 0$ as the vertical gap between the surfaces $\to \infty$.

The stability parameter is still given by Eq. 8. (It measures the reaction to a disturbance which changes the angle of attack of the configuration as a rigid unit. That is, although this configuration when in equilibrium has $\alpha = 0$, the disturbance produces a non-zero α.) The wing and tail loads for trim, from Eqs. 8, 21 and 22 with $C_M = 0$ are

$$\frac{C_{L_{ow}}}{C_L} = \frac{x_{o_T} - x_\alpha}{x_{o_T} - x_{o_w}} - \frac{\partial C_M / \partial C_L}{x_{o_T} - x_{o_w}} \tag{25}$$

$$\frac{C_{L_{o_T}}}{C_L} = -\frac{1}{S_T}\,\frac{x_{o_w} - x_\alpha}{x_{o_T} - x_{o_w}} + \frac{1}{S_T}\,\frac{\partial C_M / \partial C_L}{x_{o_T} - x_{o_w}} \tag{26}$$

The lengths $x_{o_T} - x_\alpha$ and $x_{o_w} - x_\alpha$, which are functions of $\bar{P}$ and the distance ℓ from the centroid of the wing area to the centroid of the trim surface, are evaluated in Appendix A.

The trim drag equation is then

$$\begin{aligned}\frac{C_{D_i}}{\beta C_L^2} = 0.2222\Bigg\{&\left[\left(\frac{x_{o_T} - x_\alpha}{x_{o_T} - x_{o_w}}\right)^2 + \frac{1}{S_T}\left(\frac{x_{o_w} - x_\alpha}{x_{o_T} - x_{o_w}}\right)^2\right] \\ &- 2\left[\left(\frac{x_{o_T} - x_\alpha}{x_{o_T} - x_{o_w}}\right) + \frac{1}{S_T}\left(\frac{x_{o_w} - x_\alpha}{x_{o_T} - x_{o_w}}\right)\right]\left(\frac{\partial C_M / \partial C_L}{x_{o_T} - x_{o_w}}\right) \\ &+ \left(1 + \frac{1}{S_T}\right)\left(\frac{\partial C_M / \partial C_L}{x_{o_T} - x_{o_w}}\right)^2\Bigg\}\end{aligned} \tag{27}$$

For Config. 3-b, optimally twisted and cambered wing alone, trim is effected by varying $\bar{p}$ which requires varying the distribution of local angle of attack. The drag equation is simply

$$\frac{C_{D_i}}{\beta C_L^2} = f(\bar{P}) \tag{28}$$

where $f(\bar{P})$ is given by Eq. 19. If the configuration is in trim,

the C.G. is located at the distance $\bar{P}$ ahead of the centroid of the wing. The static stability parameter is

$$\frac{\partial C_M}{\partial C_L} = -\mathcal{X}_\alpha = -\bar{P} \tag{29}$$

It is evident that the drag values for Configs. 1-b, 2-b, and 3-b are actually lower bounds in that the twist and camber of the surfaces change with Mach number, lift coefficient and C.G. position. Furthermore, in 1-b and 2-b, the interference between the wing and the trim surface is neglected. However, at the design condition one could theoretically achieve the drag values of Eq. 28 for Config. 3-b, and near the design conditions, the drag values should be close to the values of Eq. 28.

Maximum lift-to-drag ratio: In general the maximum lift to drag ratio of any zero-thickness configuration is

$$(L/D)_{MAX} = \frac{1}{2\sqrt{(C_{D_i}/C_L^2)\, S_f\, C_{D_f}}} \tag{30}$$

where C_{D_f} is the skin friction drag coefficient based on the wetted area of the configuration. C_{D_f} depends upon the Mach number and Reynold's number (and also upon the heat transfer rate). S_f is the ratio of the wetted area to the wing area:

$S_f = 2(1 + S_T)$ for the wing-plus-tail (or wing-plus-canard) configuration

$S_f = 2$ for the wing alone (with flap or twisted and cambered)

It is convenient to present the graphical results as the ratio of $(L/D)_{MAX}$ of the trimmed configuration to $(L/D)_{MAX}$ of a flat untrimmed sonic-edge delta wing alone. For this latter configuration

$$C_{D_i} / C_L^2 = .25 \beta$$

so that the $(L/D)_{MAX}$ is

$$(L/D)_{\substack{MAX,\ FLAT\ UNTRIMMED \\ SONIC\text{-}EDGE\ DELTA\ WING\ ALONE}} = \frac{1}{\sqrt{2 \beta C_{D_f}}} \tag{31}$$

The ratio of $(L/D)_{MAX}$ of a trimmed configuration to $(L/D)_{MAX}$ of the flat untrimmed sonic-edge delta wing alone at the same Mach number and skin friction drag coefficient is then

$$\frac{(L/D)_{MAX,\ TRIMMED\ CONFIGURATION}}{(L/D)_{\substack{MAX,\ FLAT\ UNTRIMMED \\ SONIC\text{-}EDGE\ DELTA\ WING\ ALONE}}} = \frac{1}{\sqrt{\left(C_{D_i} / \beta C_L^2\right)_{\substack{TRIMMED \\ CONFIG}} 2 S_f}} \tag{32}$$

IV. DISCUSSION

A. General Trends (Flat Surfaces - No Leading-Edge Thrust).

Drag as function of static margin: If the wing and trim surface aspect ratios are the same, then the coefficient of drag due to lift of a flat configuration in trim is given by

$$\frac{C_{D_i}}{\beta C_L^2} = \frac{1}{\beta C_{L_\alpha}}\left\{1 + \beta\left(C_{L_\alpha}\right)_W \left(S_T \bar{k}_{WOT} - \bar{k}_{TOW}\right) R + \beta^2 \left(C_{L_\alpha}\right)_W^2 S_T R^2\right\} \qquad (15a')$$

$$R = \frac{-\partial C_M / \partial C_L}{-\beta\left(\partial C_M / \partial \delta\right)_{C_L}} \quad , \left(\partial C_M / \partial \delta\right)_{C_L} = -C_{L_\delta}\left(\bar{x}_\delta - \bar{x}_\alpha\right)^*$$

$\left.\begin{array}{l} \bar{k}_{TOW} = 0 \\ 1 \geq \bar{k}_{WOT} \geq 0 \end{array}\right\}$ WING PLUS TAIL $\qquad\qquad$ $\left.\begin{array}{l} 1 \geq \bar{k}_{TOW} \geq 0 \\ \bar{k}_{WOT} = 0 \end{array}\right\}$ WING PLUS CANARD

The coefficient of drag due to lift of a wing-with-flap configuration in trim is given by

$$\frac{C_{D_i}}{\beta C_L^2} = \frac{1}{\beta\left(C_{L_\alpha}\right)_W} + S_T\left[\frac{\beta\left(C_{L_\alpha}\right)_T}{\beta\left(C_{L_\alpha}\right)_W} - 1\right] R + S_T \beta\left(C_{L_\alpha}\right)_T \left(1 - S_T\right) R^2 \qquad (15b)$$

$$R = \frac{-\partial C_M / \partial C_L}{-\beta\left(\partial C_M / \partial \delta\right)_{C_L}} \quad , \quad \left(\partial C_M / \partial \delta\right)_{C_L} = -C_{L_\delta}\left(\bar{x}_\delta - \bar{x}_\alpha\right)^*$$

$$\beta\left(C_{L_\alpha}\right)_T = \beta\left(C_{L_\alpha}\right)_W \quad \text{FOR} \quad \beta A R \geq 4 \quad \text{(SUPERSONIC OR SONIC LEADING EDGES)}$$

$$\beta\left(C_{L_\alpha}\right)_T > \beta\left(C_{L_\alpha}\right)_W \quad \text{FOR} \quad \beta A R < 4 \quad \text{(SUBSONIC LEADING EDGES)}$$

---

* Evaluated in Appendix A (Eq. A-4) as a function of ℓ, lift curve slopes, and magnitude and location of induced load (interference).

At zero static margin, the drag coefficient is simply the lift coefficient squared divided by the lift curve slope of the complete configuration. As the static margin increases, the drag increases: It is immediately evident that the third terms of Eqs. 15a', -b increase as $-\partial C_M/\partial C_L$ increases; it can also be shown that the second terms increase as $-\partial C_M/\partial C_L$ increases. $\left[(\partial C_M/\partial \delta)_{C_L} < 0\right.$ for a tail or flap; $\left.(\partial C_M/\partial \delta)_{C_L} > 0\right.$ for a canard.]

From Eqs. 15 it is also seen that an increase in the magnitude of $(\partial C_M/\partial \delta)_{C_L}$, the trim surface "power" decreases the magnitude of R. If this increase can be achieved without altering the coefficients of R and R^2, e.g., by increasing $|\ell|$, then a given static margin can be achieved with a smaller drag penalty.

The variation of $C_{D_i}/\beta C_L^2$ with $\partial C_M/\partial C_L$ is shown in Figs. 2 through 5, and 7.

Drag as function of geometric parameters S_T, $|\ell|$, G AND AR: In the numerical calculations of the drags of the wing-plus-tail and wing-plus-canard configurations, the trim surface has the same aspect ratio as the wing $(AR_T = AR_w = AR)$. For the wing-with-flap configurations, $AR_T \neq AR_w = AR$; however, AR_T can be expressed as a function of S_T and AR_w. Thus the effect of only four geometric parameters is studied: S_T, the ratio of the planform area of the trim surface to that of the wing; $|\ell|$, the distance between the centroid of area of the wing and that of the trim surface, measured in wing m.a.c. units; G, the vertical gap between the rear surface and the vortex sheet shed from the forward surface measured in units of wing span; and AR, the wing aspect ratio. (Note that AR always appears in combination with the Mach number parameter $\beta = \sqrt{M^2-1}$.)

For the wing-with-flap configuration two values of S_T are used: .25, .50. For most of the cases the wing with the larger flap has the less drag (Figs. 4 and 5). However, the smaller flap appears to be better for small static margins for the low aspect ratio wing with $\beta AR = 1.5$ and having no leading-edge thrust. For the wing-plus-tail (or wing-plus-canard) configurations, $S_T = .25$ for almost all the calculations. However, a few calculations of $(L/D)_{max}$ have been made for configurations with other values of S_T. The results are discussed in Section IV F.

For the wing-with-flap configuration, l cannot be varied independently of S_T but is related to S_T by the equation $l = (1 - S_T) \div (1 + \sqrt{1 - S_T})$. For the wing-plus-tail (or wing-plus-canard) configurations, two values of $|l|$ were picked: 1.5, 3.0. Increasing $|l|$ means increasing $|(\partial C_M / \partial \delta)_{C_L}|$, the trim-surface "power", and this decreases the drag according to Eq. 15a'. This trend may be seen in Table 1, in which for

TABLE 1: Effect of varying tail length

$\beta AR = 4$ $\quad -\partial C_M / \partial C_L = 0.10$ $\quad S_T = 1/4$

l	G	$C_{D_i} / \beta C_L^2$	Case	See Fig.
0.40	-	0.296	Wing with flap*	7
0.59	-	0.236	Wing plus flap*	7
1.5	∞	0.206	Wing plus tail	2g
3.0	∞	0.201	Wing plus tail	2g

* NOTE: For the wing with flap case the wing area includes the flap area. For the wing plus flap case the wing area excludes the flap area.

each of the configurations there is no interference between the wing and the trim surface. The wing and flap configurations compare as follows: In line 1 the aft part of the wing is deflected as a flap but in line 2 a flap is attached to the trailing edge of the wing.

Changing the vertical gap G affects k_{WOT} or k_{TOW}, the average induced downwash angle per unit deflection of the forward surface. This average downwash angle is a measure of the interference between the wing and tail or canard. One of the primary effects of reducing the interference is that it decreases the drag by increasing C_{L_α}. Interference also enters Eq. 15a' in the coefficient of R and to a lesser extent, in $-(\partial C_M / \partial \delta)_{C_L}$. Whether or not the rear surface is above or below the vortex sheet a given distance does not matter, since the downwash field is symmetrical with respect to the vortex sheet. The effect of changing G is illustrated in Table 2. It

is interesting to note (Table 2a) that the drag decreases much more rapidly for the canard configuration than for the tail configuration as the gap increases from zero. Already at G = 0.10 the two configurations have very nearly the same drag. At a positive static margin (Table 2b) the decrease in drag with increasing G is somewhat greater than at neutral stability.

TABLE 2: Effect of changing vertical gap

(a) $\partial C_M/\partial C_L = 0$ $\beta AR = 4$ $S_T = 1/4$ $|2| = 1.5$

	Wing Plus Tail		Wing Plus Canard		See Fig.
G	$S_T k_{WOT}$	$C_{D_i}/\beta C_L^2$	k_{TOW}	$C_{D_i}/\beta C_L^2$	
0	0.140	0.225	0.305	0.264	13,2b
0.05	0.138*	0.225*	0.236*	0.246*	-
0.10	0.127*	0.223*	0.154*	0.228*	-
0.50	0.048	0.208	0.050	0.208	13,2e
∞	0	0.200	0	0.200	2g

(b) $-(\partial C_M/\partial C_L) = 0.10$ $\beta AR = 4$ $S_T = 1/4$ $|2| = 1.5$

	Wing Plus Tail		Wing Plus Canard		See Fig.
G	$S_T k_{WOT}$	$C_{D_i}/\beta C_L^2$	k_{TOW}	$C_{D_i}/\beta C_L^2$	
0	0.140	0.239	0.305	0.297	13,2b
0.5	0.048	0.216	0.050	0.217	13,2e
∞	0	0.205	0	0.205	2g

* Approximate calculation based on expansion of Eqs. B-7,8 about G = 0 .

A range of βAR from 1.5 to 8 is studied here. In general, the drag parameter, $C_{D_i}/\beta C_L^2$, decreases as the reduced aspect ratio, βAR, increases but the rate of decrease diminishes with increasing βAR. For the wing with flap case when the wing has supersonic leading edges the drag does not vary with βAR. When the wing has subsonic leading edges and leading-edge thrust is not included, the drag decreases with increasing βAR but when leading-edge thrust is included the minimum drag point occurs near $\beta AR = 3$ (Fig. 6).

B. Comparison of Wing-Plus-Canard with Wing-Plus-Tail Configurations (No Leading-Edge Thrust)

Flat wing plus tail and wing plus canard (Configs. 1-a and 2-a): The comparison will be made only on the basis of trim drag, and the effects of various parameters on the trim drag will be examined one at a time. Since calculations have been made only for the case when the wing and tail (or canard) aspect ratios and hence lift-curve slopes are the same, it is convenient to refer to Eq. 15a' (Section IV A) rather than to Eq. 15a in making the comparisons.

First, if there is no interference between wing and tail (or canard), i.e., if $k_{WOT} = 0$ (or $k_{TOW} = 0$), and if Configs. 1-a and 2-a have the same l/l and the same static margin, then R^2 is the same for both configurations, and the coefficient of R in Eq. 15a' becomes zero. Hence the trim drag of the two configurations is the same. This can be seen more directly as follows: First examine the neutrally stable trimmed configurations of Sketch (a) for which the c.g. is at the neutral point N_o. The wing and trim surface

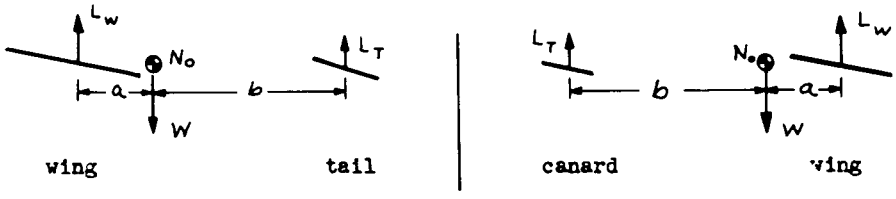

Sketch (a): Neutrally Stable Configurations

will be at the same angle of attack. Assume that the tail is geometrically similar to the wing. Then

$$\frac{L_w}{L_T} = \frac{S_w}{S_T} \qquad \text{(a)}$$

Since it is assumed that there is no interference between the wing and trim surface, the drag cannot depend upon the relative locations of the surfaces. For this neutrally stable case, the loadings on the two configurations are identical. Hence it is evident that the drags of the two configurations are the same. Now shift the center of gravity of each configuration forward by the same amount, z_α, so that each configuration has the same positive static margin. To retrim either configuration, maintaining the same total lift, it is necessary to add the load ΔL, which is proportional to z_α, to the forward surface and to subtract the same load ΔL from the rear surface as in Sketch (b). For the canard configuration,

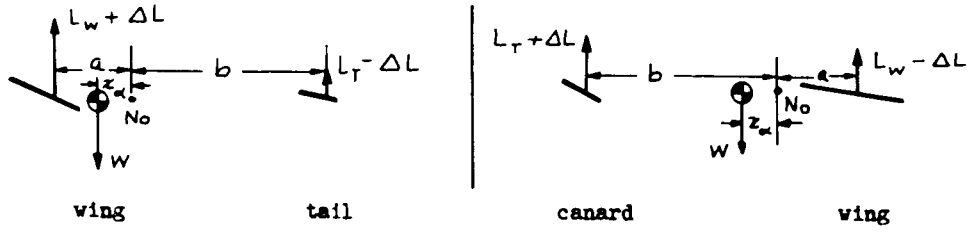

Sketch (b): Configurations with Same Positive Static Margin

additional load is carried on the trim surface and less on the wing; for the tail aft configuration, the reverse is true. The drags are then:

$$D \sim \frac{(L_w + \Delta L)^2}{S_w} + \frac{(L_T - \Delta L)^2}{S_T} \qquad \text{for tail aft case} \qquad (b)$$

$$D \sim \frac{(L_w - \Delta L)^2}{S_w} + \frac{(L_T + \Delta L)^2}{S_T} \qquad \text{for canard case} \qquad (c)$$

With the aid of (a), it is seen that the cross-product terms in both (b) and (c) disappear. Thus the flat non-interfering wing plus tail has the same trim drag as the corresponding flat non-interfering wing plus canard, both configurations having the same positive static margin. Note that in Fig. 2g, for which $G = \infty$ which means there is no interference, the drag curves for wing-plus-tail and wing-plus-canard configurations are identical.

As the gap G decreases, some unfavorable interference arises. k_{WOT} (or k_{TOW}) acquires a positive value, C_{L_α} decreases, and hence the drag increases. This effect is greater for the wing-plus-canard than for the wing-plus-tail configuration, as seen from Fig. 2. Figure 2 also shows that, as G decreases, the variation of $C_{D_i}/\beta C_L^2$ with $\partial C_M/\partial C_L$ increases, and this effect is more pronounced for the wing-plus-canard than for the wing-plus-tail configurations.

Of special interest is the case for which $S_T k_{WOT}$, for the wing-plus-tail configuration, equals k_{TOW} of the corresponding wing-plus-canard configuration.* C_{L_α}, Eqs. 5a, -b, is then the same for the two configurations. It can also be shown that $|\partial C_M/\partial \delta|$ is nearly the same (see Eqs. 6 and A-4). Thus $|R|$ is essentially the same for both configurations. Also, the magnitude of the coefficient of R is the same. Thus, for this special case, the wing-plus-tail and wing-plus-canard configurations have essentially the same drag. For $k_{TOW} < S_T k_{WOT}$, the wing-plus-canard configuration has less drag than the corresponding wing-plus-tail configuration. An example of this latter case is shown in Fig. 2e where $G = .5$, $|l| = 1.5$, $\beta AR = 8$ and $S_T = .25$. The values of k_{TOW} and $S_T k_{WOT}$ are approximately .018 and .028 respectively.

In the preceding discussion, the comparison between the trim drag of the wing plus tail and the trim drag of the wing plus canard has been made with both configurations having the same values of $G, |l|, \beta AR, S_T$ and $\partial C_M/\partial C_L$. In actually deciding between wing-plus-tail and wing-plus-canard configurations it might for some reason be more pertinent to compare the configurations at unlike values of some of the parameters. For example, perhaps a wing-plus-canard configuration is inherently suited to have a longer tail length than a wing-plus-tail configuration. Say $G = 0, \beta AR = 4$, $S_T = .25, -\partial C_M/\partial C_L = .10$ and $|l| = 1.5$ for the wing plus tail and 3.0 for the wing plus canard. Then (Figs. 2b and 2d) $C_{D_i}/\beta C_L^2 \doteq .24$ for the wing plus tail and $C_{D_i}/\beta C_L^2 \doteq .275$ for the wing plus canard (instead of $\doteq .295$ when $|l| = 1.5$).

---

* Comparing $S_T k_{WOT}$ with k_{TOW} is equivalent to comparing $S_T k_{WOT}$ with $S_W k_{TOW}$ which latter comparison displays more symmetry. However, it has been convenient throughout to divide through by the wing area.

Should subsonic stability requirements make it possible at supersonic cruise conditions for a wing-canard configuration to operate at a much smaller static margin than a wing-tail configuration, then the supersonic induced drag of the trimmed wing plus canard might be as small or smaller than the supersonic induced drag of the trimmed wing plus tail. Thus, if the two configurations are the same as in the previous example except that the static margin for the wing plus tail is .25 instead of .10, then the flat wing plus tail, with $C_{D_i} / \beta C_L^2 \doteq .28$ has about the same drag as the flat wing plus canard. With proper twist, the wing-canard configuration in such a comparison would have less drag.

Canard plus wing with uniformly twisted tip panels - Config. 2-c: The discussion of flat wings and tails (or canards) indicated that with interference present, the wing-plus-tail configuration has somewhat less drag than the corresponding wing-plus-canard configuration (except at very high βAR). However, if the wing tip panels are twisted so that the tip region is at a lower angle of attack than the center region, then the following effects occur: First, reducing the load on the tips and increasing the load in the center shifts the center of load on the wing forward. Then less load need be carried on the canard to trim the configuration so that the interference effects become less severe. Secondly, this shift in load results in a better load distribution over the wing so that the drag due to a given lift on the wing is decreased. Thirdly, the canard is more lightly loaded and hence its drag is reduced. Table 3 compares a canard-plus-flat-wing configuration with a canard-plus-wing-with-twisted-tips configuration. The corresponding flat-wing-plus-tail configuration is also included. Values of $S_T k_{WOT} = .159$ and $k_{TOW} = .295$ were computed from Trefftz-plane values of downwash assuming a flat vortex sheet (Section IV G).

TABLE 3: Angle of attack, load and drag on wing and canard (or tail) in trim. Canard plus wing with uniformly twisted tips compared with flat configurations. Interference computed by assuming flat vortex sheet.

$G = 0$, $\beta AR = 4$, $l/l = 1.5$, $s_T = 1/4$

(a) $\partial C_M / \partial C_L = 0$

	angle of attack (in radians) $\div \beta C_L$ at			fraction of total load on		coefficient of drag due to lift $\div \beta C_L^2$ of		
	wing ctr.	wing tip	canard (or tail)	wing	canard (or tail)	wing	canard (or tail)	total
Config.	$\bar{\alpha}$	$\bar{\alpha} + \bar{\alpha}_o$	$\bar{\alpha} + \bar{\delta}$	L_w/L	L_T/L	$C_{D_{i_w}}/\beta C_L^2$	$C_{D_{i_T}}/\beta C_L^2$	$C_{D_i}/\beta C_L^2$
Flat wing plus canard	.262	.262	.262	.737	.263	.193	.069	.262
Canard plus wing with twisted tips •	.325	.064	.208	.792	.207	.181	.043	.224
Flat wing plus tail	.229	.229	.229	.917	.083	.210	.019	.229

(b) $\partial C_M / \partial C_L = -.25$

Config.	$\bar{\alpha}$	$\bar{\alpha} + \bar{\alpha}_o$	$\bar{\alpha} + \bar{\delta}$	L_w/L	L_T/L	$C_{D_{i_w}}/\beta C_L^2$	$C_{D_{i_T}}/\beta C_L^2$	$C_{D_i}/\beta C_L^2$
Flat wing plus canard	.271	.271	.466	.532	.468	.144	.218	.362
Canard plus wing with twisted tips *	.366	-.028**	.384	.615	.385	.127	.148	.275
Flat wing plus tail	.271	.271	.083	1.082	-.082	.293	-.007	.286

• Angle of twist picked to minimize drag when (a) $\partial C_M / \partial C_L = 0$, (b) $\partial C_M / \partial C_L = -.25$. The off-design drag values are shown in Fig 3a.

** The tip angle of attack is negative, but the load on the tip is not necessarily negative since the tip lies in an upwash field.

Note in the table that the canard plus wing with twisted tips actually has less drag than the flat wing plus tail. The latter configuration could also be improved somewhat by twist and camber. However, not nearly as much improvement is expected because unlike the wing-plus-canard configuration, neither surface of the wing-plus-tail configuration operates in a highly non-uniform downwash field.

Thus finally it appears that on the basis of the same tail length $|\ell|$, same area ratio S_T, same aspect ratio, same gap, and same static margin - there is very little difference in the trim drag of a wing-plus-canard and a wing-plus-tail configuration, if one twists and cambers the surfaces as needed.

C. Comparison of Wing-Plus-Tail and Wing-Plus-Canard Configurations to Wing-With-Flap Configurations (Flat Surfaces - No Leading-Edge Thrust)

In the present method of analysis three effects occur in going from a wing-with-flap configuration to a wing-plus-tail (or wing-plus-canard) configuration. First the area on which a given load can be carried is increased. (Note C_{D_i} and C_L are based on the wing area.) Secondly, the interference between the wing and the trim surface is increased. This is related to decreasing the aspect ratio of the system. Thirdly, the moment arm of the system is increased.

The fact that the area increases in going from a wing-with-flap configuration to a wing-plus-tail (or wing-plus-canard) configuration is a result of defining the wing area to include the flap area. If instead the wing area were defined to be the area of that part of the wing forward of the flap, then this area increase would not occur. Furthermore this "wing-plus-flap" configuration could be treated exactly as a wing-plus-tail configuration. The drag could be found from Eq. 15a with C_{L_α} given by Eq. 5a. (Note that Eq. 15a' is applicable to this wing-plus-flap configuration for $\beta AR \geq 4$, but not for $\beta AR < 4$, since in the latter case $\beta(C_{L_\alpha})_T \neq \beta(C_{L_\alpha})_W$.) k_{TOW} would be zero and k_{WOT} would be $1 - (C_{L_\alpha})_W/(C_{L_\alpha})_T$ which is zero for $\beta AR \geq 4$. However, almost all the calculations are made with the wing area defined to include the flap area. The only exceptions are Fig. 7 and several tables in which both definitions are used alternatively.

In Table 4a, $C_{D_i}/\beta C_L^2$ of the flat wing and flap is computed alternatively using the definition of wing area that includes the flap area and using the definition that excludes the flap area. Then the flat wing and flap is compared with flat wing-plus-tail and wing-plus-canard configurations. For cases II or III as compared with I, the trim surface gives added area on which the load can be carried and this decreases the drag.

Table 4: Comparison of trim drag: Flat wing and flap, flat wing plus tail, and flat wing plus canard. $\beta AR = 4$, $S_T = 1/4$

(a) Examples to illustrate effects of increasing area and of increasing interference. $\partial C_M/\partial C_L = 0$, $|l|$ arbitrary, $\delta = 0$

Case Config.	I Wing with flap (wing includes flap)	II Wing plus flap (wing excludes flap)	III Wing plus tail (or canard)	IV Wing plus tail	V Wing plus canard
G	-	-	∞	0	0
$S_T k_{WOT}$	-	0**	0	.140	0
k_{TOW}	-	0	0	0	.305
$C_{D_i}/\beta C_L^2$	.25	.20	.20	.225*	.265*
See Fig.	4,7	7	2g	2b,d	2b,d

(b) Examples to illustrate effect of increasing moment arm. $\partial C_M/\partial C_L = -.25$, $\delta \neq 0$ Configurations as in (a).

Case	I	II	III	IV	V
$\|l\|$	.40	.59	1.5	1.5	1.5
G	-	-	∞	0	0
$S_T k_{WOT}$	-	0	0	.140	0
k_{TOW}	-	0	0	0	.305
$C_{D_i}/\beta C_L^2$	.540	.424	.235	.278	.370
See Fig.	4,7	7	2g	2b	2b

* These values differ slightly from those of Table 3 since in Table 3 the interference was computed by assuming a flat vortex sheet while here a rolled-up vortex sheet is assumed.

** For $\beta AR \geq 4$ this average interference is zero. For $\beta AR < 4$, it would be positive.

Table 4a also shows the effect, in going from flap to tail or canard configurations, of increasing the interference. For example, in going from II to IV or V the interference increases and the drag increases. It is interesting to note that in going from a wing and flap to a wing plus tail (or canard) one is decreasing the aspect ratio of the system (in the present method of analysis). Decreasing the aspect ratio of a wing in general tends to decrease its efficiency as a lifting surface and this can be explained in terms of interference. For example, on a very low aspect ratio rectangular wing most of the load is carried on the forward part of the wing and very little on the rear part. If these parts were treated as separate surfaces, then the rear part would be operating inefficiently because it is in the downwash field of the forward part.

For all the cases of Table 4a, the configurations are neutrally stable and the trim surface is undeflected with respect to the wing. However, in Table 4b, the configurations each have a positive static margin of the same amount, the trim surfaces are deflected with respect to the wing, and the effect of changes in moment arm can be demonstrated. For example, in going from a wing-flap configuration, to a wing plus tail (or canard), the moment arm increases and the drag decreases.

The maximum lift-to-drag ratios of the configurations of Table 4 are given in Table 5 (Section IV F).

D. Effects of Twist and Camber - Bounds on Wing-Plus-Tail, Wing-Plus-Canard and Wing-Alone Drags

Config. 3-b, wing with twist and camber: In general one can expect to decrease the drag of a lifting surface by giving it a proper twist and camber. Germain[3] has found the drag due to lift of a sonic-edge delta-planform wing ($\beta AR = 4$) optimally twisted and cambered to minimize the drag under the constraints of a specified lift and a specified moment. There is an optimum distribution of local angle of attack for each design condition. (At a design condition values of β, C_L, and $\partial C_M / \partial C_L$ have been specified.) These minimum drag values, which can be considered as a bound to wing-alone trim drag, are shown in the lowest curve of Fig. 4. It is seen that a considerable reduction in drag from the flat-wing-with-flap

value can be obtained by optimally twisting and cambering the wing, particularly at large $-\partial C_M/\partial C_L$. It is interesting to note that the lowest drag occurs at $-\partial C_M/\partial C_L = .0556$, a positive value of the stability.

Configs. 1-b and 2-b, wing plus tail (or canard) with twist and camber: The drag of the flat wing plus flat tail (or canard) can also be reduced by proper twist and camber of the wing and trim surface. The beneficial effect of twisting the tip panels of a wing in the downwash field of a canard has already been seen (Section IV B, Config. 2-c). Here the effect of twist and camber of the wing and of the trim surface of a configuration in which there is no interference ($G = \infty$) is examined. The wing and tail (or canard) are each a "Germain wing" of sonic-edge delta planform designed to give a minimum drag for a specified lift. The distribution of local angle of attack is fixed, but the magnitude is a function of β, C_L and $-\partial C_M/\partial C_L$. Thus, again the low drag value can be achieved only at the design condition (and with $G = \infty$) so that the lowest curves of Fig. 2g are also in the nature of a bound on the drag values of a wing-plus-tail (or wing-plus-canard) configuration. (It may not be a true lower bound in that for large $-\partial C_M/\partial C_L$ and small tail length $|l|$ a slightly lower drag for the configuration might be achieved by choosing a wing and a trim surface optimally twisted and cambered with both lift and moment specified. The drag for a given lift of the individual components would be greater, but this might be offset by getting an effectively longer moment arm.)

E. Leading-Edge Thrust

When the leading edges are subsonic ($\beta A < 4$ for delta planforms) it is possible for some leading-edge thrust to exist. In most of the calculations no leading-edge thrust has been included. However, the drag of some of the wing-with-flap configurations, and a wing-plus-tail and a wing-plus-canard configuration (each of the latter with $\beta A = 1.5$, G = 0, and interference found by assuming a flat vortex sheet) have been computed under the alternative assumptions of no leading-edge thrust and full leading-edge thrust (Figs.3,5,6).

If full leading-edge thrust is attained, there is a considerable reduction in drag at small values of βA. For example, for a flat

neutrally stable wing with $\beta AR = 1.5$, the reduction in $C_{D_i}/\beta C_L^2$ is about 40% (Figs. 5a, 6a); while with $\beta AR = 3.5$, the reduction is about 17% (Figs. 5b, 6a). Greater reductions occur at positive static margins. With full leading-edge thrust the drag of a delta wing with subsonic leading edges is about as low or lower than the drag of a delta wing with supersonic leading edges. The variation with aspect ratio is shown in Fig. 6a for $\partial C_M/\partial C_L = 0$ and in Fig. 6b for $\partial C_M/\partial C_L = -.25$. When full leading-edge thrust acts there is somewhat less variation with $\partial C_M/\partial C_L$ than when no leading-edge thrust acts (Figs. 5a, b). For a delta wing with a large flap, it is interesting to note that with full leading-edge thrust the minimum value of $C_{D_i}/\beta C_L^2$ occurs at a positive value of the static margin (Fig. 5).

D
L
2
5

F. Maximum Lift-to-Drag Ratio

Figures 8 through 12 give the ratio of $(L/D)_{MAX}$ of the various trimmed configurations to the $(L/D)_{MAX}$ of a flat untrimmed sonic-edge delta wing at the same Mach number and with the same skin-friction drag coefficient. All the configurations have zero thickness.

A comparison of configurations on the basis of $(L/D)_{MAX}$ eliminates the effect of configurations having different total areas. This is illustrated for sonic leading-edge configurations in Table 5 and also in Fig. 11. At zero static margin, there is no difference between flat wing-alone and flat wing-plus-tail (or wing-plus-canard) configurations of zero interference (infinite gap). As the interference increases, these configurations become poorer than the wing alone. For $\partial C_M/\partial C_L = -.25$, the wing plus tail or wing plus canard (except when $G = 0$) is superior to the wing and flap. The greater moment arm offsets the smaller effective aspect ratio of the wing plus tail (or canard) in the comparison to the wing and flap.

The Germain configurations of Fig. 11 and Table 5 indicate that at a given design condition, a considerable improvement in $(L/D)_{MAX}$ can be made by proper twist and camber of the surfaces. $(L/D)_{MAX}$ of the flat wing plus canard is increased appreciably just by uniformly twisting the wing tip panels (Table 5).

The effect on $(L/D)_{MAX}$ of changing the trim-surface area has not been studied in detail. However, some calculations have been made for flat wing-with-flap configurations and for flat wing-plus-

TABLE 5: Comparison of $(L/D)_{MAX}$: flat wing and flap, flat wing plus tail, flat wing plus canard, Germain wing, Germain wing plus Germain tail (or canard), canard plus flat wing with twisted tips, in trim.

$\partial C_M/\partial C_L = 0$; $\beta AR = 4$, $S_T = 1/4$, /2/ ARBITRARY, $\delta = 0$									
Case	I	II	III	IV	V	VI	VII	VIII	IX
Config.	wing with flap (wing includes flap)	wing plus flap (wing excludes flap)*	wing plus tail (or canard)	wing plus tail	wing plus canard	Germain** wing (no trim surface)	Germain** wing plus Germain tail	Germain** wing plus Germain canard	Canard *** plus flat wing with uniformly twisted tips
G	–	–	∞	0	0	–	∞	∞	0
$\frac{(L/D)_{MAX\ TRIMMED\ CONFIG.}}{(L/D)_{MAX\ FLAT\ UN-TRIMMED\ SONIC-EDGE\ WING\ ALONE}}$	1.000	1.000	1.000	.942	.870	1.050	1.057	1.057	.945
$\partial C_M/\partial C_L = -.25$; $\beta AR = 4$, $S_T = 1/4$, $\delta \neq 0$ except for Cases VI, VII and VIII, G AS ABOVE									
/2/	.40	.59	1.5	1.5	1.5	–	1.5	1.5	1.5
$\frac{(L/D)_{MAX\ TRIMMED\ CONFIG.}}{(L/D)_{MAX\ FLAT\ UN-TRIMMED\ SONIC-EDGE\ WING\ ALONE}}$	.680	.687	.922	.848	.735	.952	1.008	1.004	.853
See Fig.	10,11	–	8e,11	8a,11	8a,11	10,11	8e,11	8e,11	–

* Note that in Case II the flap area is 25% of the wing area excluding the flap, but is only 20% of the total surface area.

** See explanations of Section IV D.

*** See explanations of Table 3.

tail and flat wing-plus-canard configurations with sonic leading edges ($\beta AR = 4$). In some cases the optimum trim area (trim area such that the configuration has the highest $(L/D)_{MAX}$ at a given static margin) has been found. In general, if there is no net interference between wing and trim surface, a large trim area is desirable; if there is interference and if the static margin is not too large, a small trim area is desirable.

For the wing-with-flap configuration with $\beta AR \geq 4$, for which case there is no net interference, the optimum flap area is equal to that part of the wing area forward of the flap (Fig. 12c, $S_T = .50$). For $\beta AR < 4$, the net wing-flap interference is no longer zero and the optimum flap area has not been computed but is probably less than .50. For example, for $\beta AR = 1.5$ with no leading-edge thrust and at a small static margin the flap with $S_T = .25$ is slightly better than that with $S_T = .50$. However, in most cases the larger of these two flaps is better.

For the flat wing-tail or wing-canard configuration with sonic leading edges and at a positive static margin, increasing the trim surface area up to the area of the wing increases $(L/D)_{MAX}$ if there is no wing-tail or wing-canard interference (e.g. at $G = \infty$, Figs. 12c). At zero static margin $(L/D)_{MAX}$ is unaffected by the size of the tail or canard. For the wing-tail configuration with $G = 0$ (Fig. 12a), for which value of G there is maximum interference, $(L/D)_{MAX}$ is considerably higher if the tail area is one-fourth the wing area than if the tail area equals the wing area. For the wing-canard configuration with $G = 0$ (Fig. 12b), $(L/D)_{MAX}$ is higher if the canard area is one-fourth the wing area than if the canard area equals the wing area for low and moderate static margins, but at high static margins the reverse is true. At low static margins the lowest $(L/D)_{MAX}$ occurs at some value of $S_T < 1$ for the canard configuration. The size of the trim surface has less effect on $(L/D)_{MAX}$ for the canard configurations than for the tail configurations.

The optimum tail and canard areas and the corresponding $(L/D)_{MAX}$ values for the $\beta AR = 4$, $G = 0$, $|\ell| = 1.5$ configurations are also shown in Figs. 12a, b as functions of the static margin. At zero static margin, zero trim area is optimum. As the static margin

increases, the optimum trim area increases approximately in proportion to the static margin except that at large static margins the optimum canard has an area equal to that of the wing. In Fig.12 d various flat configurations with optimum trim areas are compared.

G. Average Downwash Angles

Calculation of k_{WOT} and k_{TOW} : Since the drag of a wing-plus-tail configuration is quite dependent upon k_{WOT} and the drag of a wing plus canard is quite dependent upon k_{TOW} , it is necessary to define these numbers clearly and to describe how they were calculated. k_{WOT} is defined to have a value such that the coefficient of induced lift on the tail is $-k_{WOT}\alpha\, s_T\,(C_{L\alpha})_T$; similarly, k_{TOW} is such that the coefficient of induced lift on the wing is $-k_{TOW}(\alpha+\delta)(C_{L\alpha})_W$. Thus k_{WOT} is an average value of $d\epsilon/d\alpha$ produced at the region of the tail by the wing and k_{TOW} is an average value of $d\epsilon/d\alpha$ produced at the wing by the canard. The values of k_{WOT} and k_{TOW} could be estimated from charts of $d\epsilon/d\alpha$. (See Ref. 4 and references cited therein.) For numerical calculations made here, they have been computed from analytical expressions for $d\epsilon/d\alpha$ in the Trefftz-plane (far downstream). This will over estimate their magnitude somewhat, particularly for short tail-length configurations.

Most of the graphs are based on values of k computed by assuming that the vortex sheet shed from the forward surface is rolled up into two vortices in the neighborhood of the rear surface. (This assumption simplifies the calculations.) The other extreme is to assume that the vortex sheet remains flat in the region of the rear surfaces. At positions far from the vortex sheet or discrete vortices (G large), the downwash values are little affected by the assumption about the vortex sheet. The greatest effect occurs when G = 0. Fig. 13 compares the values of k for G = 0, computed on these two different assumptions. The corresponding differences in $C_{D_i}/\beta C_L^2$ are seen by comparing the curves for $\beta A = 1.5$ (without leading-edge thrust) and $\beta A = 4$ of Fig. 3 with the corresponding curves of Fig. 2. The differences are small. For example, for a wing plus tail with $\beta A = 4$ and $\partial C_M/\partial C_L = 0$, $C_{D_i}/\beta C_L^2 = .225$ if a rolled-up vortex sheet is assumed as compared to .229 when a flat vortex sheet is assumed. The effect of the vortex sheet

assumption upon $(L/D)_{MAX}$ for wing-plus-tail configurations with $\beta AR = 4$ is shown in Fig. 12a.

Computing k involves computing the induced lift on the rear surface and this is done with the aid of a strip theory. The theory is exact for delta wings with supersonic and sonic leading edges, but, in general, is only approximate for delta wings with subsonic leading edges (see Appendix B). For very low effective aspect ratios of the rear surface, say $\beta AR < 1$, the value of k computed in this way is unreliable.

Determination of G: G has been defined as the vertical distance measured in units of wing span, to the rear surface from the vortex sheet shed from the forward surface. For many purposes it is probably sufficient to take G as the non-dimensional vertical distance from the forward surface to the rear surface when the configuration is at zero angle of attack. Actually the vertical distance from the vortex sheet to the rear surface will be somewhat different from this and will vary with angle of attack both because the vortex sheet is deflected downward from the x-axis (which passes through the forward surface and is aligned with the free stream) and more importantly because the rear surface lies below the x-axis when the whole configuration is at the angle of attack α . Approximations for the dependence of G upon α are given in Appendix B.

Since G depends somewhat upon the angle of attack of the forward surface, k and hence C_{L_α} also depend somewhat upon this angle of attack. (This dependence introduces a non-linearity into the problem.) However, the dependence of G upon the forward surface angle of attack is neglected in the equations of this report in finding, for example, $\partial C_M / \partial \alpha$, and G is assumed to be an independent parameter.

Drag calculations from other values of k_{WOT} and k_{TOW} - for short tail lengths, for twin tails: It may be that the values of k_{WOT} and k_{TOW} used in this report do not seem appropriate to some configurations. For example, for short tail lengths, k_{WOT} and k_{TOW} should really be obtained not from Trefftz-plane values of downwash, but from downwash values a short distance behind the wing. This would decrease k_{WOT} or k_{TOW} and hence decrease the trim drag. These new drag values could be computed directly from the basic

equations, which are expressed as functions of k_{WOT} , or k_{TOW} , or they might be estimated from the graphs, by choosing, not the actual G, but a value of G which corresponds more nearly to the new value of k_{WOT} or k_{TOW} .

There is also the possibility of modifying the configuration so that the rear surface lies in a region of lower downwash, or even of upwash. For example, instead of one tail, one might use twin tails, with the same total area as the single tail, placed to the rear and outboard of the wing tips in the upwash field of the wing. Similarly one might use twin canards so placed that they produce upwash on the wing. Then the wing, trim-surface interference will be favorable. Table 6 gives some results obtained from Eq. 15a'. (This equation is still applicable when there is no interference between the two trim surfaces.) The drag of the configurations with twin trim surfaces is considerably less than the drag of the single trim-surface configurations. However, structural requirements might penalize these unconventional arrangements, particularly the twin canard configuration so that much of this potential gain in performance might be lost.

TABLE 6: Comparison of twin and single trim surfaces showing effect of favorable wing, trim-surface interference. Flat vortex sheet assumed. $-\partial C_M/\partial C_L = .10$, G = 0, $\beta AR = 4$, $S_T = 1/4$, $l/l = 1.5$

Config.	$S_T k_{WOT}$	k_{TOW}	C_{D_i}/BC_L^2	See Fig.
wing plus single tail	+.159	—	.245	3a
wing plus twin tails	-.077*	—	.189*	—
wing plus single canard	—	+.295	.292	3a
wing plus twin canards	—	-.023*	.195*	—

* k_{WOT} and k_{TOW} are estimated to be values of $d\epsilon/d\alpha$ at centerlines of rear surfaces. k_{WOT} and k_{TOW} should be somewhat more negative since upwash at centerline is somewhat less than average upwash. It is also assumed that induced load acts at centroid of planform area.

V. CONCLUSIONS

Calculations have been made of the trim drag (drag due to lift of configurations in trim) of wing-plus-tail, wing-plus-canard and wing-alone configurations at supersonic speeds. In general it has been found that the trim drag decreases as the aspect ratio increases, as the tail length increases, as the vertical distance, the "gap" between the rear surface and the vortex sheet from the forward surface, increases, and as the static margin decreases; also suitable camber and twist decrease the trim drag. However, calculations for wing-with-flap configurations with subsonic leading edges indicate that if full leading-edge thrust exists, then there is a range of aspect ratio in which decreasing the aspect ratio decreases the trim drag. Also if leading-edge thrust exists or if the surfaces are twisted and cambered there can sometimes be less trim drag at a small positive static margin than at zero static margin.

The optimum trim-surface area depends in general upon the static margin, the tail length, and the interference between the surfaces. A limited investigation of flat sonic-edge wings and trim surfaces indicates that if there is no net interference large trim surfaces are desirable, if there is much interference small trim surfaces are desirable at least if the static margin is not too large. For wing-with-flap configurations, large flap areas are usually desirable. For wing-tail configurations, large tails are desirable if the gap is large, small tails if the gap is small. For wing-canard configurations large canards are desirable if the gap is large or for any gap size if the static margin is large, small canards if the gap is small and the static margin small. For zero gap and small or moderate static margins, the optimum trim area (to give the highest $(L/D)_{MAX}$) is approximately proportional to the static margin divided by the magnitude of the tail length according to a semi-empirical analysis.

If one compares a flat wing-tail configuration to a flat wing-canard configuration (of the same trim-surface area, tail length, aspect ratio, gap and static margin) then, if there is zero gap, the wing plus tail has significantly higher $(L/D)_{MAX}$ than has the wing plus canard. This is still true even if the comparison is made using optimum rather than the same trim-surface areas. Also the wing plus

tail is somewhat more tolerant to an unfavorable change in any of the parameters, e.g. to increasing the static margin. However, if the gap is large, or if it is possible to choose a more favorable value of some parameter for the canard configuration than for the aft tail configuration, e.g. a longer tail length or a smaller static margin, or if an optimum twist can be used for the canard configuration, then there is little difference in the cruise performance of the two types of configurations. The often quoted "popular" concept that an airplane with a canard type of trim surface is superior to one with an aft tail surface because the trim load lifts up instead of down is incorrect. If there is little wing-canard interference, or if there is proper wing twist, then the penalty for trimming by adding lift to the small low-span canard surface and subtracting the same amount of lift from the main wing is about the same as the penalty for trimming with a small down load on the tail and adding lift on the main, large-span wing. (If there is much interference and if the configurations are flat, then the penalty for trimming with a canard is greater than that for trimming with a tail, comparing configurations with the same tail length, static margin, etc.) It seems probable, then, that considerations other than supersonic trim drag will determine whether a tail or a canard is a more desirable trim surface.

At small static margins, wing-with-flap configurations may have higher $(L/D)_{MAX}$ values than the corresponding wing-plus-tail or wing-plus-canard configurations. However, at larger static margins, the inherently longer tail length of the wing plus tail (or canard) gives that configuration an advantage over the wing alone. If all the surfaces were properly twisted or cambered it seems likely that the wing plus tail (or canard) would have a slight advantage over the wing alone at almost all positive values of the static margin. For moderate stability margins the wing and flap is about as efficient as a wing-plus-tail or wing-plus-canard arrangement of not too small gap. Again the choice of the type of trim surface will probably depend upon considerations other than supersonic trim drag.

If the configurations studied here could be modified so that the rear surface would lie in a region of lower downwash or preferably of upwash, considerable drag reduction could result. An approximate calculation

in which a single tail was replaced by twin tails of the same total area but operating in a region of upwash showed a drag reduction of about 20%. An even greater drag reduction, about 33%, is calculated if a single canard is replaced by twin canards so located that the wing operates in an upwash field rather than a mixed upwash-downwash field. These improvements are large compared to differences between wing-tail, wing-canard, and wing-alone designs where each is advantageously arranged. However, structural requirements might penalize such unconventional configurations, particularly the twin canard configuration, so that much of these potential gains in performance might not be achieved.

VI. APPENDICES

A. Superposition Procedures, Lift Curve Slopes, Centers of Load

Superposition procedures: Since it is assumed that the flow is governed by linear equations, the local load on a surface with a complicated angle of attack distribution (actual or apparent) may be found by superimposing the loads due to several simpler angle of attack distributions. The superposition procedures used in this report are shown in the following sketches.

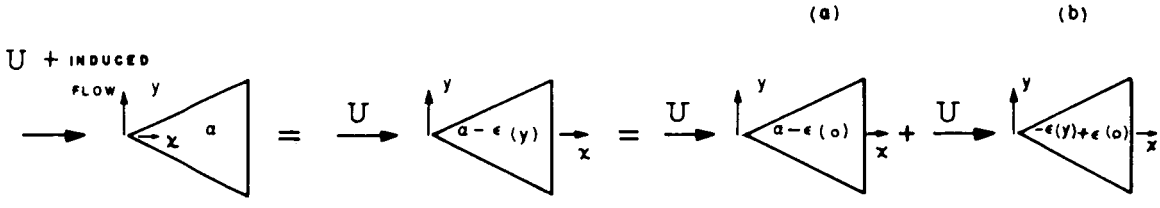

Local load on wing, $\ell_w(x,y) = \ell_{(a)}(x,y) + \ell_{(b)}(x,y)$

SKETCH 1: Wing at geometrical angle of attack α in downwash field of canard (Config. 2-a)

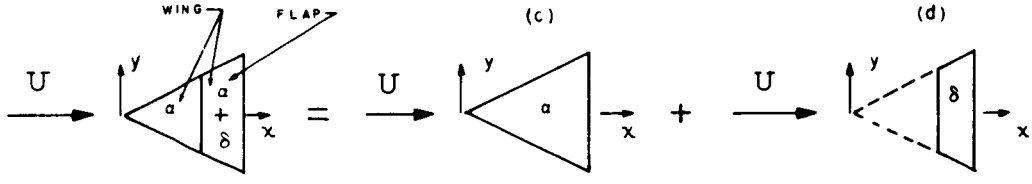

Local load on flap, $\ell_w(x,y) = \ell_{(c)}(x,y) + \ell_{(d)}(x,y)$

SKETCH 2: Wing with full trailing-edge flap at geometrical angle of attack $\alpha + \delta$ (Config. 3-a).

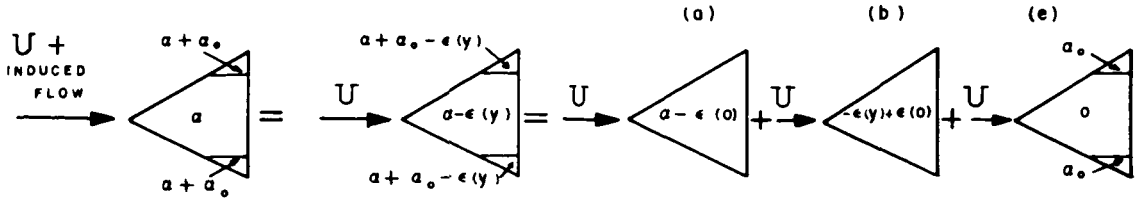

Local load on wing, $\ell_w(x,y) = \ell_{(a)}(x,y) + \ell_{(b)}(x,y) + \ell_{(c)}(x,y)$

SKETCH 3: Wing with twisted tips in downwash field of canard (Config. 2-c).

The purpose of the superposition procedure of Sketch 1 is not clear without further explanations: The local load due to the twisted surface (b) is computed by a strip theory [1] which is exact for a wing with subsonic leading edges ($m = \beta AR/4 < 1$) only if in the central part of the wing between $y = \pm \frac{1-m_w}{1+m_w}\frac{b_w}{2}$ the "effective" angle of attack $-\epsilon(y)+\epsilon(0)$ is zero. That is, the region of influence of an elementary streamwise strip must intersect at most only one leading edge of the delta planform. However, the strip theory should be a good approximation if the angle of attack is small in this region. Since $\epsilon(y) - \epsilon(o)$ is zero at $y = 0$, the strip theory will be more accurate, and in some cases exact, if applied to (b), while if applied directly to the surface with effective twist $\alpha - \epsilon(y)$, it would in general always give an approximate and less accurate result. For sonic or supersonic leading edges ($m \geq 1$), the strip theory is exact whatever the angle of attack distribution, but it is still convenient to use the superposition procedure of Sketch 1.

Lift curve slopes: The lift curve slopes for a delta wing, Ref. (4), pp. 199, 200 are

$$\beta C_{L_{\alpha_w}} = \begin{cases} (\pi/2)(1/E)\beta AR, & m \leq 1 \quad \text{(subsonic or sonic edges)} \\ 4, & 1/m \leq 1 \quad \text{(supersonic or sonic edges)} \end{cases}$$

where $E = E\left(\sqrt{1-m^2}\right)$, the complete elliptic integral of the second kind and $m = \beta AR/4$.

The lift curve slope for the flap may be obtained directly from Fig. A, 14f, page 196, of Ref. 4 by first computing the aspect ratio of the trapezoidal planform of the flap.

Centers of load - $(z_\delta - z_\alpha)$, $(z_o - z_\alpha)$: In general, the distance from the center of the load on a configuration at angle α to the center of load on the configuration when the trim surface is at angle δ (and $\alpha = 0$) is (see Fig. 1)*

$$x_\delta - x_\alpha = l + C.P._\delta - C.P._\alpha \qquad \text{(A-1)}$$

where l is the distance from the centroid of the wing planform (which includes the flap in Config. 3) to the centroid of the trim surface. (Note that distances are positive when measured in the downstream direction so that l is positive for a wing-tail configuration, and negative for a wing-canard configuration.) $C.P._\delta$ is the center of the load due to δ measured from the centroid of area of the trim surface, and and $C.P._\alpha$ is the center of the load due to α measured from the centroid of the wing. Let x_w and x_T be the centers of the "direct" load on the flat wing and on the flat trim surface respectively, and let x_{TOW} and x_{WOT} be the centers of the induced loads on the wing and on the trim surface respectively. x_w and x_{TOW} are measured from the wing centroid and x_T and x_{WOT} from the trim-surface centroid. Then, for Configs. 1 and 2 (wing plus tail and wing plus canard)

$$C.P._\delta = \frac{x_T S_T (C_{L_\alpha})_T + (x_{TOW} - l)(-k_{TOW})(C_{L_\alpha})_w}{C_{L_\delta}} \qquad \text{(A-2a)}$$

$$C.P._\alpha = \frac{x_w (C_{L_\alpha})_w + x_{TOW}(-k_{TOW})(C_{L_\alpha})_w + (x_T + l) S_T (C_{L_\alpha})_T + (x_{WOT} + l)(-k_{WOT}) S_T (C_{L_\alpha})_T}{C_{L_\alpha}} \qquad \text{(A-3a)}$$

*Note: These distances are all in units of $\bar{c}$.

For Config. 3 (wing with flap)

$$C.P._{\delta} = \chi_T \tag{A-2b}$$

$$C.P._{\alpha} = \chi_W \tag{A-3b}$$

For a flat delta planform, the direct load acts at the centroid, so for Configs. 1, 2, and 3 $\chi_W = 0$ always and $\chi_T = 0$ except for Config. 3. Then

$$\chi_{\delta} - \chi_{\alpha} = l - \frac{S_T (C_{L_\alpha})_T}{C_{L_\alpha}} \left[l - (l + \chi_{WOT}) k_{WOT} \right] \text{wing plus tail} \tag{A-4a}$$

$$\chi_{\delta} - \chi_{\alpha} = l + \frac{(C_{L_\alpha})_W}{C_{L_\delta}} (l - \chi_{TOW}) k_{TOW} + \frac{(C_{L_\alpha})_W}{C_{L_\alpha}} k_{TOW} \chi_{TOW} - S_T \frac{(C_{L_\alpha})_T \, l}{C_{L_\alpha}} \quad \text{wing plus canard} \tag{A-4b}$$

$$\chi_{\delta} - \chi_{\alpha} = l + \chi_T \quad \text{wing with flap} \tag{A-4c}$$

χ_{WOT} and χ_{TOW} are evaluated in Appendix B. For a trapezoidal flap

$$\chi_T = 0 \qquad \text{for } \beta AR \geq 4 \text{ (supersonic and sonic leading edges)}$$

$$\chi_T = e_{m \leq 1} - e_{m \geq 1} \quad \text{for } \beta AR < 4 \text{ (subsonic leading edges)} \tag{A-5}$$

$$= \frac{\frac{m-1}{4} \left(\frac{C_2}{C}\right)^2 \left(1 - \frac{C_2}{C}\right)}{4m - (3m+1)\frac{C_2}{C} + \frac{m+1}{2}\left(\frac{C_2}{C}\right)^2}$$

where $m = \frac{\beta AR}{4}$ and e = the distance from the leading edge of the flap to the center of pressure due to the δ deflection.

$e_{m \geq 1}$ is also equal to the distance from the leading edge to the centroid of area of the flap

$$\left(e_{m \geq 1} = \frac{1 - \frac{1}{3}\frac{C_2}{C}}{2 - \frac{C_2}{C}} \frac{3}{2} \frac{C_2}{C} \right) \qquad \text{where } \frac{C_2}{C} = 1 - \sqrt{1 - S_T}.$$

In general, the distance from the center of the load on a configuration at angle α to the center of load due to twist and camber is

$$\bar{x}_o - \bar{x}_\alpha = \frac{(\bar{x}_{ow} - \bar{x}_\alpha)\, C_{L_{ow}} + (\bar{x}_{oT} - \bar{x}_\alpha) S_T\, C_{L_{oT}}}{C_{L_o}} \tag{A-6}$$

where

$$\bar{x}_{o_w} - \bar{x}_\alpha = C.P._{o_w} - C.P._\alpha$$

$$\bar{x}_{o_T} - \bar{x}_\alpha = l + C.P._{o_T} - C.P._\alpha$$

$C.P._{o_w}$ is the center of the load on the wing due to twist and camber, measured from the controid of the wing, and $C.P._{o_T}$ is the center of the load on the trim surface due to twist and camber, measured from the centroid of the trim surface.

For Config. 2-c (canard plus wing with twisted tips), $C_{L_{oT}} = 0$, $C_{L_{ow}} = C_{L_o}$ and $C.P._{o_w}$ is at the centroid of the area affected by the tip panel deflection. (The load distribution due to this elementary twist is conical.) Thus,

$$C.P._{o_w} = (1/2)\left[1 - \sqrt{S_P}\right] \tag{A-7}$$

Then

$$\bar{x}_o - \bar{x}_\alpha = (1/2)\left[1 - \sqrt{S_P}\right] + \frac{(C_{L_\alpha})_w}{C_{L_\alpha}}\, k_{TOW}\, \bar{x}_{TOW} - \frac{S_T (C_{L_\alpha})_T}{C_{L_\alpha}}\, l \tag{A-8}$$

For Config. 1-b and 2-b (twisted and cambered wing plus tail and wing plus canard) interference is neglected, $C.P._{o_w} = -\bar{P}$ and $C.P._{o_T} = -\sqrt{S_T}\ \bar{P}$.

Then

$$\bar{x}_{o_w} - \bar{x}_\alpha = -\bar{P} - l\, \frac{S_T (C_{L_\alpha})_T}{C_{L_\alpha}} \tag{A-9}$$

$$\bar{x}_{o_T} - \bar{x}_\alpha = l - \bar{P}\sqrt{S_T} - l\, \frac{S_T (C_{L_\alpha})_T}{C_{L_\alpha}} \tag{A-10}$$

$$\bar{x}_{o_T} - \bar{x}_{o_w} = l + \bar{P}\left(1 - \sqrt{S_T}\right) \tag{A-11}$$

B. Induced Loads - Values of k_{WOT}, k_{TOW}, χ_{WOT}, χ_{TOW}, - Dependence of G upon α :

In general, for wing-tail and wing-canard configurations, when the forward surface is at an angle of attack, the rear surface will be operating in a non-uniform downwash field. k_{WOT} (or k_{TOW}) is an average value of $d\epsilon/d\alpha$ (the downwash angle per unit deflection of the forward surface) such that the induced load on the tail (or wing) per unit deflection of the forward surface is

$$\text{Induced load on tail} = q\, S_w (1-k_{WOT}) \quad S_T \, (C_{L_\alpha})_T \, \alpha \tag{B-1}$$

$$\text{Induced load on wing} = q\, S_w (-k_{TOW}) \, (C_{L_\alpha})_w \, (\alpha + \delta) \tag{B-2}$$

k_{WOT} (or k_{TOW}) could be estimated by looking at downwash charts and picking a value of $d\epsilon/d\alpha$ which seems representative of the region in which the tail (or wing) operates. However, for this report, k_{WOT} and k_{TOW} were calculated with the aid of a strip theory after making the assumption that the downwash values at the downstream surface were essentially Trefftz-plane values (values infinitely far downstream). The downwash then varies over the tail (or wing) in the spanwise (y) direction, but not in the streamwise (x) direction.

For most of the calculations it was assumed that the vortex sheet from the wing (or canard) was rolled up into two vortices at the position of the tail (or wing). Then in the Trefftz plane,

$$\frac{d\epsilon}{d\alpha}(y) = \frac{1}{2\pi}\left(\frac{\Gamma}{\alpha_F U \frac{b_F}{2}}\right)\left[\frac{a-\bar{y}}{(a+\bar{y})^2+\bar{G}^2} + \frac{a+\bar{y}}{(a+\bar{y})^2+\bar{G}^2}\right] \tag{B-3}$$

where Γ is the vortex strength, $2a\frac{b_F}{2}$ is the lateral spacing between the two vortices, $G\, b_w$ is the vertical distance of the rear surface from the vortex lines, bars denote distances measured in units of $b_F/2$, and the subscript F denotes the forward surface (F = W for a wing-tail configuration, F = T for a wing-canard configuration.) If the forward surface has a delta planform, then

$$\frac{\Gamma}{\alpha_F U b_F/2} = \frac{2}{E_F} \quad \text{for } m_F \leq 1 \text{ (subsonic or sonic leading edges)}$$
$$= \frac{4f \cos^{-1} f}{\pi \sqrt{1-f^2}} \text{ for } f = \frac{1}{m_F} < 1 \text{ (supersonic leading edges)} \tag{B-4}$$

where E_F is a complete elliptic integral of the second kind with modulus $\sqrt{1-m_F^2}$.

$$a = \frac{\pi}{4} \quad \text{for} \quad m_F \leq 1$$
$$= \frac{\pi}{4} \frac{\sqrt{1-f^2}}{\cos^{-1} f} \quad \text{for} \quad f = \frac{1}{m_F} < 1 \tag{B-5}$$

Γ was found by computing the circulation around the root chord of the wing. The vortex spacing was found by equating the momentum associated with the two vortices to the momentum imparted by the forward surface[5].

For a few cases it was assumed that the vortex sheet was still flat in the region of the downstream surface. In the plane of the vortex sheet (G = 0) shed from a delta wing (or delta canard), the Trefftz-plane value of $d\epsilon/d\alpha$ is, for $m_F \leq 1$:

$$\frac{d\epsilon}{d\alpha}(y) = \frac{d\epsilon}{d\alpha}(0) = \frac{1}{E_F} \quad \text{for} \quad |\bar{y}| = \frac{y}{b_F/2} \leq 1$$
$$= \frac{d\epsilon}{d\alpha}(0)\left[1 - \frac{\bar{y}}{\sqrt{\bar{y}^2-1}}\right] \quad \text{for} \quad |\bar{y}| > 1 \tag{B-6a}$$

and for $f = \frac{1}{m_F} < 1$:

$$\frac{d\epsilon}{d\alpha}(y) = \frac{d\epsilon}{d\alpha}(0) = \frac{f}{\pi\sqrt{1-f^2}} \ln\left|\frac{1+\sqrt{1-f^2}}{1-\sqrt{1-f^2}}\right| \quad \text{for} \quad |\bar{y}| \leq f$$
$$= \frac{d\epsilon}{d\alpha}(0) - \frac{f}{\pi\sqrt{1-f^2}} \ln\left|\frac{\sqrt{1-(\frac{f}{\bar{y}})^2}+\sqrt{1-f^2}}{\sqrt{1-(\frac{f}{\bar{y}})^2}-\sqrt{1-f^2}}\right| \quad \text{for} \quad |\bar{y}| \geq f \tag{B-6b}$$

A surface in a non-uniform downwash field has an effective twist. The load and center of load can be computed with the aid of a strip theory (Appendix A, and Ref. 1). Then the average $d\epsilon/d\alpha$ is

$$k_{FOR} = \left(\frac{d\epsilon}{d\alpha}\right)_{AVERAGE} = \frac{d\epsilon}{d\alpha}(0)\left\{1 + \frac{(c_{l_\alpha})_R}{(C_{L_\alpha})_R}\int_{-1}^{+1}\left[\frac{\frac{d\epsilon}{d\alpha}(y) - \frac{d\epsilon}{d\alpha}(0)}{\frac{d\epsilon}{d\alpha}(0)}\right]\left(1-\left|\frac{y}{b_R/2}\right|\right) d\,\frac{y}{b_R/2}\right\} \tag{B-7}$$

where

$$\frac{(C_{\ell_\alpha})_R}{(C_{L_\alpha})_R} = \frac{2}{\pi}\frac{E_R}{\sqrt{m_R}} \qquad \text{for} \qquad m_R \leq 1$$

$$= 1 \qquad \text{for} \qquad m_R \geq 1$$

$(C_{\ell_\alpha})_R$ is the lift-curve slope produced by deflecting a single strip and is based on the area of the strip. $(C_{L_\alpha})_R$ is the lift-curve slope of a flat delta surface. The subscripts F and R refer to the forward (upstream) and rear (downstream) surfaces respectively. With $d\epsilon/d\alpha$ given by Eq. B-3, the integral of Eq. B-7 becomes

$$\int_{-1}^{+1} [\ \ ](\ \ )\, d\frac{y}{b_R/2} = \frac{a^2 + \bar{G}^2}{a r}\left\{\begin{matrix}\text{BRACE OF}\\ \text{EQ. 13 OF REF 1}\end{matrix}\right\} \tag{B-8}$$

$$\text{with } r = b_R / b_F$$

(The brace is a function of $\bar{\bar{x}}_2$, r, and a, with $\bar{\bar{x}}_2 = \bar{G} = \frac{G b_w}{b_F/2}$.)
With $d\epsilon/d\alpha$ given by Eq. B-6, the integral of Eq. B-7 becomes, for $m_F \leq 1$

$$\int_{-1}^{1} [\ \ ](\ \ )\, d\frac{y}{b_R/2} = 0 \qquad \text{for} \qquad r = \frac{b_R}{b_F} \leq 1 \tag{B-9a}$$

$$= \left[-\frac{1}{r}\sqrt{r^2-1} + \frac{1}{r^2}\ln\left|r + \sqrt{r^2-1}\right|\right] \tag{B-9b}$$

$$\text{for} \qquad r \geq 1$$

and for $m_F > 1$

$$\int_{-1}^{+1} [\ \ ](\ \ )\, d\frac{y}{b_R/2} = 0 \qquad \text{for} \qquad r \leq f = \frac{1}{m_F} < 1 \tag{B-9c}$$

(The integration for $m_F > 1$, $r > f$ was not carried out.) Note that the cases for which $r < 1$ correspond to wing-tail configurations and $r > 1$ to wing-canard configurations.

The streamwise center of the load due to the deflection of a single strip is at the midchord of the strip. Knowing this, χ_{FOR}, the center of the total induced load measured from the centroid of area of the rear surface (in units of wing m.a.c.) can be obtained by an integration similar to that of Eq. B-7. With $d\epsilon/d\alpha$ given by Eq. B-3, the result is

$$\chi_{FOR} = \frac{3}{2}\,\frac{b_R}{b_W}\,\frac{m_W}{m_R}\left(1 - \frac{\frac{d\epsilon}{d\alpha}(0)}{k_{FOR}}\right)\left(-\frac{2}{3} - \frac{\left[\begin{array}{c}\text{BRACKET OF}\\ \text{EQ. 14 OF REF. 1}\end{array}\right]}{\left\{\begin{array}{c}\text{BRACE OF}\\ \text{EQ. 13 OF REF. 1}\end{array}\right\}}\right) \qquad \text{(B-10)}$$

with the brace and the bracket functions of $\bar{\bar{\chi}}_2 = \bar{G}$, a and r. With $d\epsilon/d\alpha$ given by Eq. B-6,

$$\chi_{FOR} = 0 \quad \text{for} \quad m_F \le 1\,,\ r \le 1 \qquad \text{AND for} \quad m_F \ge 1\,,\ r \le f = \frac{1}{m_F} < 1 \qquad \text{(B-11a,c)}$$

$$\chi_{FOR} = \frac{3}{2}\,\frac{b_R}{b_W}\,\frac{m_W}{m_R}\left(1 - \frac{\frac{d\epsilon}{d\alpha}(0)}{k_{FOR}}\right)\left(-\frac{2}{3} + \frac{2}{3}\,\frac{(r - \frac{1}{r})\sqrt{r^2-1}}{r\sqrt{r^2-1} - \ln\left|r + \sqrt{r^2-1}\right|}\right) \qquad \text{(B-11b)}$$

for $m_F \le 1\,,\ r > 1$

Dependence of G upon α : It is convenient to let $G = G_o + G_\alpha$ where G_o is that part which is independent of α and which is commonly called the gap (but measured in units of wing span) and G_α is that part which depends upon α. An approximate equation for G_α is the following

$$G_\alpha \doteq \frac{-4\alpha\,|\Gamma|}{3AR_W}\left[1 - \frac{w}{\alpha U}\right] \qquad \text{(B-12)}$$

This approximation (which is based upon a rolled-up vortex sheet) assumes that the vortex sheet is deflected downward from the free-stream direction by the angle w/U. w is the downwash velocity induced by one vortex at the other vortex:

$$w/U = \left(\Gamma/2\pi a\, b_F\, \alpha_F\, U\right)\alpha_F \qquad \text{(B-13)}$$

where Γ is the vortex strength, $a b_F$ the vortex spacing, and α_F the angle of attack of the forward surface.

The factor in the parentheses of Eq. B-13 can be obtained from Eqs. B-4, -5 and lies between 0 and $2/\pi^2$. α_F is α for the wing-plus-tail configurations and $\alpha + \delta$ for the wing-plus-canard configurations. Actually the values of α and δ for trim depend upon the interference and hence upon G. However, for the purpose of finding G_α it is sufficient to find α and δ from Eqs. 13, 14 using the interference computed by assuming $G_\alpha = 0$.

C. Wing With Twisted Tips (Config. 2-c)

Coefficients A_o, A_α, A_δ of Eq. 16: The coefficient A_o is a dimensionless number proportional to the load carried on the wing tip panels per radian of twist α_o of the panels. Similarly A_α is proportional to the load carried on the wing tip panels per radian of angle of attack α of the configuration. Note that A_α includes a load, $\ell_{\alpha_{IND.}}$, induced by the canard on the wing tips as well as the direct load, $\ell_{\alpha_{DIR}}$, due to the wing being at an angle of attack. Finally A_δ is proportional to the load induced by the canard on the wing tips per radian of deflection δ of the canard.

$$A_o = \frac{\beta}{\alpha_o q S_w} \iint_{\substack{WING \\ TIPS}} \ell_o(x,y)\, dx\, dy \qquad (C\text{-}1)$$

$$A_\alpha = \frac{\beta}{\alpha q S_w} \iint_{\substack{WING \\ TIPS}} \left[\ell_{\alpha_{DIR.}}(x,y) + \ell_{\alpha_{IND.}}(x,y) \right] dx\, dy \qquad (C\text{-}2)$$

$$A_\delta = \frac{\beta}{\delta q S_w} \iint_{\substack{WING \\ TIPS}} \ell_\delta(x,y)\, dx\, dy \qquad (C\text{-}3)$$

A_o, A_α, and A_δ have been evaluated only for the case where the canard and wing are each of delta planform with sonic leading edges ($\beta AR = 4$), the wing lies in a flat vortex sheet shed by the canard ($G = 0$), and the tip panels of the wing outboard of the canard span ($|y| \geq b_T/2$) are deflected with respect to the center by the angle α_o. (α_o is positive if the tip angle of attack is increased.) Under these conditions

$b_T/2 = \sqrt{S_T}\, b_w/2$ and the ratio of the total area of both tip panels to the wing area $S_p = (1-\sqrt{S_T})^2$.

The flow field due to the elementary twist of the right wing tip is conical and the local load $\ell_o(x,y)$ is[4]

$$\ell_o(x,y) = \frac{4q\alpha_o}{\pi\beta}\sqrt{\frac{1+\tau_o}{1-\tau_o}} \qquad \text{(C-4)}$$

$$\text{with} \qquad \tau_o = \frac{\beta(y-b_T/2)}{x-\beta b_T/2}$$

The direct load $\ell_{\alpha_{DIR.}}$ due to the wing being at angle of attack α also comes, of course, from a conical flow solution [4]

$$\ell_{\alpha_{DIR.}}(x,y) = \frac{8q\alpha}{\pi\beta}\frac{1}{\sqrt{1-\tau^2}} \qquad \text{(C-5)}$$

$$\text{with} \qquad \tau = \beta y/x$$

The local induced load $\ell_{\alpha_{IND.}}$ produced when the wing tip operates in the upwash field of the canard consists of the local load due to the surface being at an apparent constant angle of attack $-\alpha\,\frac{d\epsilon}{d\alpha}(0)$ plus the sum of the loads due to a set of infinitesimal strips (see Appendix A). The local load due to a single strip at $y = \eta$ with apparent angle of attack $-\alpha\left[\frac{d\epsilon}{d\alpha}(\eta) - \frac{d\epsilon}{d\alpha}(0)\right]$ is given in Appendix D (Eq. D-7 with m = 1). The angle of attack distribution is taken from Eq. B-6A. The load due to the constant deflection plus an approximate integration of the loads due to the strips is

$$\ell_{\alpha_{IND.}}(x,y) \doteq \frac{-16q\alpha x}{\pi^2\beta\sqrt{x^2-\beta^2y^2}} + \frac{q\alpha}{\pi\beta\sqrt{\theta}}\sqrt{\frac{x+\beta y}{x-\beta y}}\left(7+\frac{\beta b_T}{x+\beta y}\right) \qquad \text{(C-6)}$$

(The exact integration yields elliptic integrals for the second term of Eq. C-6. See Eq. D-13. This approximation is exact at the most forward point of the tip panel where $x+\beta y = \beta b_T$. At the tip,

D
4
2
5

where $x + \beta y = \beta b_w$, the second term is only .3% too small for the case $S_T = 0.25$.) The local induced load ℓ_δ is given by the same equation as $\ell_{\alpha\ IND.}$, that is

$$\frac{\ell_\delta}{\delta} = \frac{\ell_{\alpha\ IND}}{\alpha} \tag{C-7}$$

Integration of these local loads over the two tip panels yields

$$A_o = 2\left(\frac{2}{\pi} + 1\right)\left(1 - \sqrt{S_T}\right)^2 \tag{C-8}$$

$$A_\alpha = A_{DIR.} + A_{IND.} \tag{C-9}$$

$$A_\delta = A_{IND.} \tag{C-10}$$

where

$$A_{DIR} = \frac{8}{\pi}\left[\cos^{-1}\sqrt{S_T} - \sqrt{S_T(1 - S_T)}\right]$$

$$A_{IND} = -\frac{16}{\pi^2}\left[\cos^{-1}\sqrt{S_T} - \sqrt{S_T(1 - S_T)}\right]$$

$$+ \frac{\sqrt{2}}{\pi}\left[\left(1.75 + \sqrt{S_T}\right)\cos^{-1}\sqrt{S_T}\right.$$

$$\left. -2.75\, S_T \ln\left(\frac{1 + \sqrt{1 - S_T}}{\sqrt{S_T}}\right) + 1.75\left(1 - \sqrt{S_T}\right)\sqrt{1 - S_T}\right]$$

For $S_T = 0.25$

$$A_o = .8183,\ A_\alpha = 1.5623,\ A_\delta = -.0019 \tag{C-11}$$

Coefficients B_1, B_2: The optimum twist $\bar{\alpha}_o$ is evaluated by setting $\frac{d}{d\bar{\alpha}_o}\left(\frac{C_{Di}}{\beta C_L^2}\right) = 0$ where $C_{Di}/\beta C_L^2$ is given by Eq. 16. (Note that $\bar{\alpha}$ and $\bar{\delta}$, through Eqs. 13, 14 and 17, are functions of $\bar{\alpha}_o$ as well as being functions of βC_{L_α}, βC_{L_δ}, $(x_o - x_\alpha)$, $(x_\delta - x_\alpha)$ and $\partial C_M / \partial C_L$.) The result can always be expressed in the form

$$(\bar{\alpha}_o)_{OPT} = B_1 + B_2 \left(\partial C_M / \partial C_L\right) \tag{18}$$

B_1 and B_2 depend on the geometry and Mach number only. For the special case $S_T = .25, /// = -1.5$ (and $\beta R = 4$, G = 0)

$$B_1 = -0.2608, \quad B_2 = 0.537 \tag{C-12}$$

D. Leading-Edge Thrust

One form of the basic equation for leading-edge thrust is (putting together several equations from Ref. 6)*

$$\Delta T = 2\pi q \int_{SPAN} \beta_n \left[\frac{\ell \sqrt{x_n}}{4q \sin\omega}\right]^2 dy \tag{D-1}$$

The bracket is evaluated along the leading edge. Close to a subsonic leading edge the local lift $\ell \sim 1/\sqrt{x_n}$ where x_n is the perpendicular distance from the leading edge to the point at which ℓ is evaluated. Thus as $x_n \to 0$, $\ell\sqrt{x_n}$ remains a finite non-zero quantity. ω is the angle between the free stream and the tangent to the leading edge. β_n is the Mach number parameter of the component of the free stream Mach number perperndicular to the leading edge, so that

$$\beta_n = \sqrt{1 - M^2 \sin^2\omega} = (\cos\omega)\sqrt{1 - \beta^2 \tan^2\omega}$$

---

* Equation D-1 is also equivalent to Eq. 14-7 plus Eq. 14-5 of Ref. 7 since the component of the perturbation velocity parallel to the leading edge is zero on the wing at the leading edge.

At a thin subsonic leading edge the component of the flow normal to the edge has a square root singularity. This same type of singularity occurs at the leading edge of a thin two-dimensional airfoil in subsonic flow. The leading-edge thrust on this two-dimensional subsonic airfoil is well known. By analogy, the suction force normal to the leading edge of the three-dimensional supersonic wing per unit length of the edge is assumed to depend upon the local pressure and normal component of the free stream velocity in the same way as the suction force normal to the leading edge of the two-dimensional subsonic airfoil depends upon the local pressure and free stream velocity. The leading-edge thrust of Eq. D-1 is the integral along the leading edge of the streamwise components of this local normal suction force.

In practice, only a part of the leading-edge thrust is achieved, and this will require some rounding of the leading edges. On the following pages, the full theoretical value of leading-edge thrust is calculated. In Figs. 3, 5, 6, 9, and 10 the drag or the $(L/D)_{MAX}$ of certain configurations is presented under the alternative assumptions of no leading-edge thrust and of the full theoretical leading-edge thrust.

The leading-edge thrust gives a negative drag increment. To find this drag increment for the flat configurations, Eq. D-1 is written in the form

$$\frac{\Delta C_{D_i}}{\beta C_L^2} = -\int_{\substack{\text{WING}\\ \text{SPAN}}} \frac{\pi \beta_n}{8\beta} \frac{b_w/2}{S_w} \left[\frac{\ell_w \sqrt{x_{n_w}}}{q C_L \sin \omega_w} \right]^2_{\substack{\text{WING}\\ \text{LEADING EDGES}}} d\frac{y}{b_w/2}$$

$$-\int_{\substack{\text{TAIL (OR CANARD)}\\ \text{SPAN}}} \frac{\pi \beta_n}{8\beta} \frac{b_T/2}{S_w} \left[\frac{\ell_T \sqrt{x_{n_T}}}{q C_L \sin \omega_T} \right]^2 d\frac{y}{b_T/2} \qquad \text{(D-2)}$$

(Here the subscript W refers to the wing, which may include a flap, and T to the tail or canard.) The superposition procedures described in Appendix A are utilized to find the local loads on the wing (or wing plus flap) and on the tail (or canard). Let $m_w = \beta \tan \omega_w$ and $m_T = \beta \tan \omega_T$. Then

$$\sqrt{\frac{\pi\beta n}{8\beta}\,\frac{b_w/2}{S_w}}\left[\frac{\ell_w\sqrt{x n_w}}{q C_L \sin\omega_w}\right]_{\substack{\text{WING}\\ \text{LEADING EDGE}}} = f_1\left(\frac{y}{b_w/2}, m_w\right)\bar{\alpha}_{\text{FLAT WING PLUS TAIL}} \tag{D-3a}$$

$$= f_1\left(\frac{y}{b_w/2}, m_w\right)\left[\bar{\alpha} - (\bar{\alpha}+\bar{\delta})\frac{d\epsilon}{d\alpha}(0, m_T)\right] + f_2\left(\frac{y}{b_w/2}; m_w, \frac{b_T}{b_w}\right)\left[\bar{\alpha}+\bar{\delta}\right]\left[\frac{d\epsilon}{d\alpha}(0, m_T)\right] \tag{D-3b}$$

FLAT WING PLUS CANARD

$$= f_1\left(\frac{y}{b_w/2}, m_w\right)\bar{\alpha} + f_F\left(\frac{y}{b_w/2}; m_w, S_T\right)\bar{\delta} \tag{D-3c}$$

FLAT WING WITH FLAP

$$\sqrt{\frac{\pi\beta n}{8\beta}\,\frac{b_T/2}{S_w}}\left[\frac{\ell_T\sqrt{x n_T}}{q C_L \sin\omega_T}\right]_{\substack{\text{TAIL}\\ \text{(OR CANARD)}\\ \text{LEADING EDGE}}} = f_1\left(\frac{y}{b_T/2}, m_T\right)\left[\bar{\alpha}+\bar{\delta} - \bar{\alpha}\frac{d\epsilon}{d\alpha}(0, m_w)\right] \tag{D-4a}$$

FLAT WING PLUS TAIL WITH $G = 0$ AND ASSUMING A FLAT VORTEX SHEET

$$= f_1\left(\frac{y}{b_T/2}, m_T\right)(\bar{\alpha}+\bar{\delta}) \tag{D-4b}$$

FLAT WING PLUS CANARD

The functions, $f_1\left(\frac{y}{b/2}, m\right)$ which is proportional to the local load near the leading edge of a flat delta, $f_2\left(\frac{y}{b_w/2}; m_w, \frac{b_T}{b_w}\right)$ which is proportional to the local leading-edge load of a certain twisted delta surface, and $f_F\left(\frac{y}{b_w/2}; m_w, S_T\right)$ which is proportional to the local load at the tip leading edges of a flat trapezoidal surface, will now be evaluated.

Local Loads: The load distribution per unit angle of attack, $\frac{d\ell}{d\alpha}$, on a flat surface of delta planform with subsonic leading edges is[4]

$$\frac{d\ell}{d\alpha} = \frac{4q m^2}{\beta E(k)\sqrt{m^2-\tau^2}} \tag{D-5}$$

where

$$\tau = \frac{\beta y}{x},\quad m = \beta\tan\omega = \frac{\beta R}{q} < 1,\quad k = \sqrt{1-m^2}$$

The load distribution per unit angle of attack on the right tip of a wing of trapezoidal planform for which the leading edge of the tip is subsonic is[4]

$$\frac{d\ell}{d\alpha} = \frac{8q}{\pi\beta}\left[\frac{m}{1+m}\sqrt{\frac{1+\tau'}{m-\tau'}} + \tan^{-1}\sqrt{\frac{m-\tau'}{1+\tau'}}\right] \tag{D-6}$$

where

$$\tau' = \frac{\beta(y - y_1)}{x - \frac{\beta y_1}{m}}$$

y_1 = spanwise location of beginning of tip

$$= \frac{b_w}{2}\sqrt{1 - S_T}$$

$m = \beta \tan \omega < 1$, with ω the angle of inclination of the side edge to the free stream direction

D 4 2 5

If a flat surface at zero angle of attack is operating in a downwash field it will carry an induced load. If the downwash varies only in the spanwise direction across the surface, this induced load is the same, within linear theory, as the load on a twisted surface with the angle of attack distribution due to twist equal to the negative of the downwash angle. The local load $d\ell(x,y)$ due to a single strip of width $d\eta$, located at the spanwise position $\eta > 0$ and with angle of attack $-\alpha_F\left[\frac{d\epsilon}{d\alpha}(\eta) - \frac{d\epsilon}{d\alpha}(0)\right]$ is *

$$d\ell(x,y) = -\frac{qq\sqrt{m}}{\pi\beta} \frac{\alpha_F\left[\frac{d\epsilon}{d\alpha}(\eta) - \frac{d\epsilon}{d\alpha}(0)\right]\tau''\, d\eta}{(y-\eta)\sqrt{(1+\tau'')(m-\tau'')}} \qquad \text{(D-7)}$$

where $m = \beta \tan \omega \leq 1$ with ω the angle of inclination of the leading edge to the free stream direction

$$\tau'' = \frac{\beta(y-\eta)}{x - \frac{\beta\eta}{m}}$$

α_F = angle of attack of forward surface

---

* This solution is found by superimposing two solutions of the type given, for example, in Ref. 4 , page 164, flow field 24.

If $\eta > \frac{1-m}{1+m}\frac{b_w}{2}$, Eq. D-7 is valid anywhere on the delta surface within the Mach cone from the leading edge of the strip.

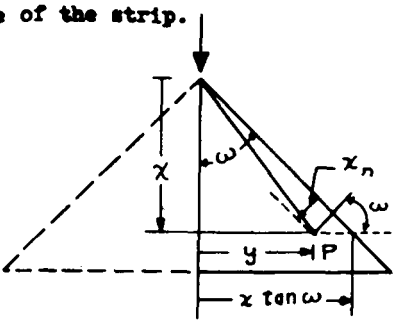

Local loads near a leading edge:

Consider the point P (see sketch) on a ray near the right leading edge of the wing (or tail or canard). Introduce the coordinate x_n measured perpendicularly from the leading edge to P. Then

$$x_n = (x \tan\omega - y)\cos\omega$$

or
$$x = \frac{\beta y}{m}\left(1 + \frac{x_n}{y\cos\omega}\right) \qquad \text{(D-8)}$$

If $x_n << y\cos\omega$, and one neglects $x_n/y\cos\omega$ compared to 1, then

$$m - \tau \doteq m\frac{x_n}{y\cos\omega} \qquad \text{(D-9a)}$$

$$m - \tau' \doteq \frac{m}{(1-y_1/y)}\frac{x_n}{y\cos\omega} \qquad \text{(D-9b)}$$

$$m - \tau'' \doteq \frac{m}{(1-\eta/y)}\frac{x_n}{y\cos\omega} \qquad \text{(D-9c)}$$

Along the right leading edge, the local load per unit angle of attack of Eq. D-5 then becomes

$$\left(\frac{dl}{d\alpha}\right)_{l.e.} = \frac{4qm}{\sqrt{2}\,\beta E(k)\sqrt{\frac{x_n}{y\cos\omega}}} \qquad \text{(D-10)}$$

and of Eq. D-6, becomes

$$\frac{dl}{d\alpha} = \frac{8q}{\pi\beta}\left[\sqrt{\frac{m}{1+m}}\,\frac{\sqrt{1-\frac{y_1}{y}}}{\sqrt{\frac{x_n}{y\cos\omega}}}\right] \qquad \text{(D-11)}$$

The local load along the right leading edge, due to a single strip at angle of attack $-\alpha_F\left[\frac{d\epsilon}{d\alpha}(\eta) - \frac{d\epsilon}{d\alpha}(0)\right]$ becomes

$$d\ell = \frac{-4qm\alpha_F}{\beta\pi\sqrt{1+m}} \frac{\left[\frac{d\epsilon}{d\alpha}(\eta) - \frac{d\epsilon}{d\alpha}(0)\right] d\frac{\eta}{y}}{\sqrt{1-\frac{\eta}{y}}\sqrt{\frac{x_n}{y\cos\omega}}} \qquad \text{(D-12)}$$

If the vortex sheet is assumed flat, then in the plane of the vortex sheet (i.e., for G = 0) $\frac{d\epsilon}{d\alpha}(\eta) - \frac{d\epsilon}{d\alpha}(0)$ is given by Eq. B-6a: Over all the tail, in Config. 1-a, $\frac{d\epsilon}{d\alpha}(\eta) - \frac{d\epsilon}{d\alpha}(0) = 0$. On the wing of Config. 2-a, $\frac{d\epsilon}{d\alpha}(\eta) - \frac{d\epsilon}{d\alpha}(0)$ is zero for $\eta < b_T/2$, but is $-\frac{d\epsilon}{d\alpha}(0)\,\eta/\sqrt{\eta^2 - (b_T/2)^2}$ for $\eta > b_T/2$. (Then the strip theory applied to this distribution of twist is exact for $\frac{b_T}{b_w} \geq \frac{1-m}{1+m}$.) Summing up all the strips which affect the load at x, y:

$$\ell(x,y) = \frac{4qm(\alpha+\delta)}{\beta\pi\sqrt{1+m}} \frac{d\epsilon}{d\alpha}(0,m_T) \sqrt{\frac{y\cos\omega}{x_n}}\, \mathcal{J} \qquad \text{(D-13)}$$

where

$$\mathcal{J} = \int_{\frac{b_T/2}{y}}^{1} \frac{\left(\frac{\eta}{y}\right) d\left(\frac{\eta}{y}\right)}{\sqrt{1-\frac{\eta}{y}}\sqrt{\left(\frac{\eta}{y}\right)^2 - \left(\frac{b_T/2}{y}\right)^2}}$$

$$= 2\sqrt{1+\frac{b_T/2}{y}}\, E\left(\sqrt{\frac{1-\frac{b_T/2}{y}}{1+\frac{b_T/2}{y}}}\right) - \frac{2\frac{b_T/2}{y}}{\sqrt{1+\frac{b_T/2}{y}}}\, K\left(\sqrt{\frac{1-\frac{b_T/2}{y}}{1+\frac{b_T/2}{y}}}\right)$$

$$\doteq \frac{\pi}{8\sqrt{2}}\left(7 + \frac{b_T/2}{y}\right)$$

with K and E elliptic integrals of the first and second kinds respectively, each with modulus $\sqrt{\left(1-\frac{b_T/2}{y}\right)/\left(1+\frac{b_T/2}{y}\right)}$. The approximation to the elliptic integrals is exact for $y = b_T/2$, and is only 3% too small when $y = 2(b_T/2)$.

The load functions in Eqs. D-3,4 can now be written out explicitly, using Eqs. D-10, -11, -13.

$$f_1\left(\frac{y}{b/2}; m\right) = \frac{b/b_w}{E(k)}\sqrt{\pi m k}\,\sqrt{\frac{y}{b/2}} \qquad \text{(D-14)}$$

with $k = \sqrt{1-m^2}$, $m = m_w$ or m_T and $b = b_w$ or b_T

$$f_2\left(\frac{y}{b_w/2}\,;\, m_w, \frac{b_T}{b_w}\right) \doteq \frac{\sqrt{\pi}}{8}\sqrt{\frac{m_w k_w}{1+m_w}}\left[7\sqrt{\frac{y}{b_w/2}} + \frac{b_T}{b_w}\sqrt{\frac{b_w/2}{y}}\right] \qquad \text{(D-15)}$$

with $k_w = \sqrt{1-m_w^2}$

$$f_F\left(\frac{y}{b_w/2}\,;\, m_w, s_T\right) = \sqrt{\frac{8k_w}{\pi(1+m_w)}}\sqrt{\frac{y}{b_w/2} - \sqrt{1-s_T}} \qquad \text{(D-16)}$$

Final results: The spanwise integrations of Eq. D-2 may now be carried out, using the leading-edge load functions of Eqs. D-14, -15, -16. Note that the drag is proportional to the squares of the loads so that interference terms occur. The final results are given below.

Config. 1-a (flat wing plus tail) with G = 0 and assuming a flat vortex sheet:

$$\left(\frac{\Delta C_{D_i}}{\beta C_L^2}\right)_{WING} = -\bar{\alpha}^2\, I_1\,(m_w) \qquad \text{(D-17a)}$$

$$\left(\frac{\Delta C_{D_i}}{\beta C_L^2}\right)_{TAIL} = -s_T\left[\bar{\alpha} + \bar{\delta} - \bar{\alpha}\frac{d\epsilon}{d\alpha}(0,m_w)\right]^2 I_1\,(m_T) \qquad \text{(D-17b)}$$

Config. 2-a (flat wing plus canard) with G = 0 and assuming a flat vortex sheet:

$$\left(\frac{\Delta C_{D_i}}{\beta C_L^2}\right)_{WING} = -\left[\bar{\alpha} - (\bar{\alpha}+\bar{\delta})\frac{d\epsilon}{d\alpha}(0,m_T)\right]^2 I_1(m_w) - \left[(\bar{\alpha}+\bar{\delta})\frac{d\epsilon}{d\alpha}(0,m_T)\right]^2 I_2\left(m_w, \frac{b_T}{b_w}\right) \qquad \text{(D-18a)}$$

$$- \left[\bar{\alpha} - (\bar{\alpha}+\bar{\delta})\frac{d\epsilon}{d\alpha}(0,m_T)\right]\left[(\bar{\alpha}+\bar{\delta})\frac{d\epsilon}{d\alpha}(0,m_T)\right] I_{12}\left(m_w, \frac{b_T}{b_w}\right)$$

$$\left(\frac{\Delta C_{D_i}}{\beta C_L^2}\right)_{CANARD} = -s_T\,(\bar{\alpha}+\bar{\delta})^2\, I_1\,(m_T) \qquad \text{(D-18b)}$$

where $\frac{d\epsilon}{d\alpha}(0,m) = \frac{1}{E(k)}$ with $E(k)$ an elliptic integral of the second kind with modulus $k = \sqrt{1-m^2}$. $m = m_w$ or m_T.

Config. 3-a (flat wing with flap):

$$\left(\frac{\Delta C_{Di}}{\Delta C_L^2}\right)_{\text{WING + FLAP}} = -\bar{\alpha}^2 I_1(m_w) - \bar{\delta}^2 I_F(m_w, s_T) - \bar{\alpha}\bar{\delta} I_{1F}(m_w, s_T) \qquad \text{(D-19)}$$

$\bar{\alpha}$ and $\bar{\delta}$, if the configuration is in trim, are given as functions of the static margin by Eqs. 13 and 14. The integrals of Eqs. D-17, -18, -19 are

$$I_1(m) = 2\int_0^1 \left[f_1\left(\frac{y}{b/2}; m\right)\right]^2 d\left(\frac{y}{b/2}\right) = \frac{\pi m\sqrt{1-m^2}}{\left[E\left(\sqrt{1-m^2}\right)\right]^2} \qquad \text{(D-20a)}$$

with $m = m_w$ or m_T and $b = b_w$ or b_T

$$I_2\left(m_w, \frac{b_T}{b_w}\right) = 2\int_{b_T/b_w}^1 \left[f_2\left(\frac{y}{b_w/2}; m_w, \frac{b_T}{b_w}\right)\right]^2 d\left(\frac{y}{b_w/2}\right)$$

$$\doteq \frac{\pi}{32}\frac{m_w}{1+m_w}\sqrt{1-m_w^2}\left[\frac{49}{2} + 14\left(\frac{b_T}{b_w}\right) - \frac{77}{2}\left(\frac{b_T}{b_w}\right)^2 + \left(\frac{b_T}{b_w}\right)^2 \ln\frac{b_w}{b_T}\right] \qquad \text{(D-20b)}$$

$$I_{12}\left(m_w, \frac{b_T}{b_w}\right) = 4\int_{b_T/b_w}^1 \left[f_1\left(\frac{y}{b_w/2}; m_w\right)\right]\left[f_2\left(\frac{y}{b_w/2}; m_w, \frac{b_T}{b_w}\right)\right] d\left(\frac{y}{b_w/2}\right)$$

$$\doteq \frac{\pi}{2}\frac{m_w\sqrt{1-m_w}}{E\left(\sqrt{1-m_w^2}\right)}\left[\frac{7}{2} + \frac{b_T}{b_w} - \frac{9}{2}\left(\frac{b_T}{b_w}\right)^2\right] \qquad \text{(D-20c)}$$

$$I_F(m_w, s_T) = 2\int_{\sqrt{1-s_T}}^1 \left[f_F\left(\frac{y}{b_w/2}; m_w, s_T\right)^2 d\left(\frac{y}{b_w/2}\right)\right.$$

$$\doteq \frac{8}{\pi}\sqrt{\frac{1-m}{1+m}}\left(1-\sqrt{1-s_T}\right)^2 \qquad \text{(D-20d)}$$

$$I_{1F}(m_w, s_T) = 4\int_{\sqrt{1-s_T}}^1 \left[f_1\left(\frac{y}{b_w/2}, m_w\right)\right]\left[f_F\left(\frac{y}{b_w/2}; m_w, s_T\right)\right] d\left(\frac{y}{b_w/2}\right)$$

$$\doteq \frac{2\sqrt{2m(1-m)}}{E\left(\sqrt{1-m^2}\right)}\left[\left(1+\frac{c_2}{c}\right)\sqrt{\frac{c_2}{c}} - \frac{\left(1-\frac{c_2}{c}\right)^2}{2}\ln\left|\frac{2\sqrt{\frac{c_2}{c}} + \left(1+\frac{c_2}{c}\right)}{1-\frac{c_2}{c}}\right|\right] \qquad \text{(D-20e)}$$

with $\frac{c_2}{c} = 1-\sqrt{1-s_T}$

Note that the ratio of maximum tail (or canard) span b_T to the maximum wing span is proportional to the square root of the ratio s_T of the trim surface area to the wing area:

$$\frac{b_T}{b_w} = \sqrt{s_T}\sqrt{\frac{m_T}{m_w}} \qquad \text{wing plus tail (or canard)} \qquad \text{(D-21)}$$

If the wing and tail (or canard) have the same planform, as is the case for all the numerical calculations of this report, then $b_T/b_w = \sqrt{s_T}$.

Douglas Aircraft Company, Inc.,
Santa Monica, Calif., July 1959.

VII. REFERENCES

1. Graham, M. E. "Some Linearized Computations of Supersonic Wing-Tail Interference." Douglas Aircraft Company, Inc., Report No. SM-13430, December 1948.

2. Graham, M. E. "Drag due to Lift at Supersonic Speeds of a Delta Wing-Tail Combination." Douglas Aircraft Company, Inc., Report No. SM-13601, September 1949.

3. Germain, Paul. "Sur le Minimum de Traînée d'une Aile de Forme en Plan Donnée." Comptes Rendus des Séances de l'Académie des Sciences, Vol. 244, pp. 1135-1138, February 1957.

4. Donovan, A. F. and Lawrence, H. R., Editors. Aerodynamic Components of Aircraft at High Speeds. Volume VII, Princeton Series on High Speed Aerodynamics and Jet Propulsion, 1957.

5. Lagerstrom, P. A., and Graham, M. E. "Aerodynamic Interference in Supersonic Missiles." Douglas Aircraft Company, Inc., Report No. SM-13743, April 1950.

6. Puckett, A. E. and Stewart, H. J., "Aerodynamic Performance of Delta Wings at Supersonic Speeds." Journal of the Aeronautical Sciences, Vol. 14, pp. 567-578, October 1947.

7. Sears, W. R., Editor. General Theory of High Speed Aerodynamics. Volume VI, Princeton Series on High Speed Aerodynamics and Jet Propulsion, 1954.

VIII. FIGURES

1. Plan view and side view of configurations.

   a. Wing plus tail - Config. 1-a
   b. Wing plus canard - Config. 2-a
   c. Flat wing with twisted tip panels plus flat canard - Config. 2-c
   d. Wing alone with full-span trailing-edge flap - Config. 3-a

2. Drag due to lift of trimmed wing plus tail and trimmed wing plus canard as function of static margin and aspect ratio.

   a. $G = 0$, $|\ell| = 1.5$, $\beta AR < 4$
   b. $G = 0$, $|\ell| = 1.5$, $\beta AR \geq 4$
   c. $G = 0$, $|\ell| = 3.0$, $\beta AR < 4$
   d. $G = 0$, $|\ell| = 3.0$, $\beta AR \geq 4$
   e. $G = 0.5$, $|\ell| = 1.5$, $1.5 \leq \beta AR \leq 8$
   f. $G = 0.5$, $|\ell| = 3.0$, $1.5 \leq \beta AR \leq 8$
   g. $G = \infty$, $|\ell| = 1.5, 3.0$, $\beta AR \geq 4$

3. Drag due to lift of trimmed wing plus tail and trimmed wing plus canard as function of static margin. Assumes flat vortex sheet.

   a. Effect of leading-edge thrust and of twisting wing tip panels, $|\ell| = 1.5$
   b. Effect of leading-edge thrust, $|\ell| = 3.0$

4. Drag due to lift of trimmed wing alone as function of static margin and aspect ratio.

5. Drag due to lift of flat wing with flap in trim as function of static margin. Effect of leading-edge thrust.

   a. $\beta AR = 1.5$
   b. $\beta AR = 3.5$

6. Drag due to lift of trimmed wing alone as function of aspect ratio. Effect of leading-edge thrust.

   a. $\partial C_M / \partial C_L = 0$
   b. $\partial C_M / \partial C_L = -0.25$

7. Drag due to lift of trimmed configurations with no interference between wing and trim surface. Comparison of wing plus tail (or canard), wing with flap (wing includes flap) and wing plus flap (wing excludes flap).

8. Maximum lift to drag ratio of trimmed zero-thickness wing plus tail and wing plus canard as function of static margin and aspect ratio.

   a. $G = 0$, $|\ell| = 1.5$
   b. $G = 0$, $|\ell| = 3.0$
   c. $G = 0.5$, $|\ell| = 1.5$
   d. $G = 0.5$, $|\ell| = 3.0$
   e. $G = \infty$, $|\ell| = 1.5, 3.0$

9. Maximum lift to drag ratio of trimmed zero-thickness wing plus tail and wing plus canard as function of static margin. Effect of leading-edge thrust. Assumes flat vortex sheet.

   a. $|\ell| = 1.5$
   b. $|\ell| = 3.0$

10. Maximum lift to drag ratio of trimmed zero-thickness wing alone as function of static margin and aspect ratio.

11. Maximum lift to drag ratio of trimmed zero-thickness configurations with sonic leading edges ($\beta AR = 4$). Comparison of various wing-plus-tail, wing-plus-canard, and wing-alone configurations.

12. Maximum lift to drag ratio of trimmed zero-thickness configurations with sonic leading edges ($\beta AR = 4$). Effect of changing trim-surface area.

    a. Flat wing plus flat tail, G = 0
    b. Flat wing plus flat canard, G = 0
    c. Flat wing plus flat tail (or canard) G = ∞, and flat wing with flap.
    d. Flat configurations, trim area optimum.

13. Average value of downwash produced by forward surface on rear surface as function of aspect ratio and gap.

FIGURE 1. PLAN VIEW AND SIDE VIEW OF CONFIGURATIONS.

a. WING PLUS TAIL — Config. 1-a

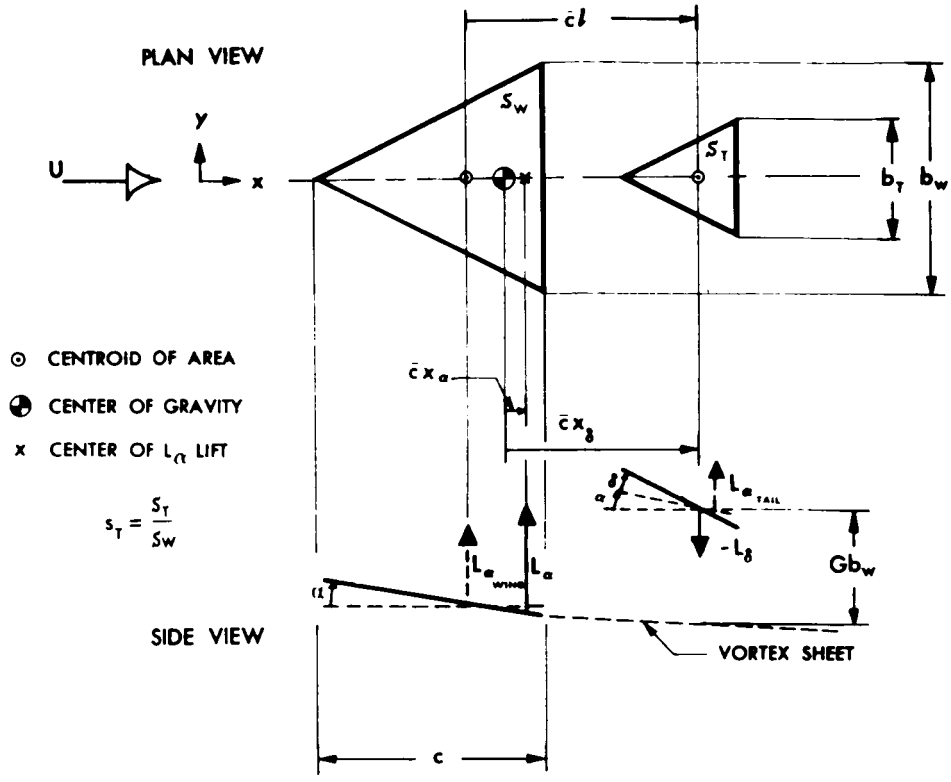

$\bar{c}$ = MEAN AERODYNAMIC CHORD (2/3 c)

GEOMETRIC VALUES SHOWN IN THIS SKETCH ARE AS FOLLOWS:

$l = 1.5$

$s_T = 1/4$

$AR_T = AR_w = 2$

$G = 0.5$

FIGURE 1. CONTINUED

b. WING PLUS CANARD — Config. 2-a

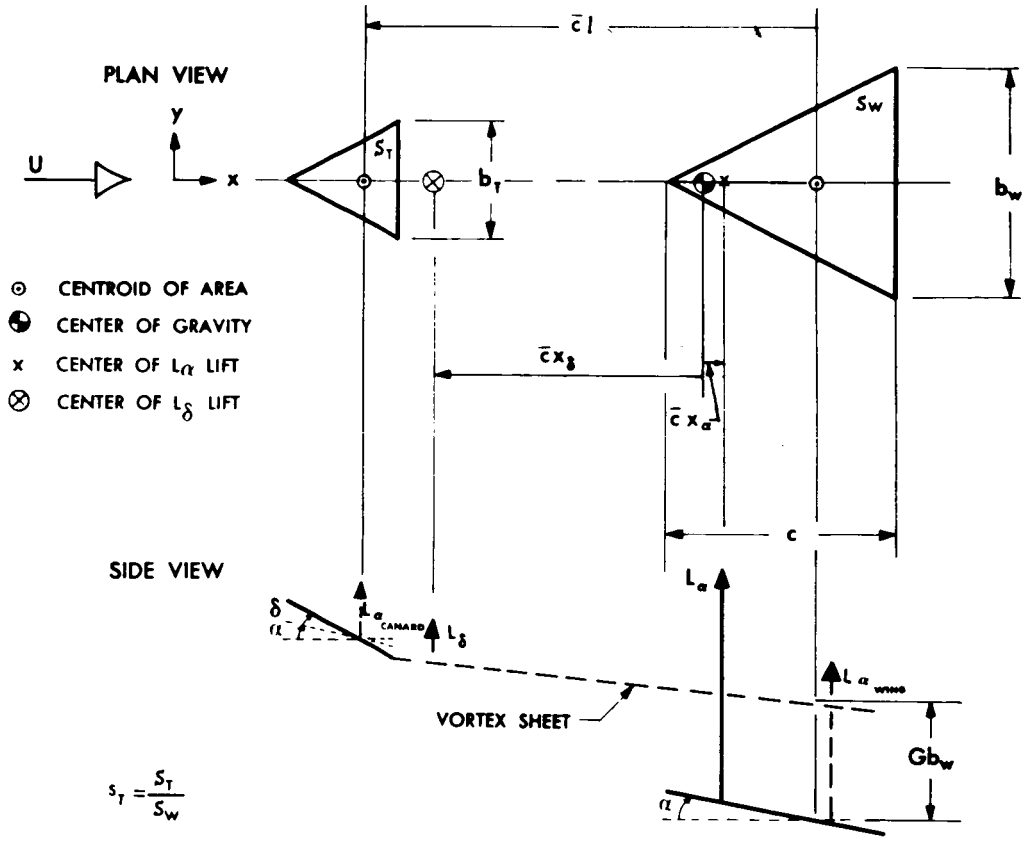

$\bar{c}$ = MEAN AERODYNAMIC CHORD (2/3 c)

GEOMETRIC VALUES SHOWN IN THIS SKETCH ARE AS FOLLOWS:

l = -3.0
s_1 = 1/4
$AR_T = AR_W = 2$
G = 0.5

FIGURE 1. CONTINUED

c. FLAT WING WITH TWISTED TIP PANELS PLUS FLAT CANARD — Config. 2-c

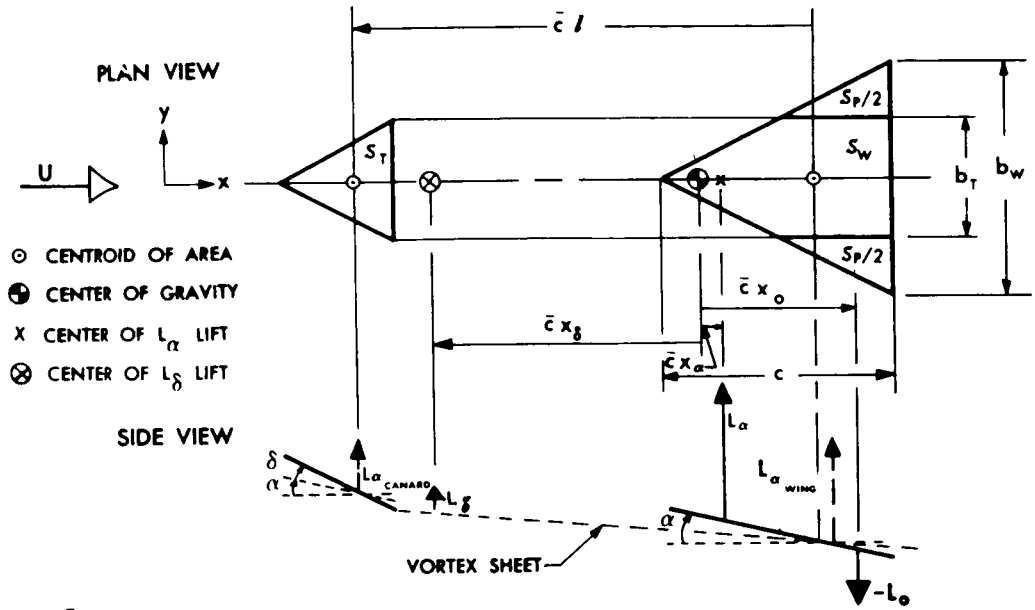

$s_T = \frac{S_T}{S_W}$

$s_P = \frac{S_P}{S_W}$

NOTE:
S_W = AREA ENTIRE WING
$\bar{c}$ = MEAN AERODYNAMICS CHORD (2/3 c)
THE TIP PANELS ARE AT A UNIFORM ANGLE OF ATTACK α_o

GEOMETRIC VALUES SHOWN IN THIS SKETCH ARE AS FOLLOWS:

$$l = -3.0$$

$$s_T = s_P = 1/4$$

$$AR_T = AR_W = 2$$

$$G = 0$$

FIGURE 1. CONCLUDED

d. WING ALONE WITH FULL-SPAN TRAILING-EDGE FLAP — Config. 3-a

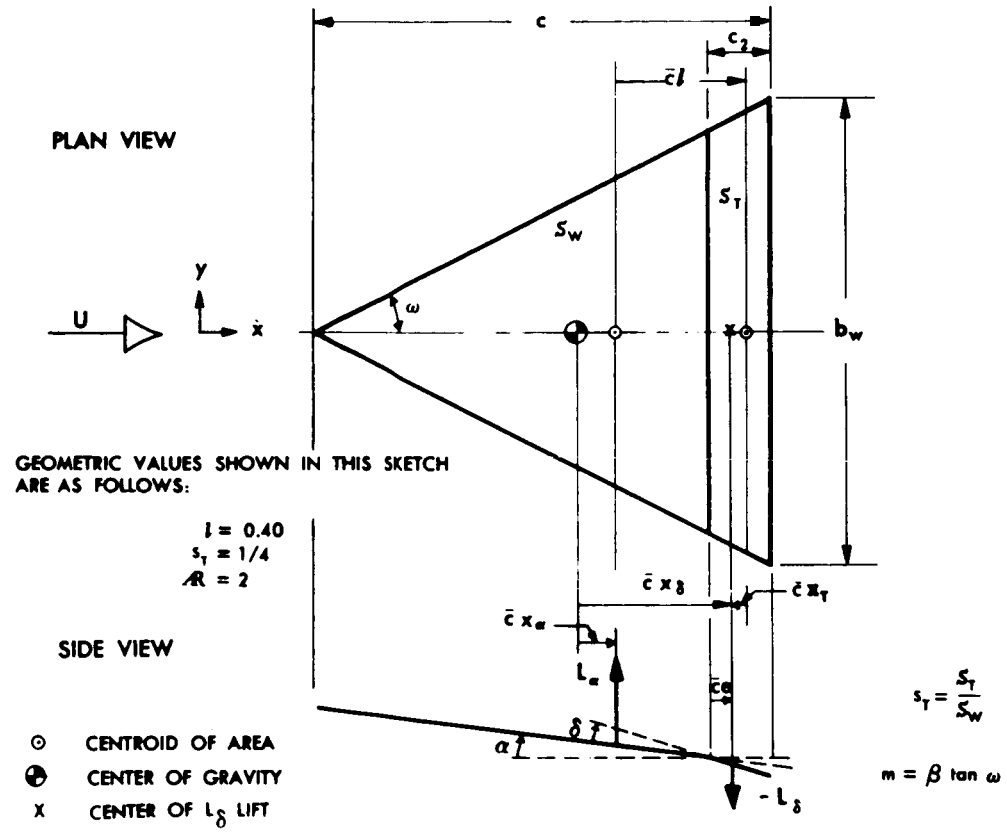

NOTE:
POSITIONS OF CENTER OF LIFT ON FLAP AND CENTROID OF AREA OF FLAP ARE EXAGGERATED

$\bar{c}\,x_T$, DISTANCE FROM CENTROID OF AREA OF FLAP TO L_δ IS EXAGGERATED

$x_T \doteq 0$ $m < 1$ (SUBSONIC LEADING EDGES)

$x_T = 0$ $m \geq 1$ (SONIC OR SUPERSONIC LEADING EDGES)

S_W IS AREA OF ENTIRE WING WITH FLAP

FIGURE 2. DRAG DUE TO LIFT OF TRIMMED WING PLUS TAIL AND TRIMMED WING PLUS CANARD AS FUNCTION OF STATIC MARGIN AND ASPECT RATIO.

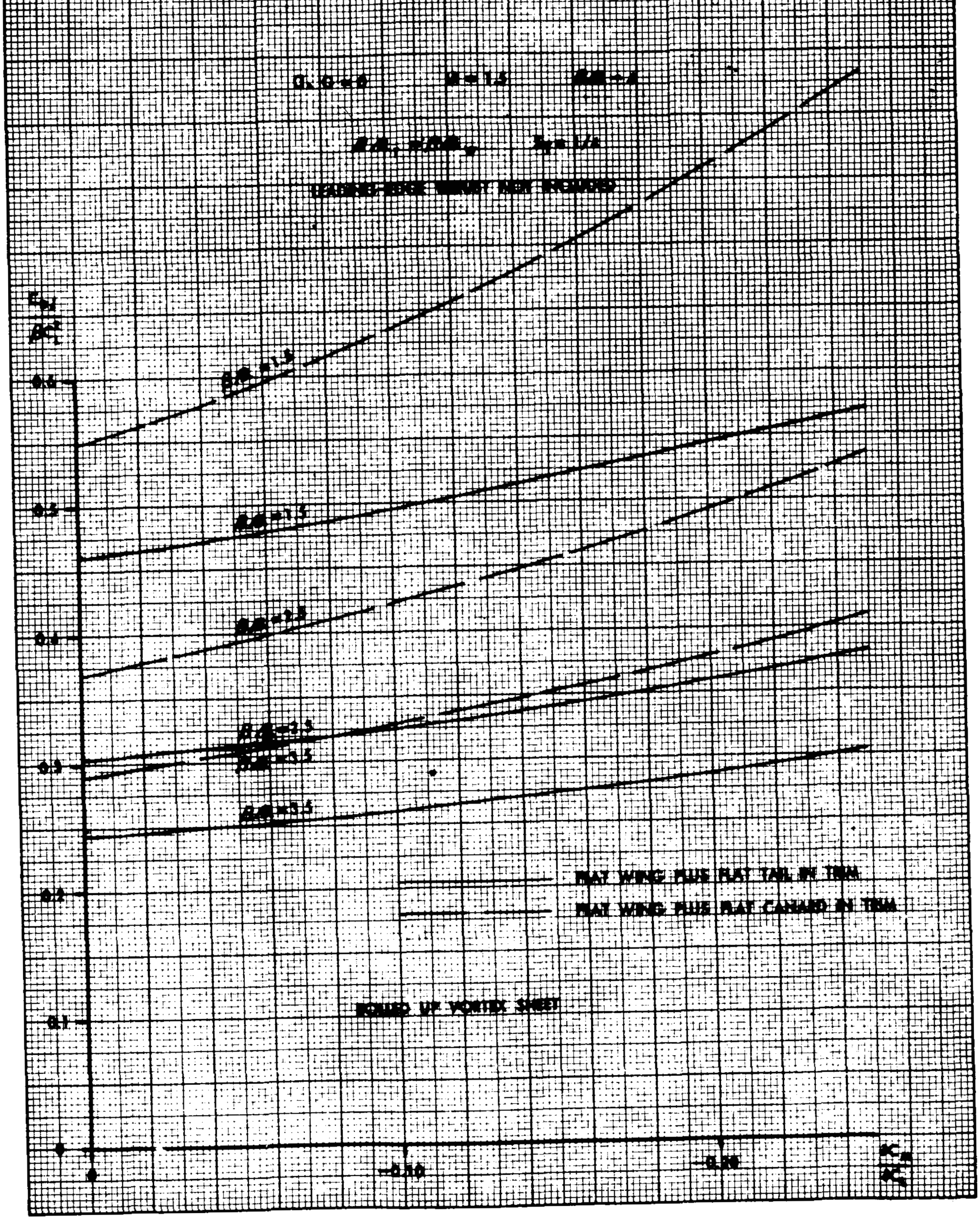

D-425

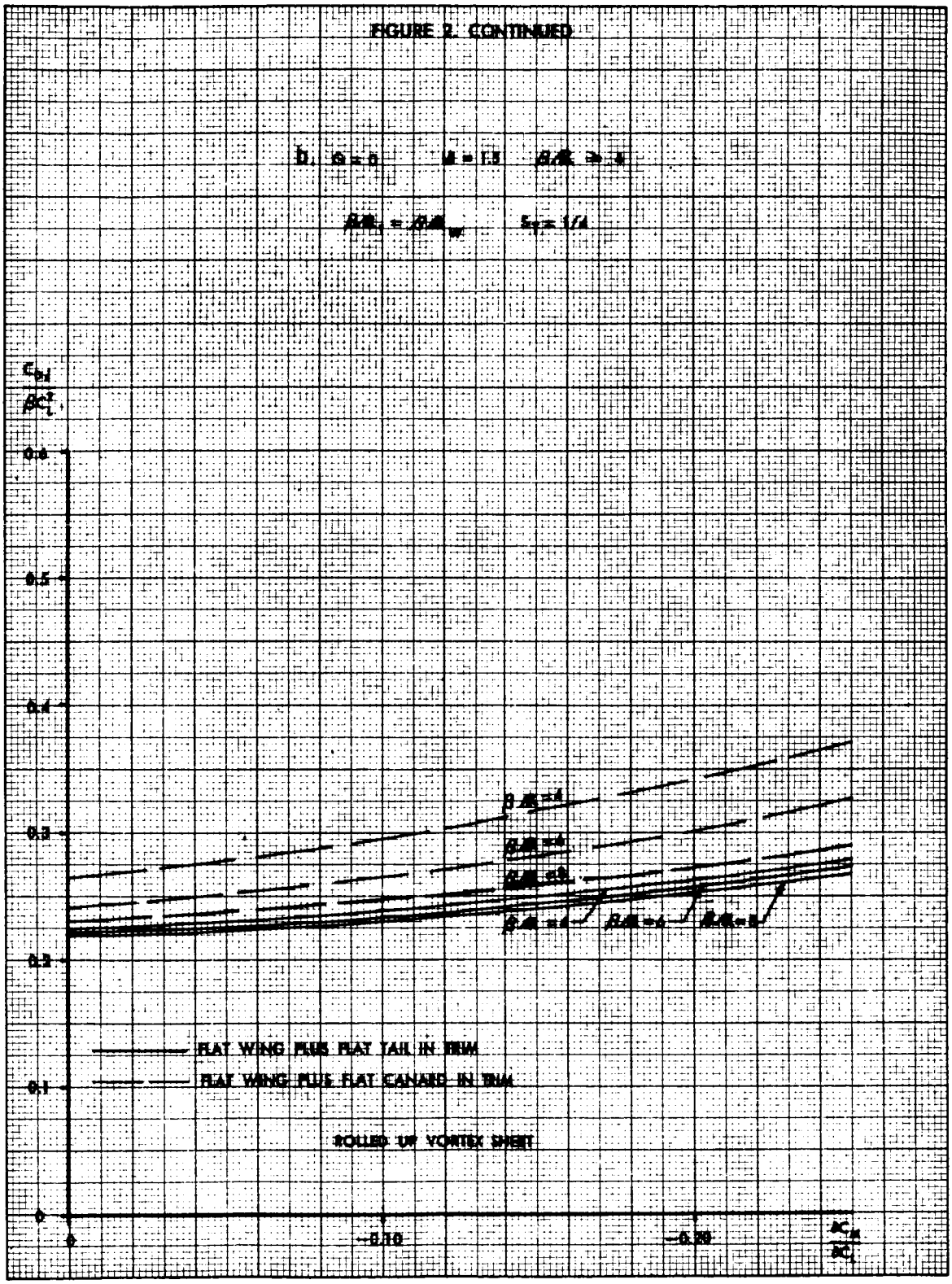
FIGURE 2. CONTINUED
b. $\Phi = 0$ $M = 1.5$ $\beta A R = 4$
$\beta A R_t = \beta A R_w$ $\lambda_t = 1/4$
$\frac{C_{Bl}}{\beta C_L^2}$
0.6
0.5
0.4
0.3
0.2
0.1
0
$\beta A R = 4$
$\beta A R = 3$
$\beta A R = 2$
$\beta A R = 1$
$\beta A R = 4$
$\beta A R = 3$
$\beta A R = 2$
FLAT WING PLUS FLAT TAIL IN TRIM
FLAT WING PLUS FLAT CANARD IN TRIM
ROLLED UP VORTEX SHEET
0
-0.10
-0.20
$\frac{\Delta C_m}{\Delta C_L}$

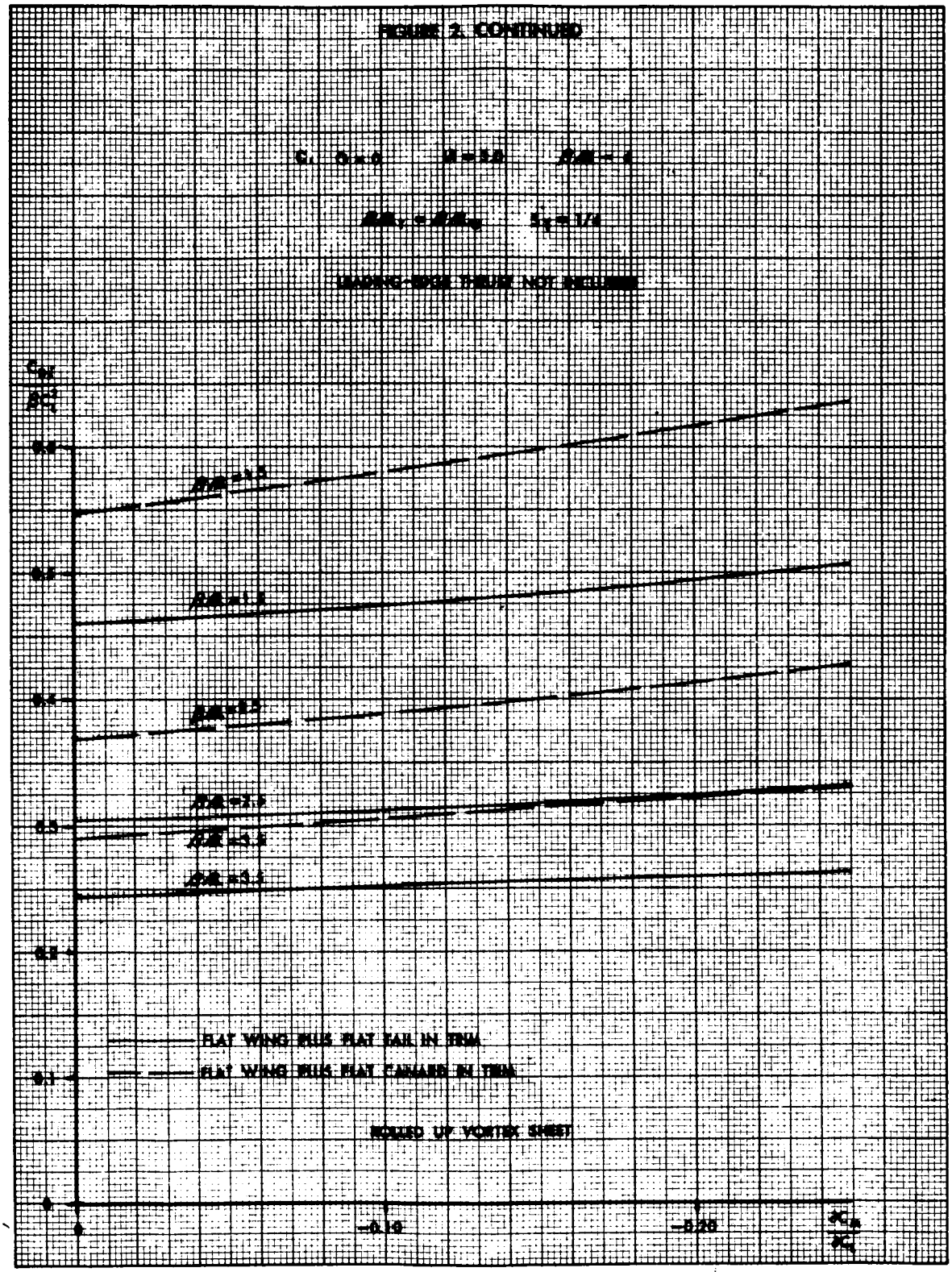
FIGURE 2. CONTINUED
C_L 0 x 0 M = 3.0 $\Delta\alpha_c$ = 4
$\Delta\alpha_{c_V} = \Delta\alpha_{c_H}$ $S_E = 1/4$
LEADING-EDGE THRUST NOT INCLUDED
$\frac{C_{m_{cg}}}{\beta C_L}$
$\Delta\alpha_c$=5.5
$\Delta\alpha_c$=4.5
$\Delta\alpha_c$=3.5
$\Delta\alpha_c$=2.5
$\Delta\alpha_c$=1.5
$\Delta\alpha_c$=0.5
0.4
0.3
0.2
0.1
0
-0.10
-0.20
$\frac{x_{cg}}{x_t}$
FLAT WING PLUS FLAT TAIL IN TRIM
FLAT WING PLUS FLAT CANARD IN TRIM
ROLLED UP VORTEX SHEET

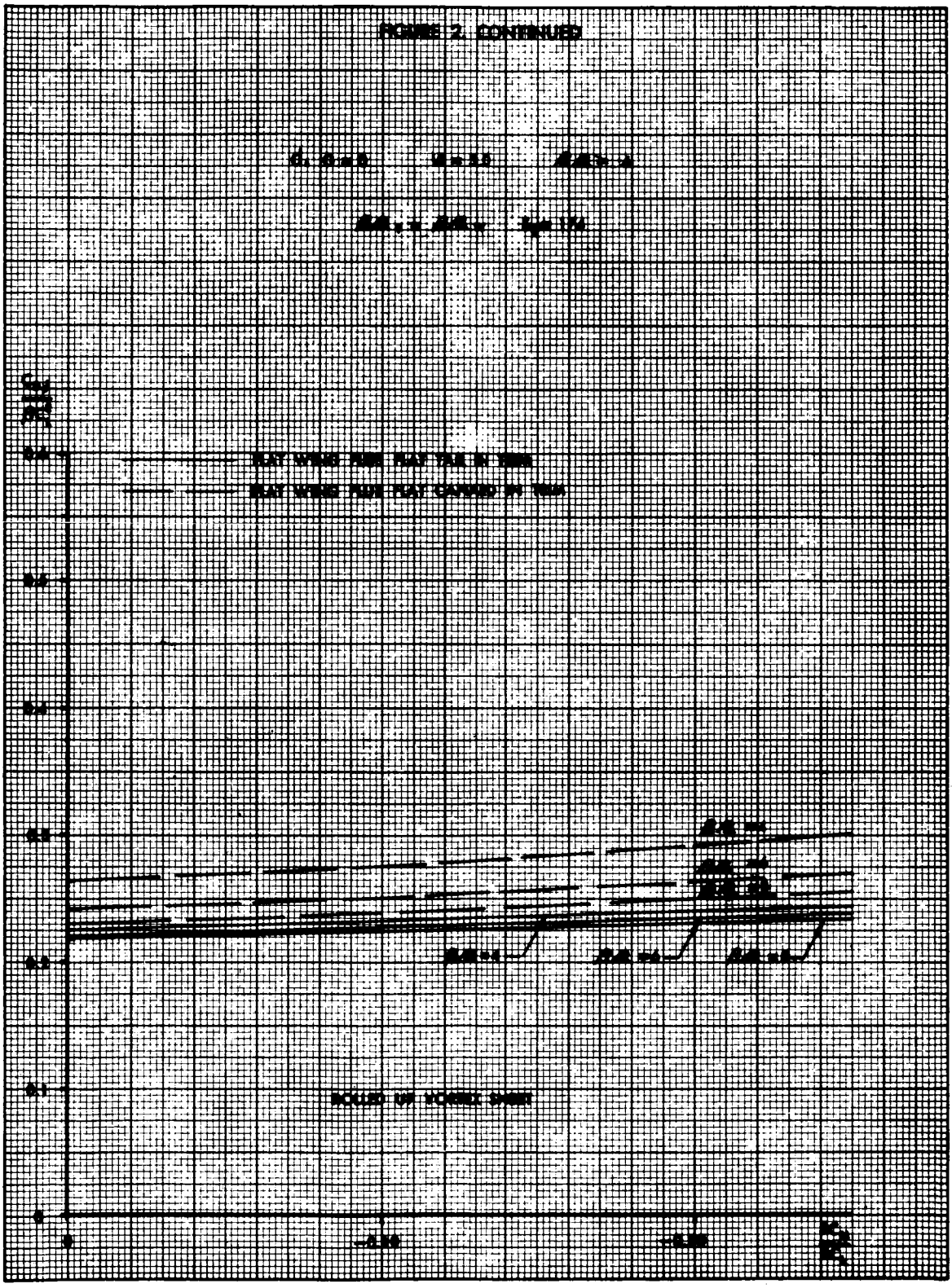
FIGURE 2. CONTINUED
FLAT WING FOR FLAT TAIL IN TRIM
FLAT WING FOR FLAT CAMBER IN TRIM
ROLLED UP VORTEX SHEET

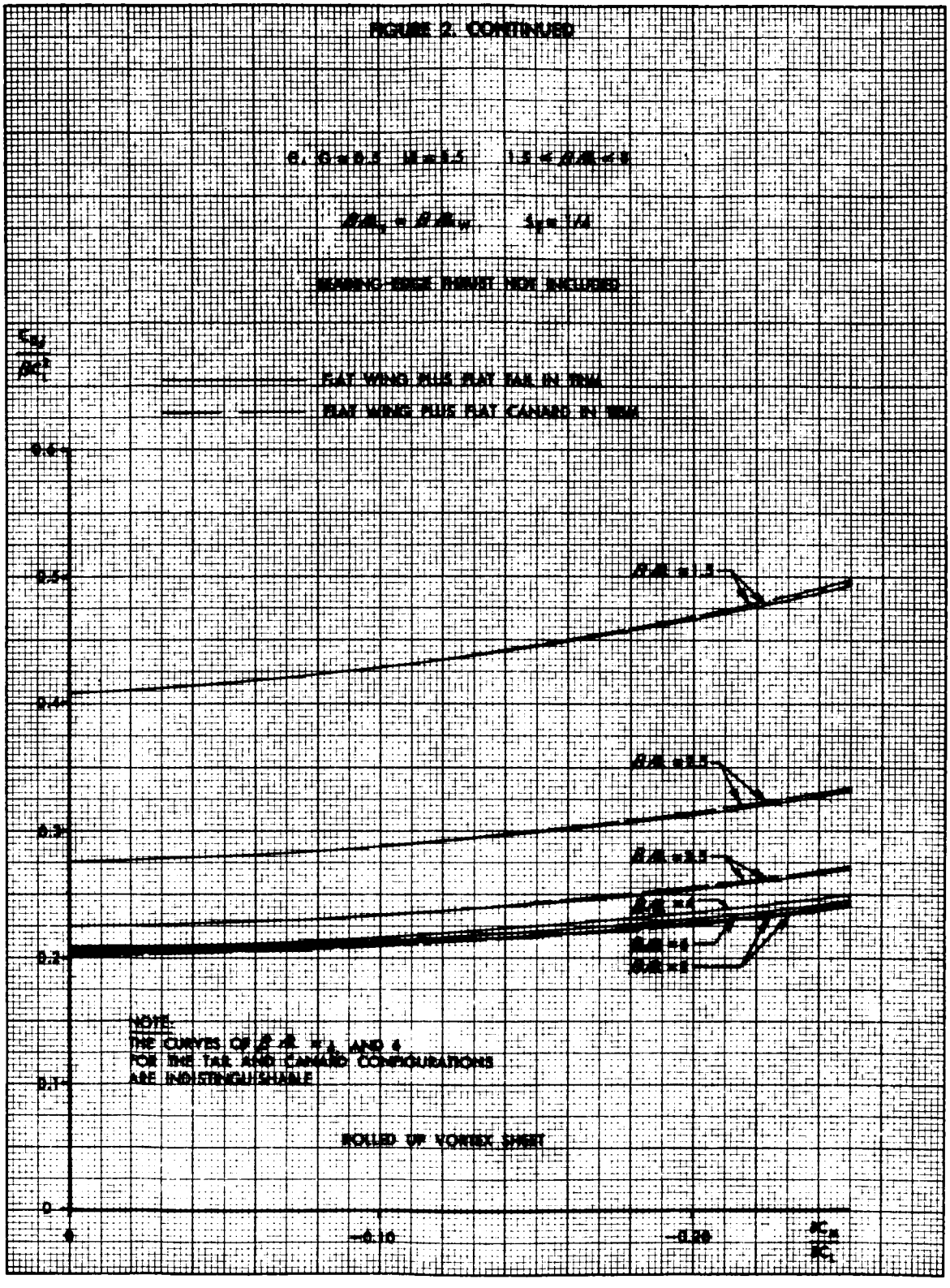
FIGURE 2. CONTINUED
FLAT WING PLUS FLAT TAIL IN WAKE
FLAT WING PLUS FLAT CANARD IN WAKE
NOTE:
THE CURVES OF
FOR THE TAIL AND CANARD CONFIGURATIONS
ARE INDISTINGUISHABLE
ROLLED UP VORTEX SHEET
0.4
0.3
0.2
0.1
0
-0.10
-0.20

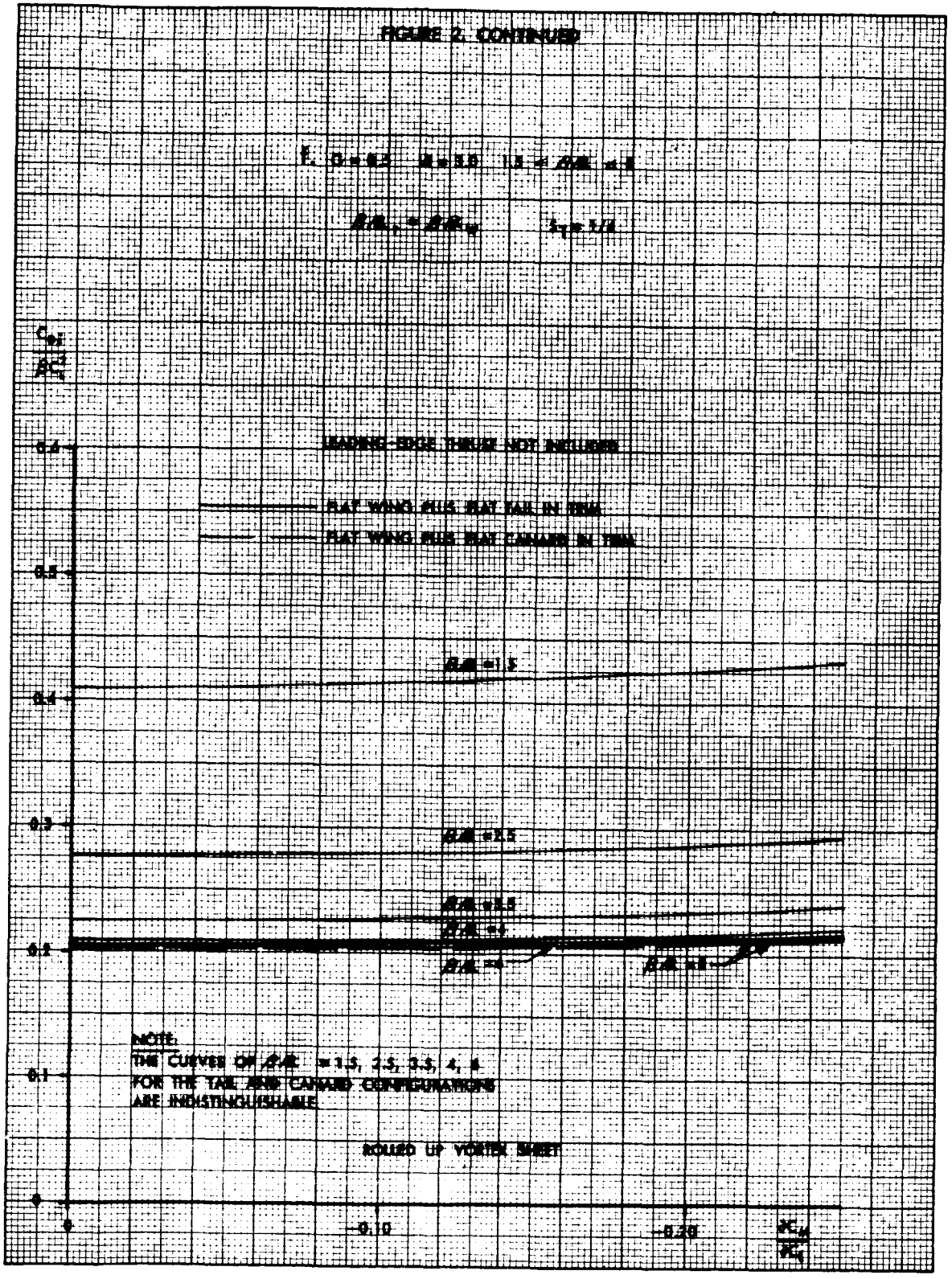
FIGURE 2. CONTINUED
$C_{D_i}/\beta C_L^2$
LEADING-EDGE THRUST NOT INCLUDED
FLAT WING PLUS FLAT TAIL IN TRIM
FLAT WING PLUS FLAT CANARD IN TRIM
$\beta/AR = 1.5$
$\beta/AR = 2.5$
$\beta/AR = 3.5$
$\beta/AR = 4$
$\beta/AR = 6$
$\beta/AR = 8$
0.6
0.5
0.4
0.3
0.2
0.1
0
NOTE:
THE CURVES OF β/AR = 1.5, 2.5, 3.5, 4, 6
FOR THE TAIL AND CANARD CONFIGURATIONS
ARE INDISTINGUISHABLE.
ROLLED UP VORTEX SHEET
0
-0.10
-0.20
$\Delta C_M / C_L$

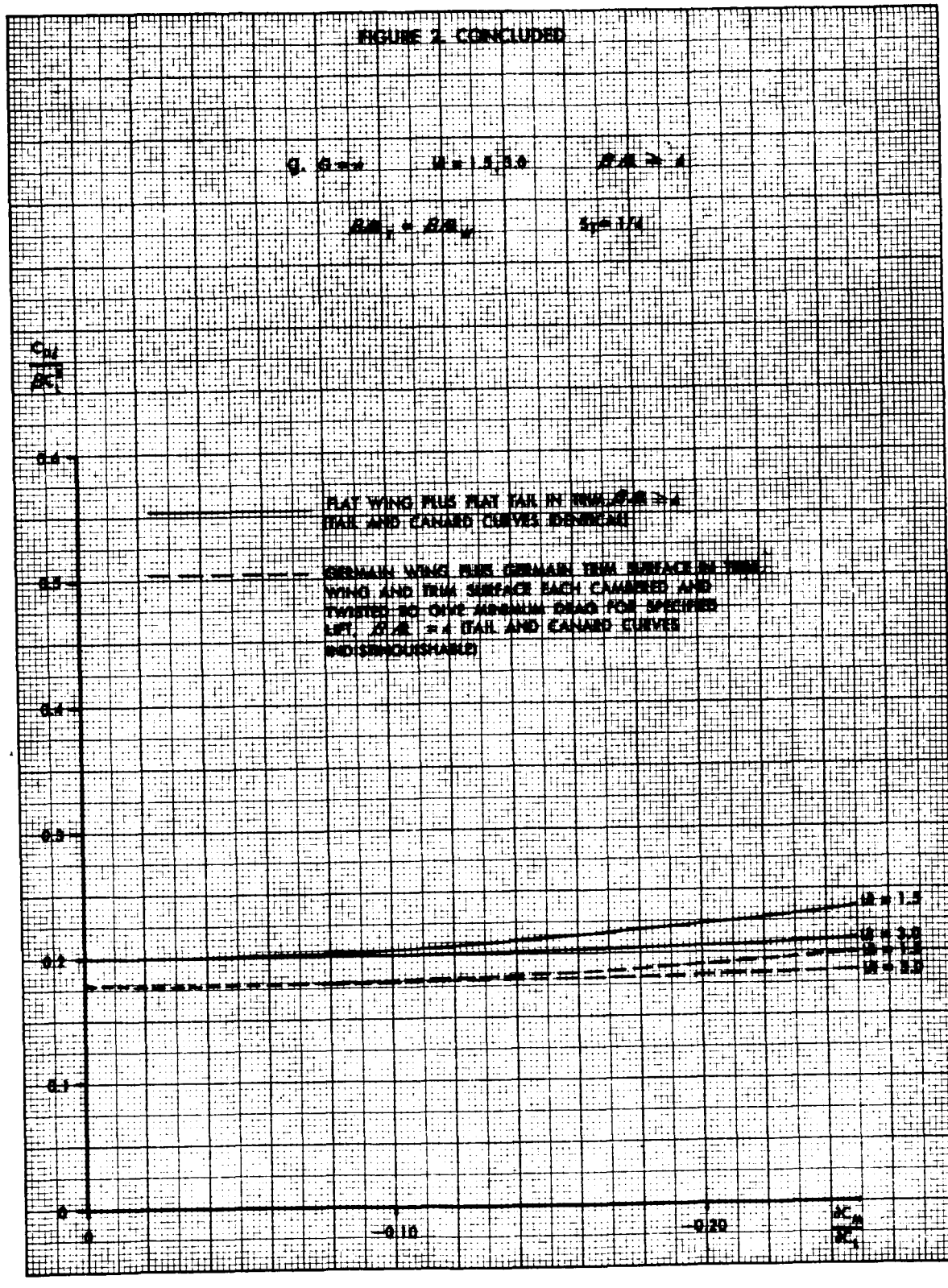
FIGURE 2. CONCLUDED
C_{D_i}
ΔC_L^2
0.6
0.5
0.4
0.3
0.2
0.1
0
FLAT WING PLUS FLAT TAIL IN TRIM, $\delta_f/\delta_t = 4$
TAIL AND CANARD CURVES INDISTINGUISHABLE
GERMAIN WING PLUS GERMAIN TRIM SURFACE IN TRIM, WING AND TRIM SURFACE EACH CAMBERED AND TWISTED TO GIVE MINIMUM DRAG FOR SPECIFIED LIFT, $\delta_f/\delta_t = 4$ (TAIL AND CANARD CURVES INDISTINGUISHABLE)
M = 1.5
M = 2.0
M = 2.5
M = 3.0
0
-0.10
-0.20
ΔC_m
ΔC_L

FIGURE 3. DRAG DUE TO LIFT OF TRIMMED WING PLUS TAIL AND TRIMMED WING PLUS CANARD AS FUNCTION OF STATIC MARGIN. ASSUMES FLAT VORTEX SHEET.

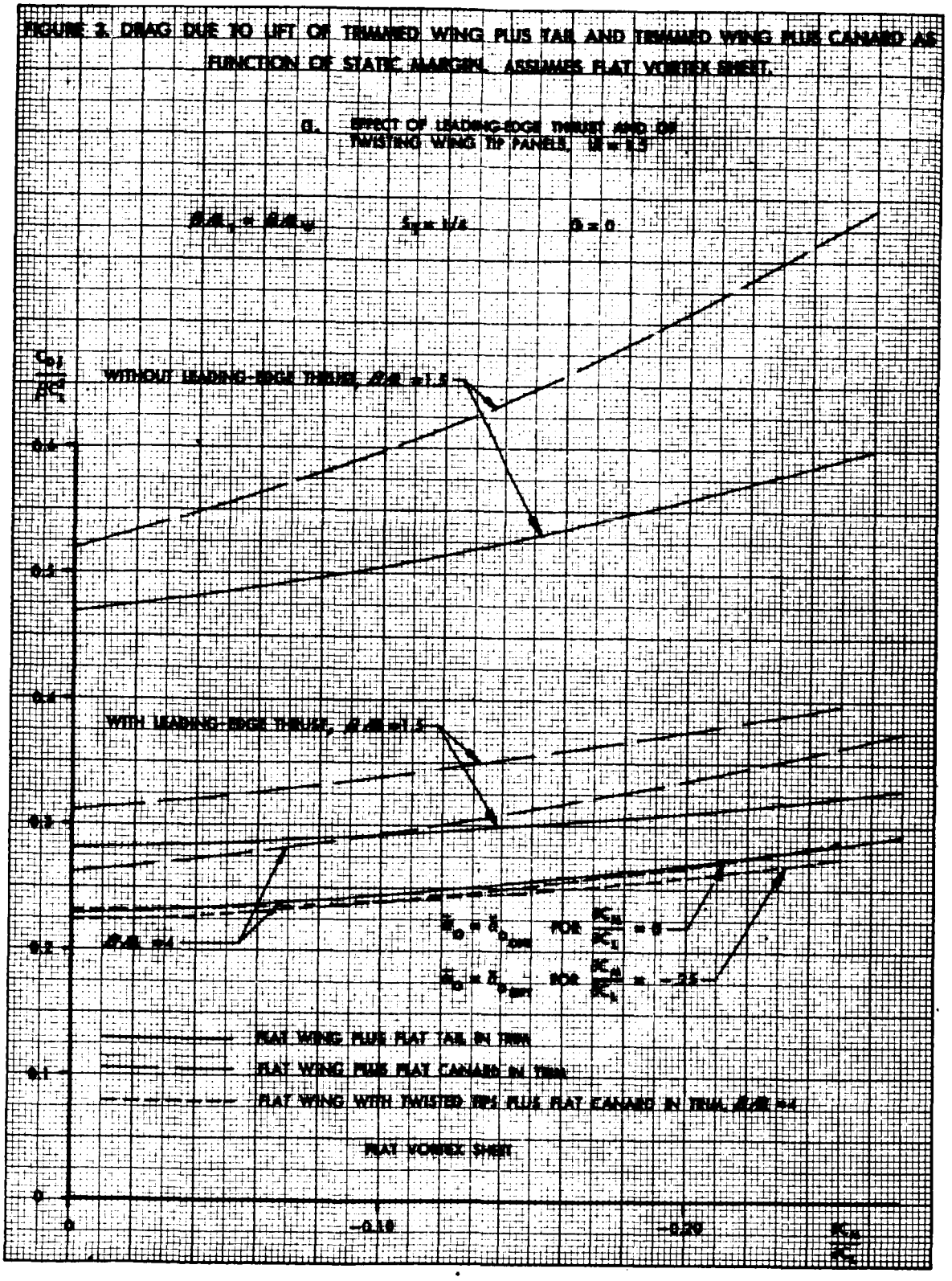

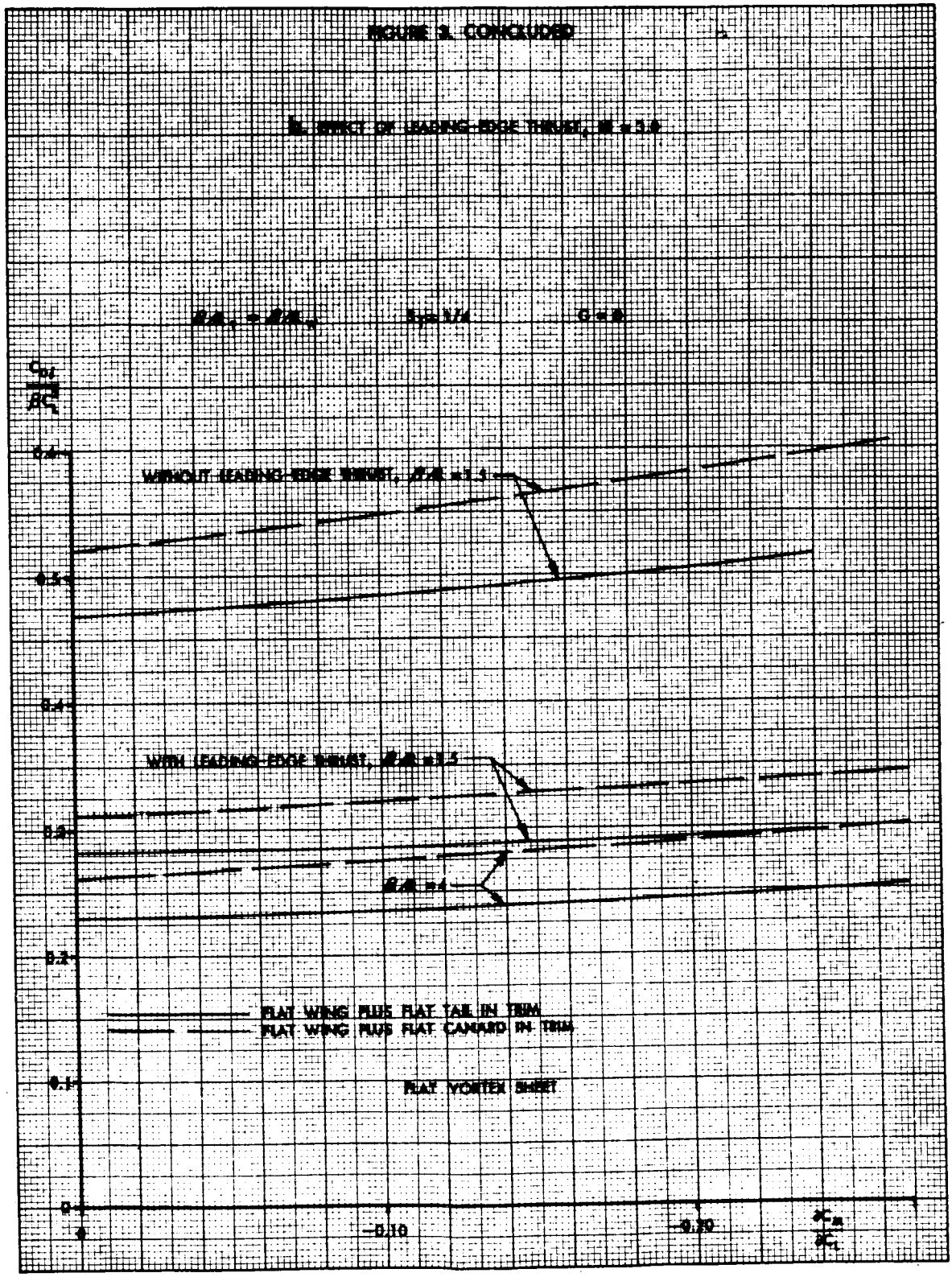
FIGURE 3. CONCLUDED
WITHOUT LEADING-EDGE THRUST, $T'/R = 1.4$
WITH LEADING-EDGE THRUST, $T'/R = 1.5$
$T'/R = 4$
FLAT WING PLUS FLAT TAIL IN TRIM
FLAT WING PLUS FLAT CANARD IN TRIM
FLAT VORTEX SHEET
0.4
0.3
0.2
0.1
0
-0.10
-0.20

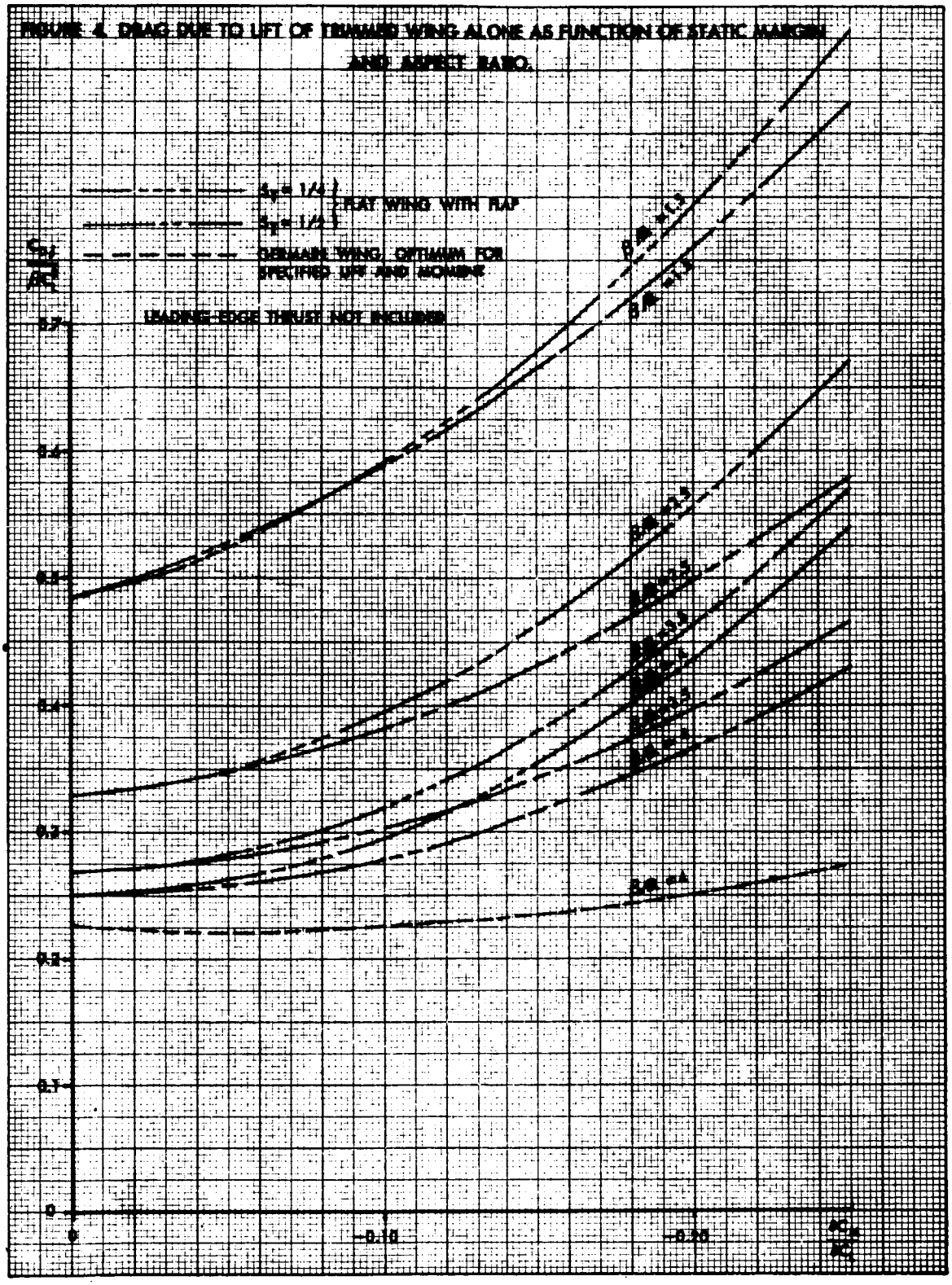

FIGURE 4. DRAG DUE TO LIFT OF TRIMMED WING ALONE AS FUNCTION OF STATIC MARGIN AND ASPECT RATIO.

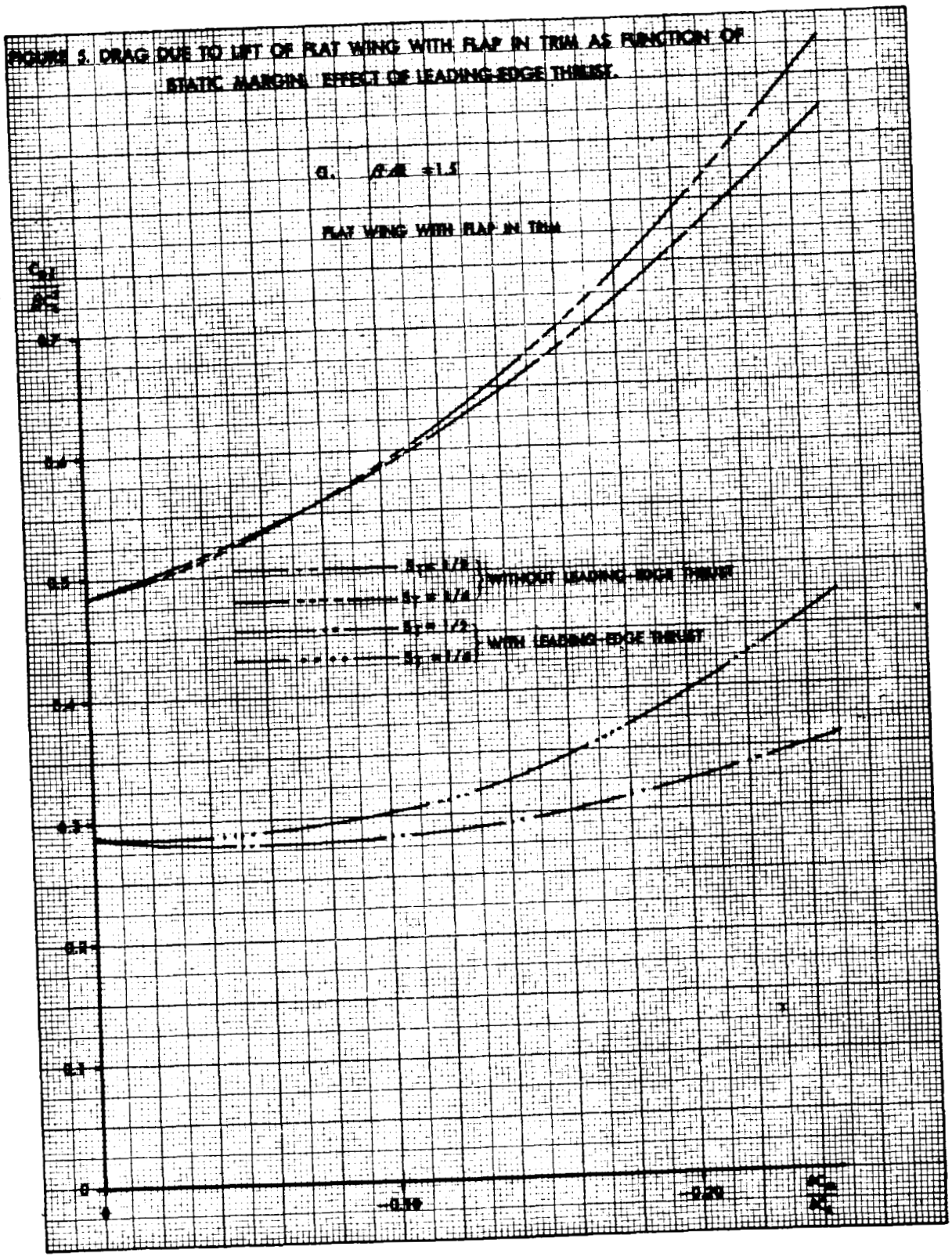

FIGURE 5. DRAG DUE TO LIFT OF FLAT WING WITH FLAP IN TRIM AS FUNCTION OF STATIC MARGIN. EFFECT OF LEADING-EDGE THRUST.

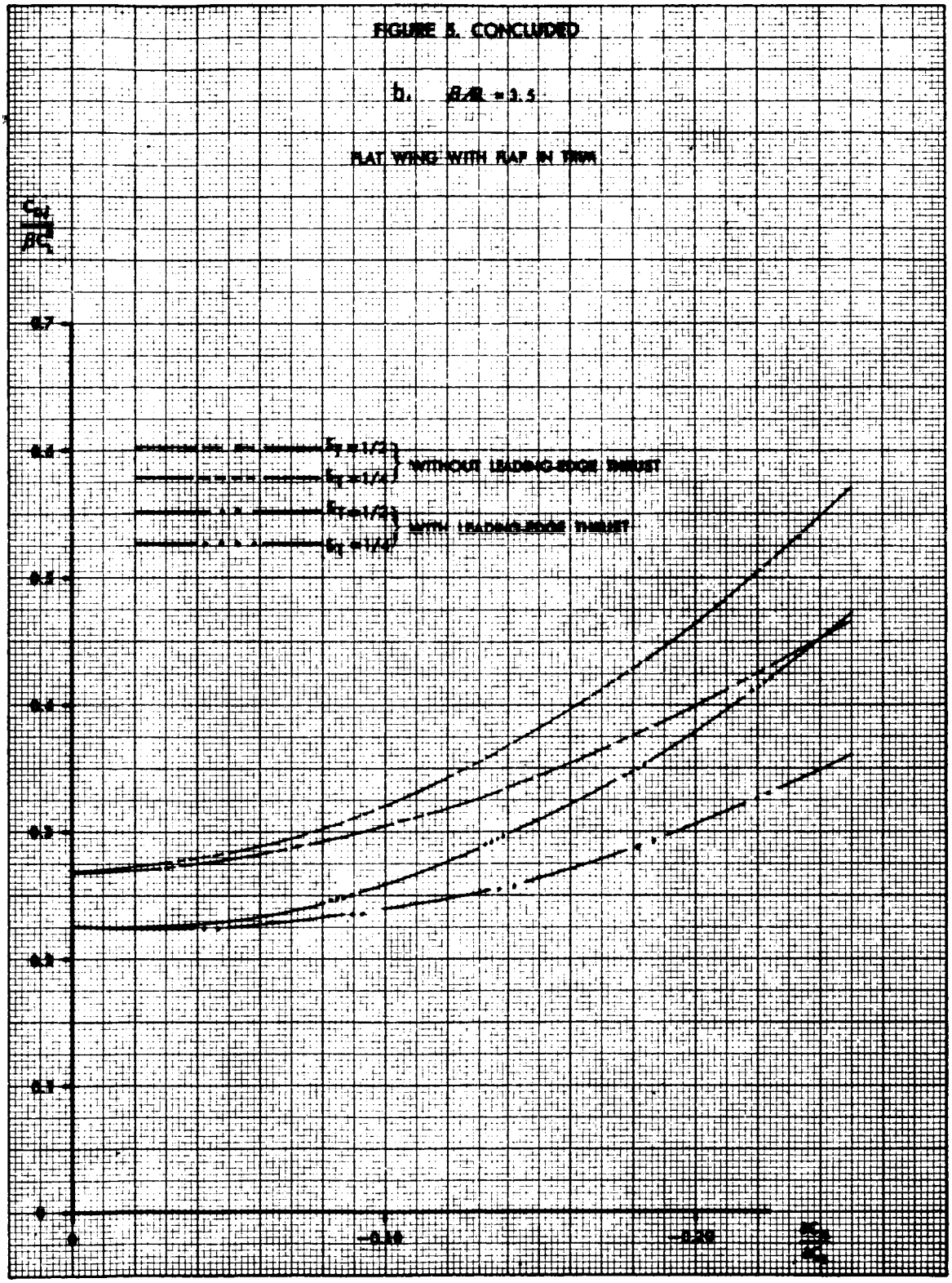
FIGURE 5. CONCLUDED
b. B/R = 3.5
FLAT WING WITH FLAP IN TRIM
$\frac{C_{M_{\alpha_t}}}{\beta C_{L_\alpha}}$
0.7
0.6
0.5
0.4
0.3
0.2
0.1
0
$\delta_T = 1/2$
$\delta_T = 1/4$
WITHOUT LEADING-EDGE THRUST
$\delta_T = 1/2$
$\delta_T = 1/4$
WITH LEADING-EDGE THRUST
-0.10
-0.20
$\frac{C_{D_i}}{C_{L_\alpha}}$

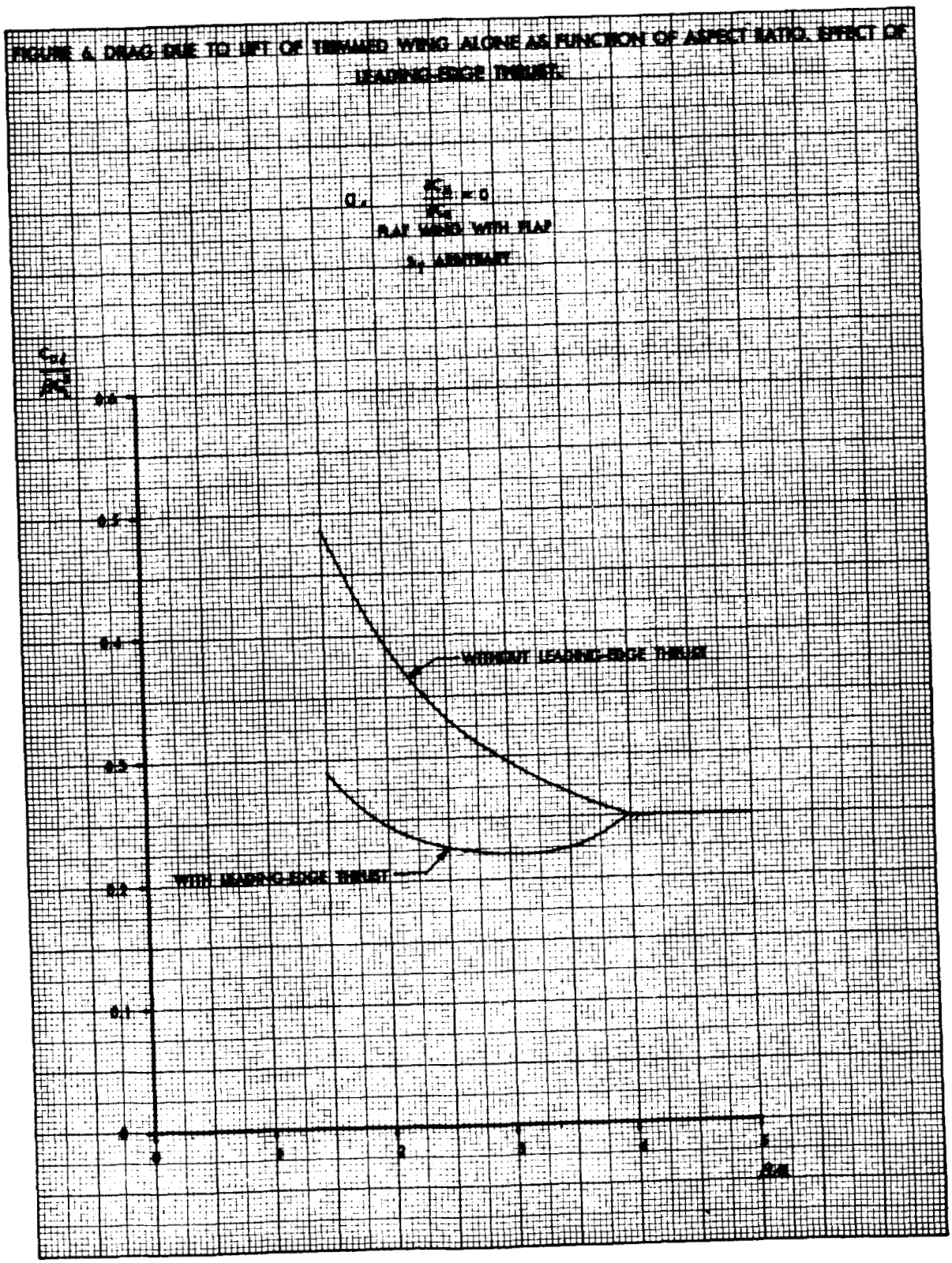

FIGURE 6. DRAG DUE TO LIFT OF TRIMMED WING ALONE AS FUNCTION OF ASPECT RATIO, EFFECT OF LEADING-EDGE THRUST.

D-425

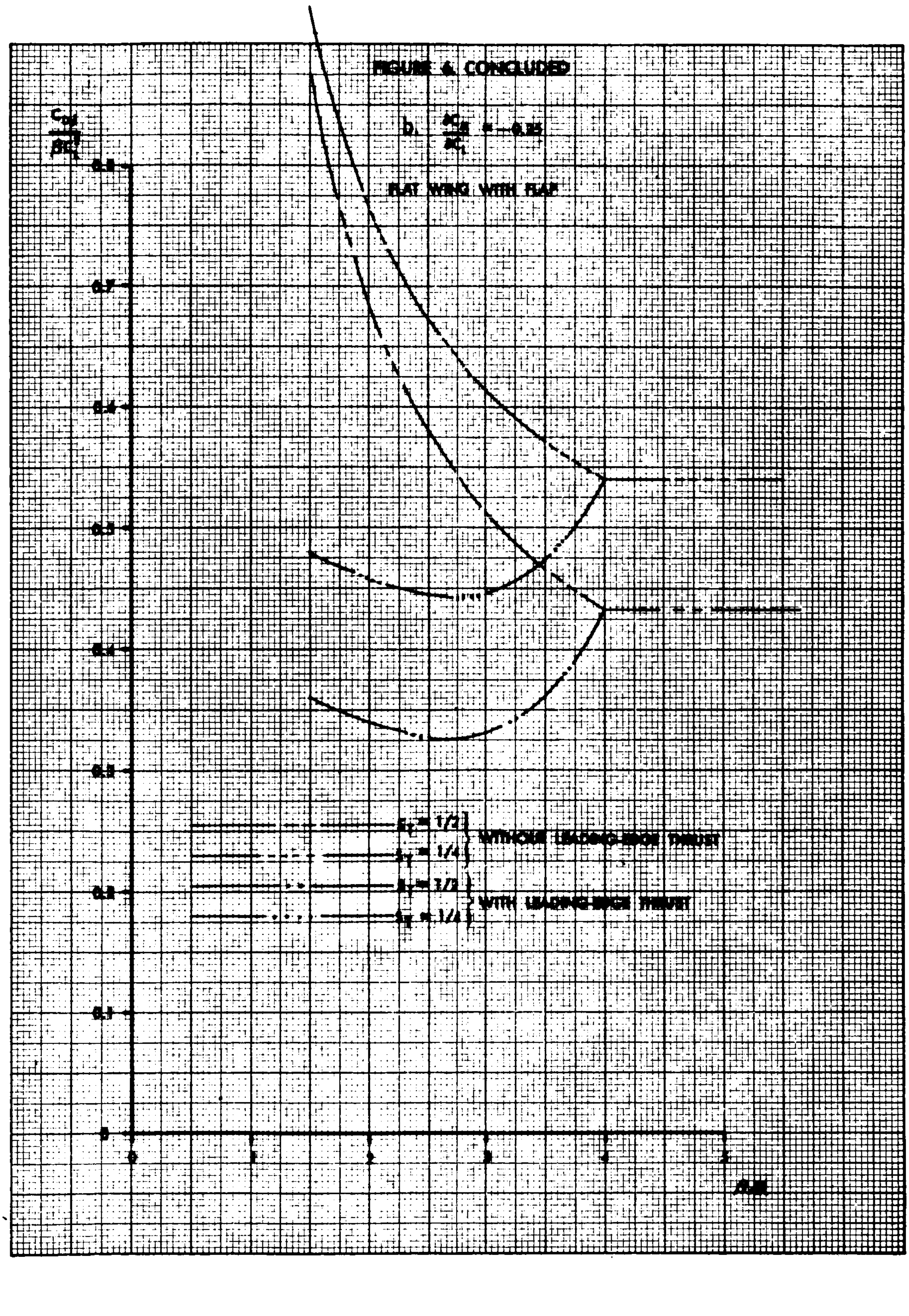
FIGURE 6. CONCLUDED
b.
FLAT WING WITH FLAP
0.8
0.7
0.6
0.5
0.4
0.3
0.2
0.1
0
0
1
2
3
4
5
= 1/2
= 1/4
WITHOUT LEADING-EDGE THRUST
= 1/2
= 1/4
WITH LEADING-EDGE THRUST

FIGURE 7. DRAG DUE TO LIFT OF TRIMMED CONFIGURATIONS WITH NO INTERFERENCE BETWEEN WING AND TRIM SURFACE. COMPARISON OF WING PLUS TAIL (OR CANARD), WING WITH FLAP (WING INCLUDES FLAP) AND WING PLUS FLAP (WING EXCLUDES FLAP).

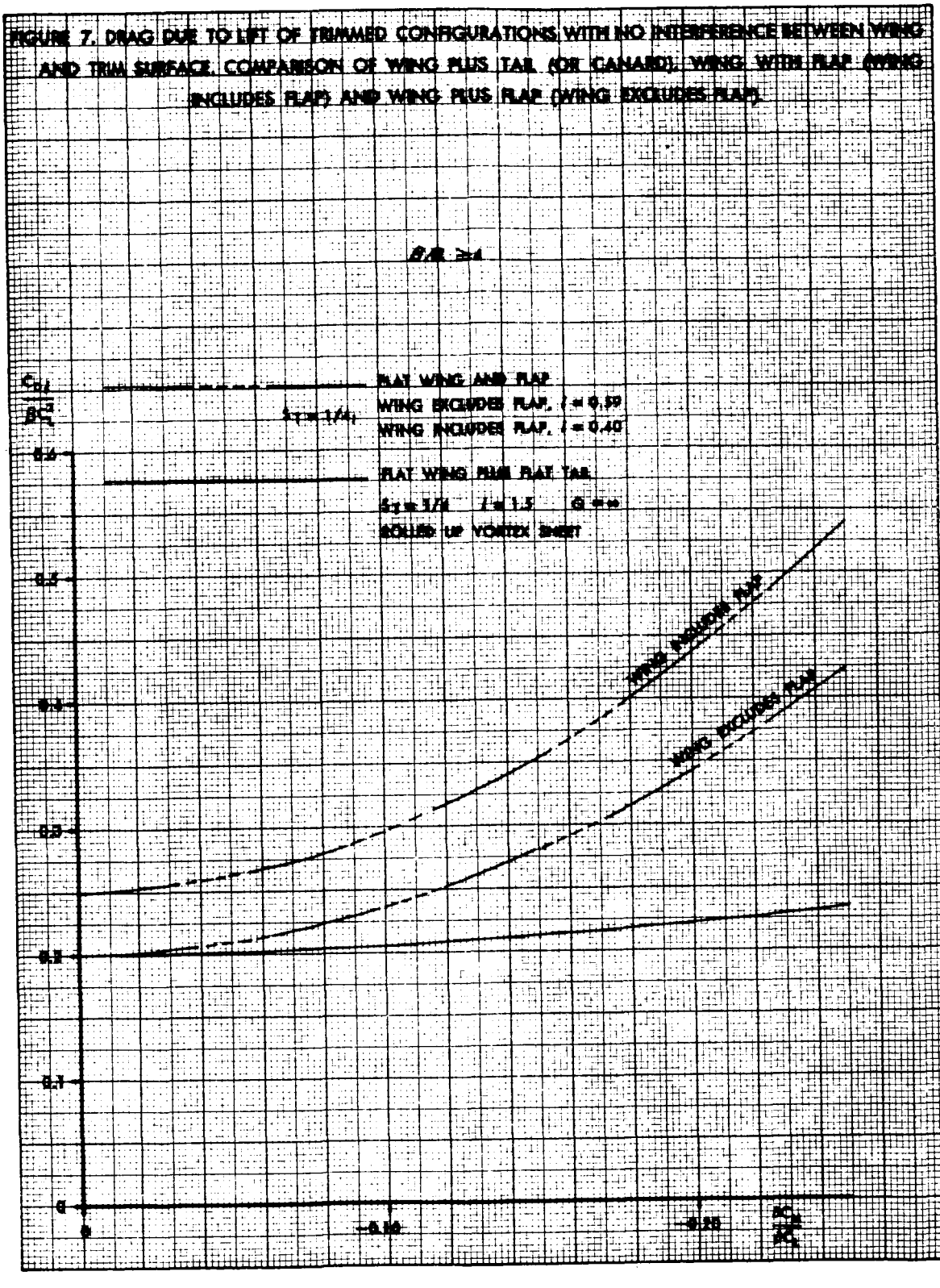

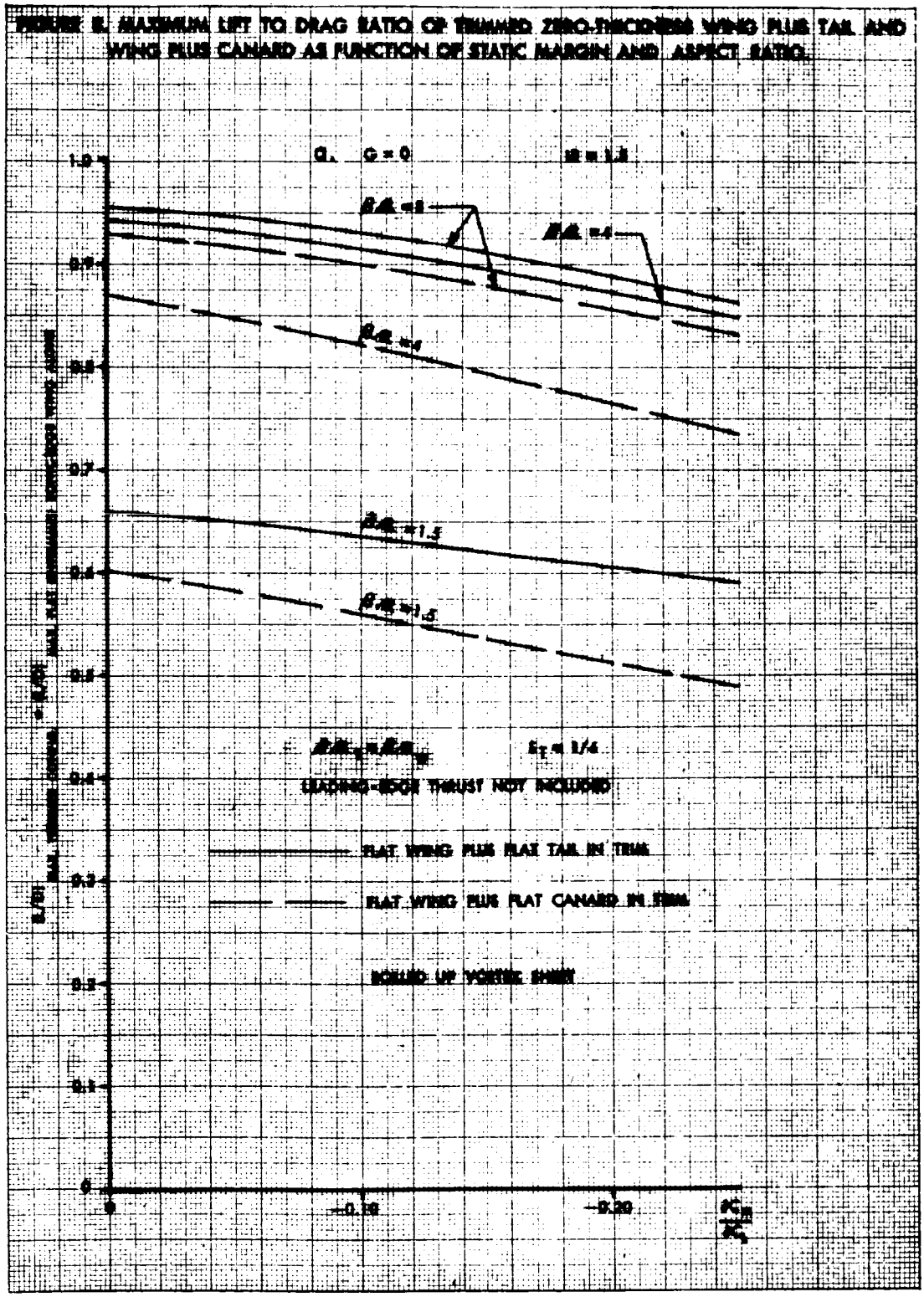
C_L, $G = 0$
$\Lambda_{LE} = 8$
$\Lambda_{LE} = 4$
$\Lambda_{LE} = 4$
$\Lambda_{LE} = 1.5$
$\Lambda_{LE} = 1.5$
$\Lambda_{LE_W} = \Lambda_{LE_W}$
$\xi_T = 1/4$
LEADING-EDGE THRUST NOT INCLUDED
FLAT WING PLUS FLAT TAIL IN TRIM
FLAT WING PLUS FLAT CANARD IN TRIM
ROLLED UP VORTEX SHEET
1.0
0.9
0.8
0.7
0.6
0.5
0.4
0.3
0.2
0.1
0
0
−0.10
−0.20

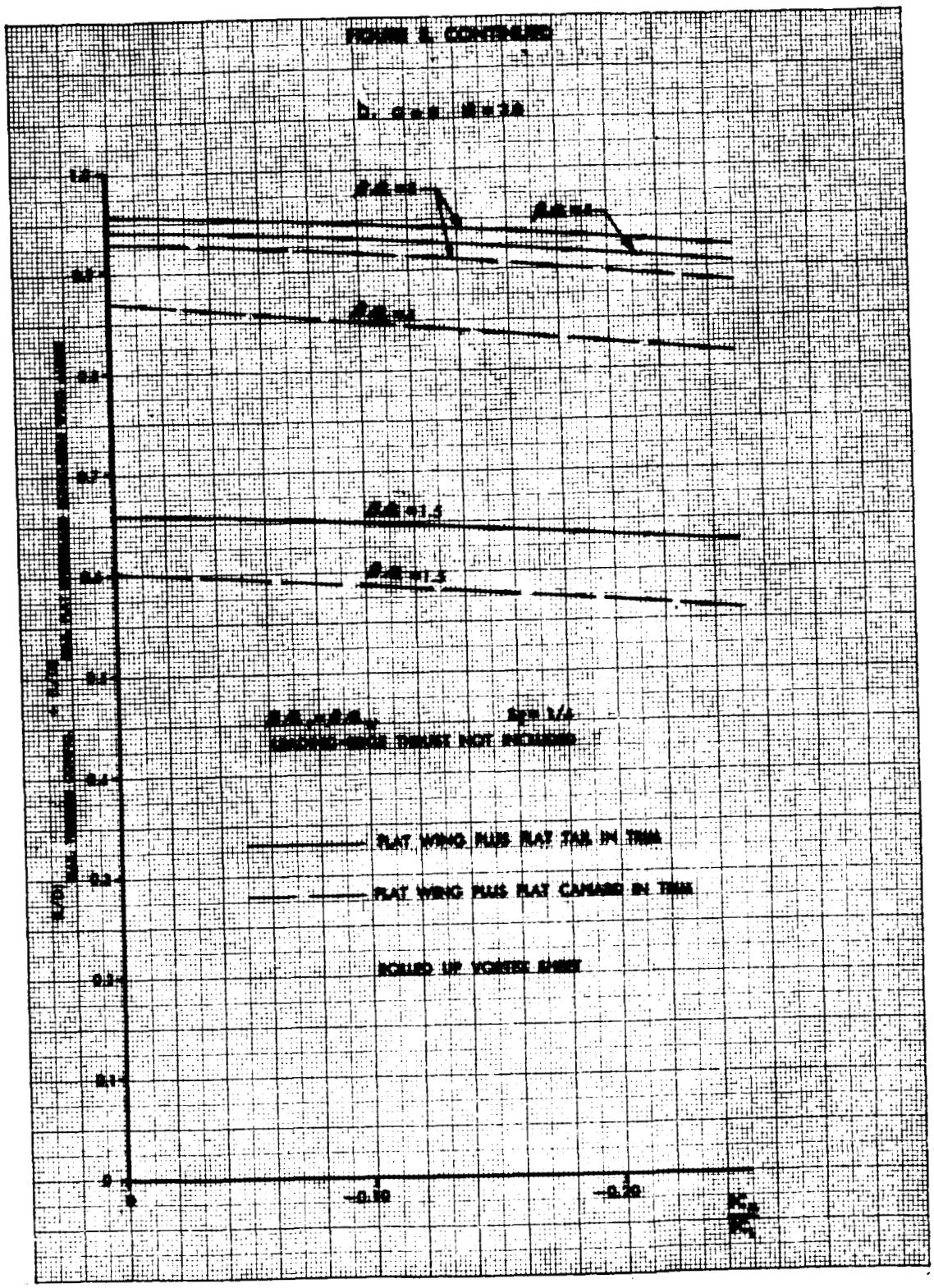
FLAT WING PLUS FLAT TAIL IN TRIM
FLAT WING PLUS FLAT CANARD IN TRIM
ROLLED UP VORTEX SHEET

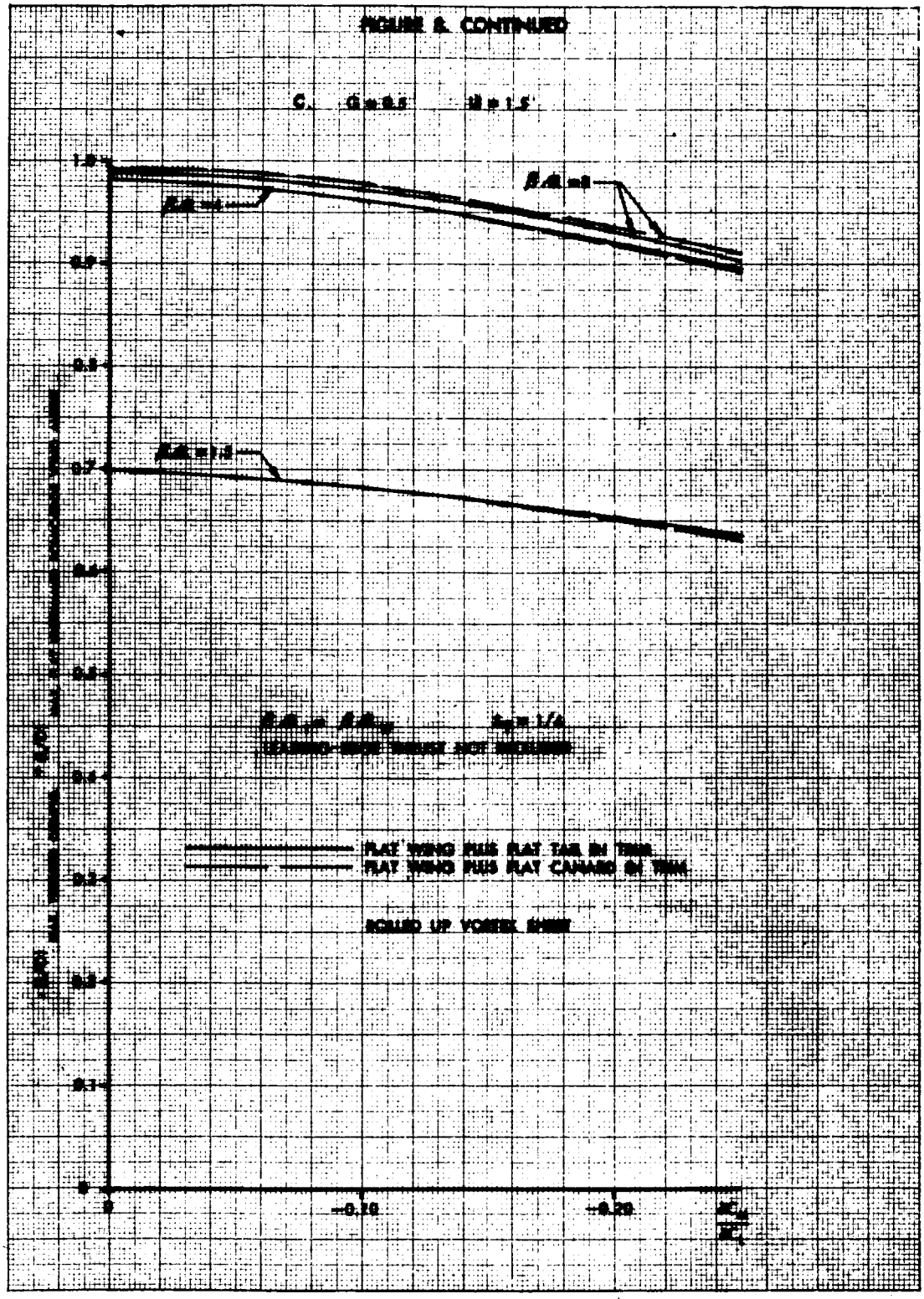
FIGURE 8. CONTINUED
C. G. = 0.5 M = 1.5
1.0
0.9
0.8
0.7
0.6
0.5
0.4
0.3
0.2
0.1
0
-0.20
+0.20
FLAT WING PLUS FLAT TAIL IN TRIM
FLAT WING PLUS FLAT CANARD IN TRIM
SCALED UP VORTEX SHEET

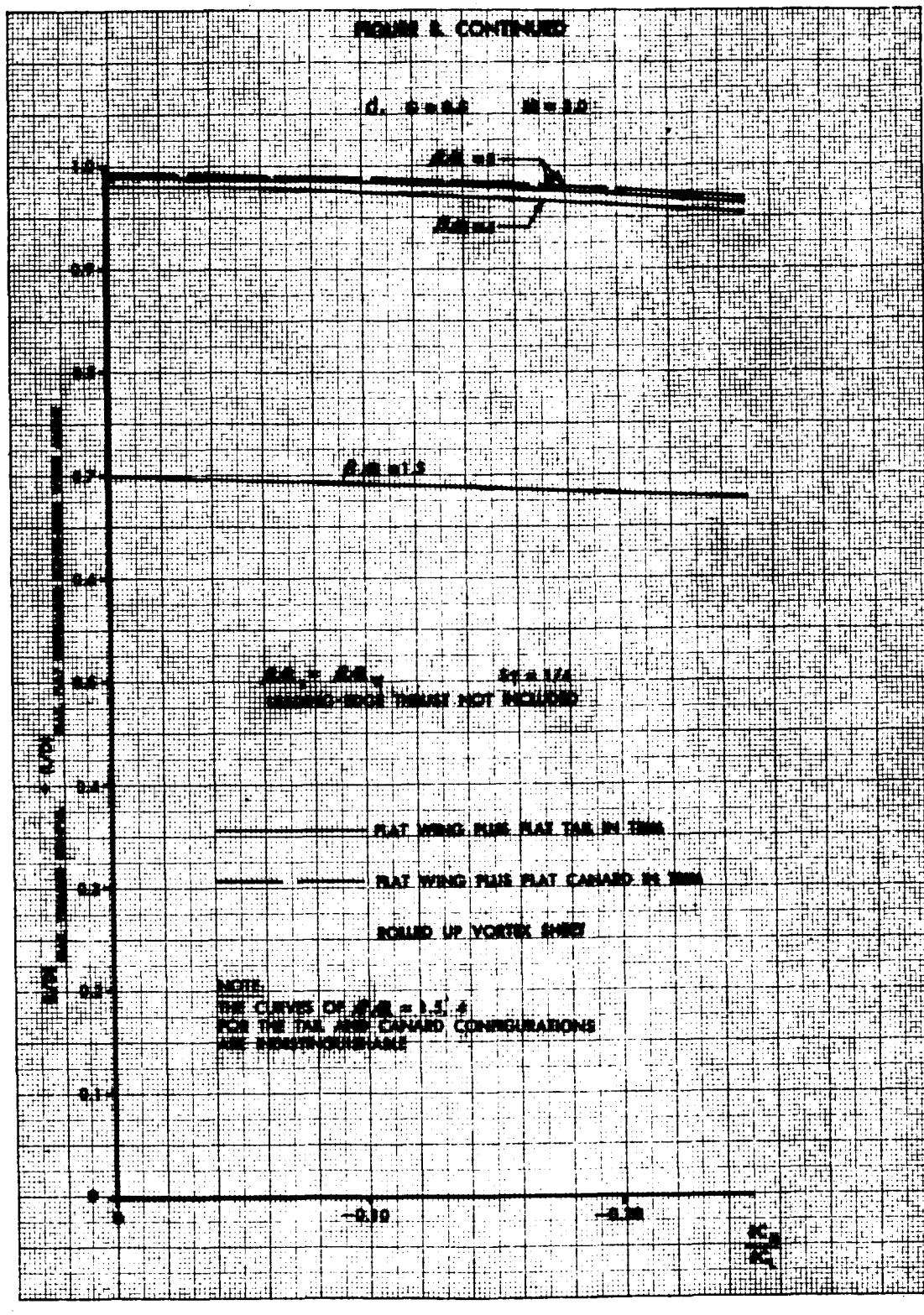
FLAT WING PLUS FLAT TAIL IN THIS
FLAT WING PLUS FLAT CANARD IN THIS
ROLLED UP VORTEX SHEET
NOTE:
THE CURVES OF
FOR THE TAIL AND CANARD CONFIGURATIONS
ARE INDISTINGUISHABLE

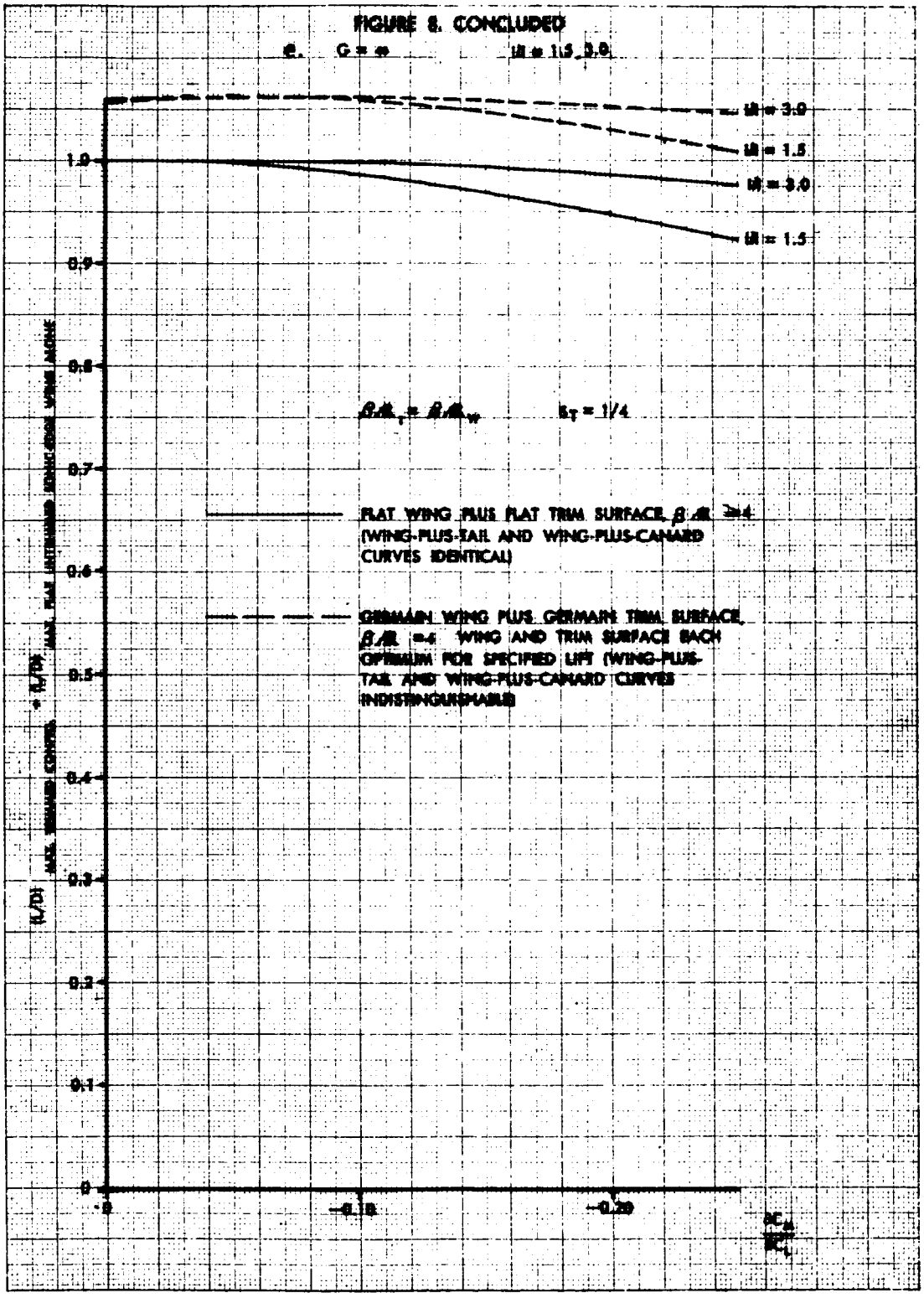
FIGURE 8. CONCLUDED
e. G = ∞
1.0
0.9
0.8
0.7
0.6
0.5
0.4
0.3
0.2
0.1
0
-0.10
-0.20
FLAT WING PLUS FLAT TRIM SURFACE, β/β = 4
(WING-PLUS-TAIL AND WING-PLUS-CANARD
CURVES IDENTICAL)
GERMAIN WING PLUS GERMAIN TRIM SURFACE,
β/β = 4 WING AND TRIM SURFACE EACH
OPTIMUM FOR SPECIFIED LIFT (WING-PLUS-
TAIL AND WING-PLUS-CANARD CURVES
INDISTINGUISHABLE)

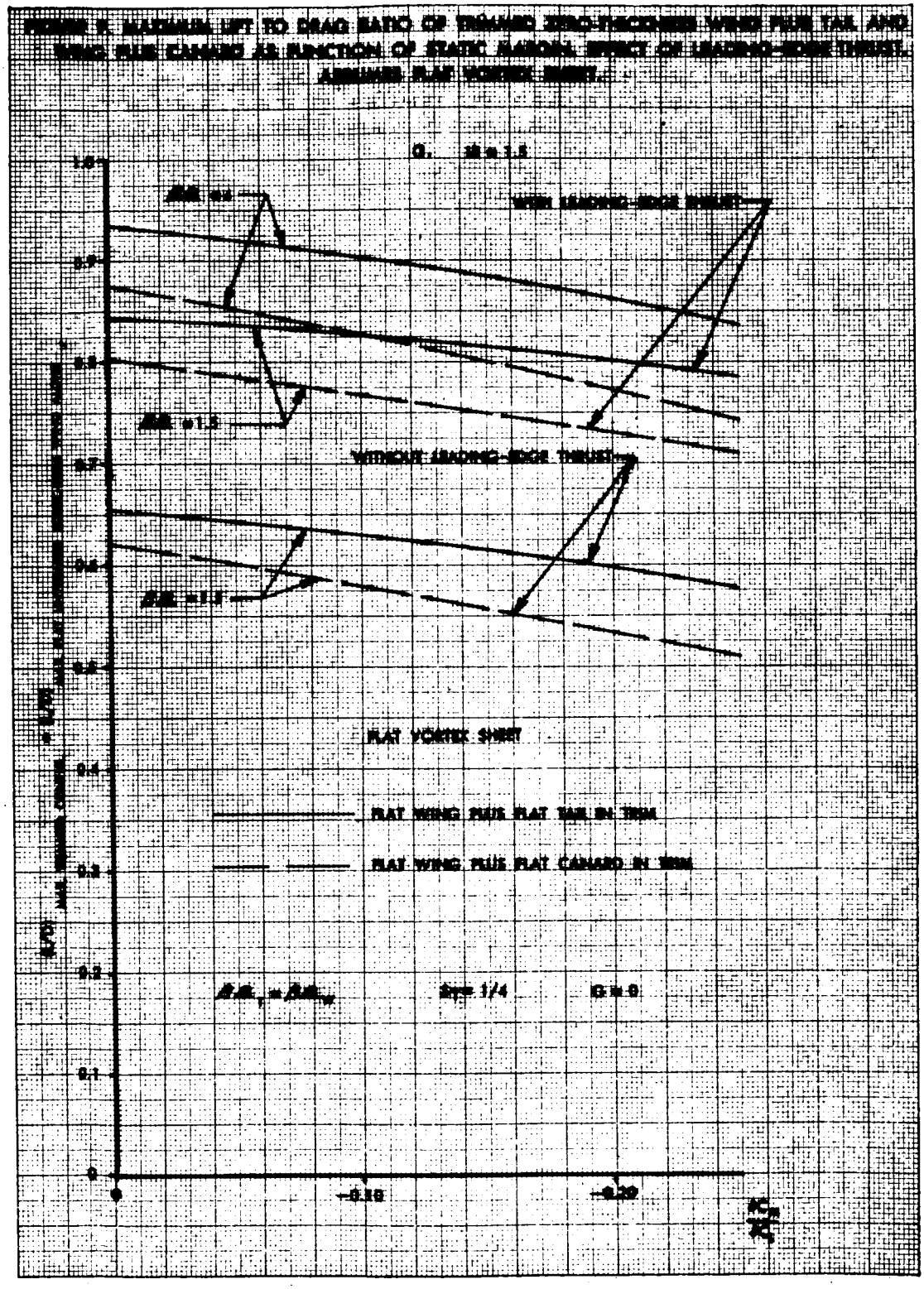
WITH LEADING-EDGE THRUST
WITHOUT LEADING-EDGE THRUST
FLAT VORTEX SHEET
FLAT WING PLUS FLAT TAIL IN TRIM
FLAT WING PLUS FLAT CANARD IN TRIM
Λ = 1/4
-0.10
-0.20

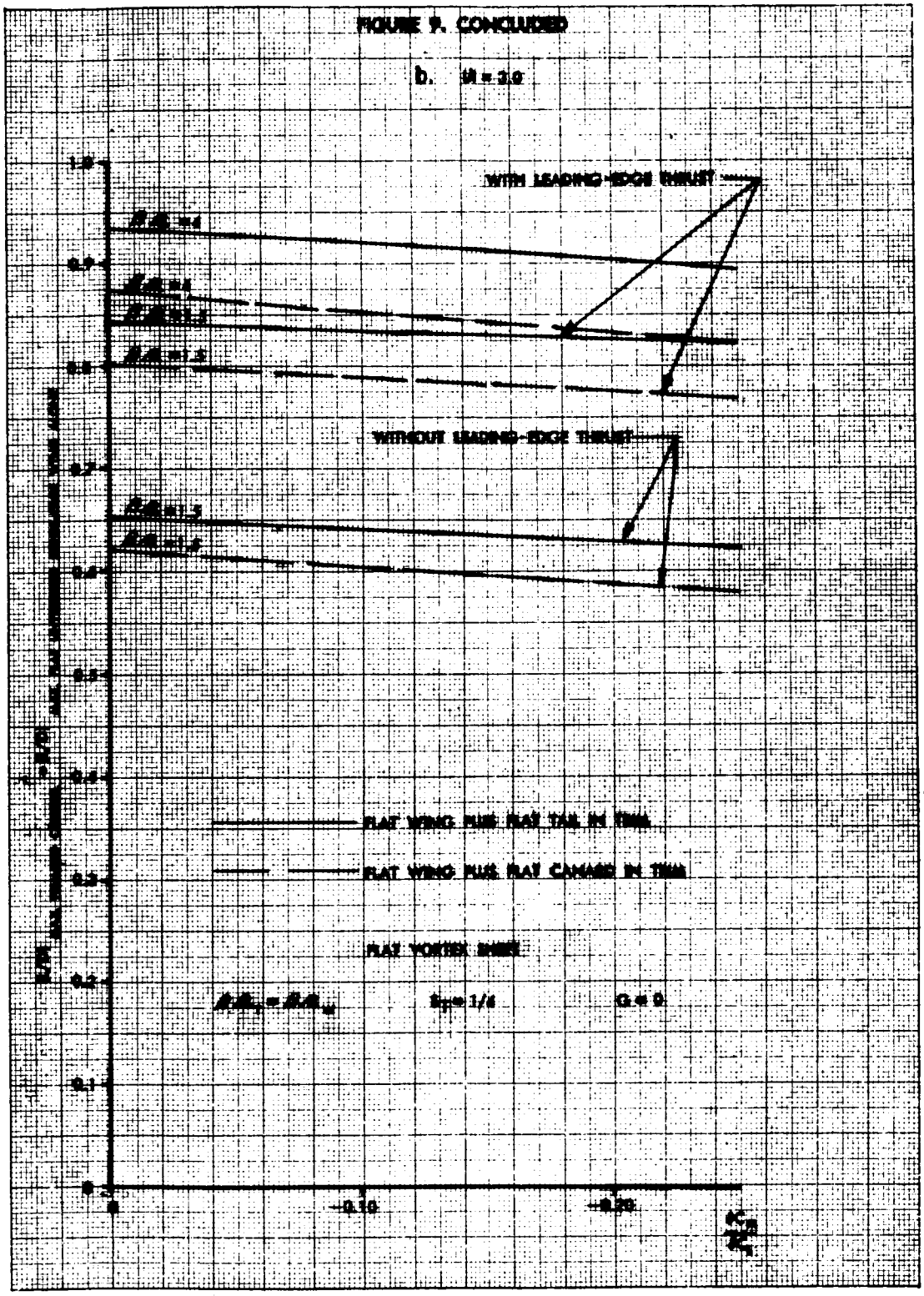
FIGURE 9. CONCLUDED
b. M = 3.0
WITH LEADING-EDGE THRUST
WITHOUT LEADING-EDGE THRUST
FLAT WING PLUS FLAT TAIL IN TRIM
FLAT WING PLUS FLAT CANARD IN TRIM
FLAT VORTEX SHEET
$\Lambda_{LE_c} = \Lambda_{LE_w}$
$\lambda_c = 1/4$
$\alpha = 0$
-0.10
-0.20

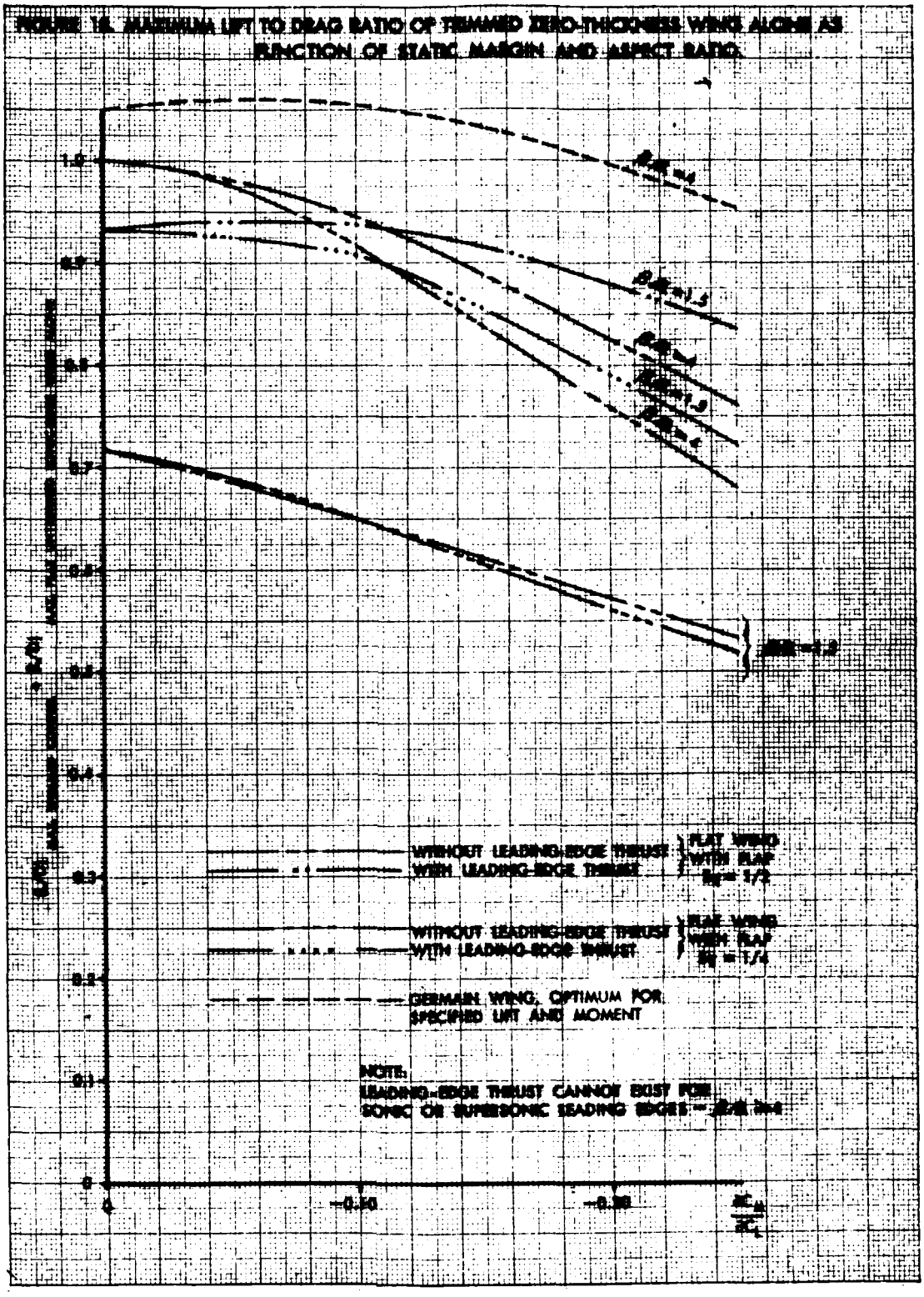

FIGURE 16. MAXIMUM LIFT TO DRAG RATIO OF TRIMMED ZERO-THICKNESS WING ALONE AS FUNCTION OF STATIC MARGIN AND ASPECT RATIO.

FIGURE 11. MAXIMUM LIFT TO DRAG RATIO OF TRIMMED ZERO-THICKNESS CONFIGURATIONS WITH SONIC LEADING EDGES ($\beta A/B = 4$). COMPARISON OF VARIOUS WING-PLUS-TAIL, WING-PLUS-CANARD AND WING-ALONE CONFIGURATIONS.

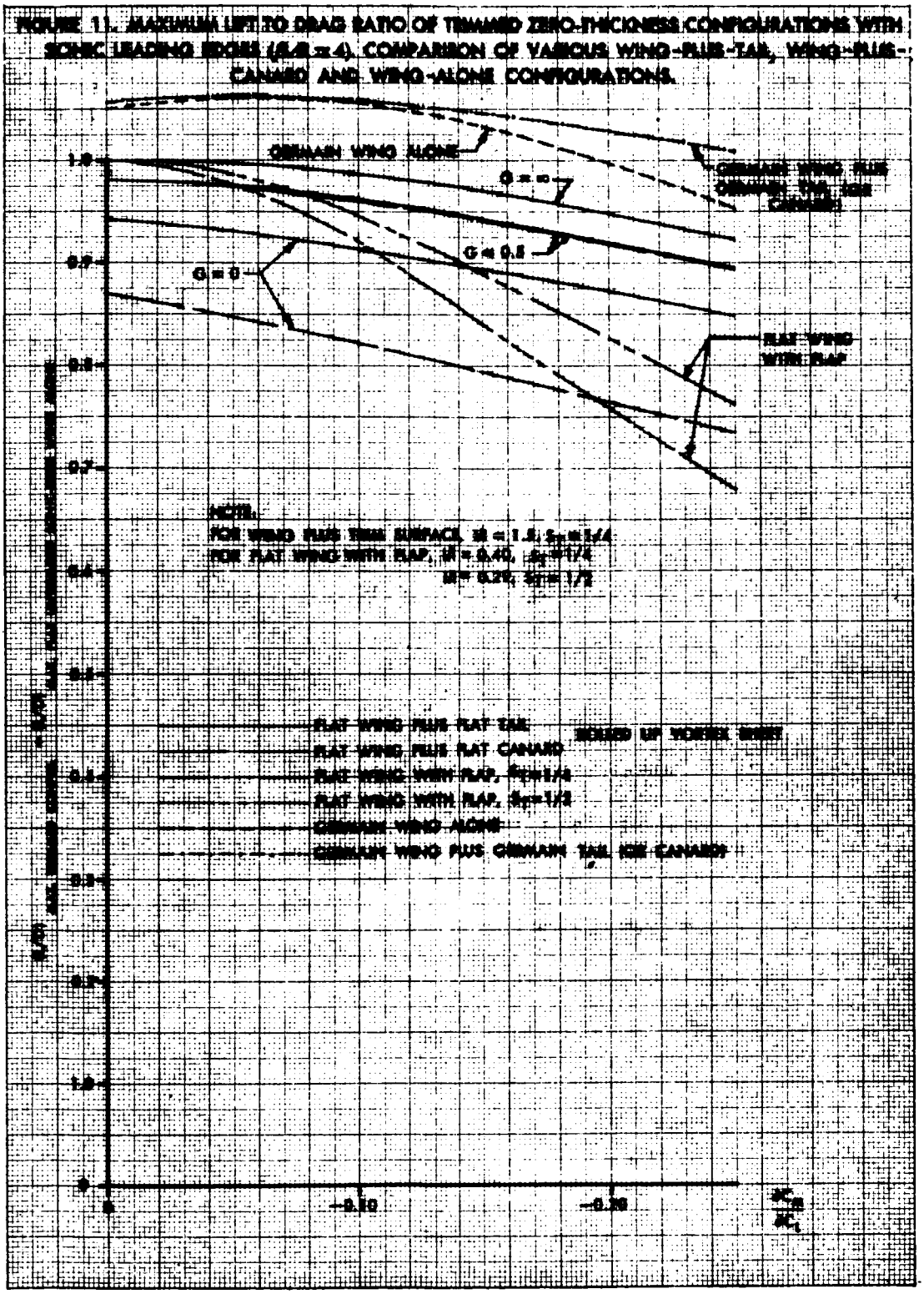

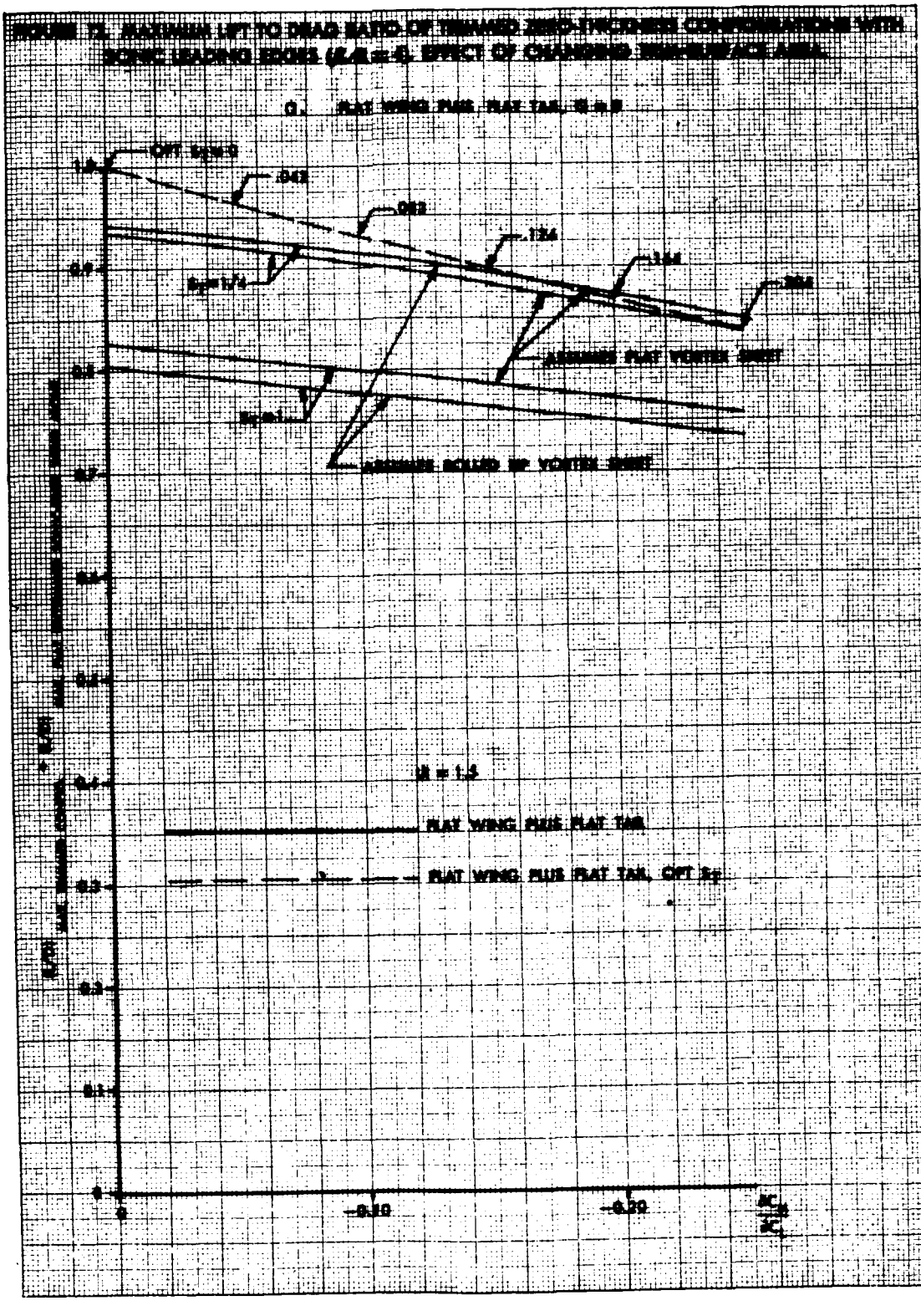
OPT s_p/s_t
.043
.083
.124
.164
.204
$s_p = 1/4$
$s_p = 1$
M = 1.5
FLAT WING PLUS FLAT TAIL
FLAT WING PLUS FLAT TAIL, OPT s_p
-0.10
-0.20

D-425

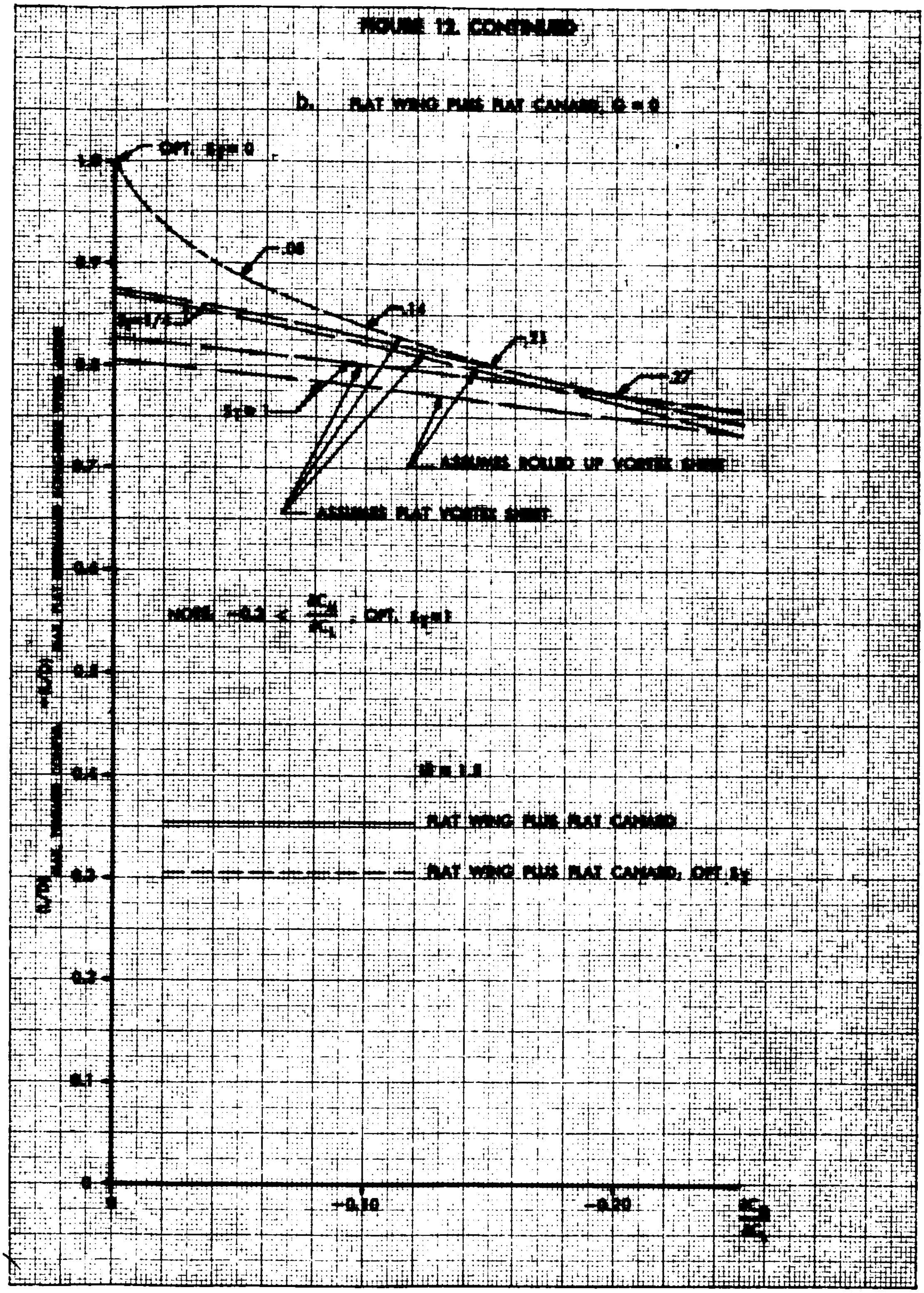
FIGURE 12. CONTINUED
b. FLAT WING PLUS FLAT CANARD
ASSUMES ROLLED UP VORTEX SHEET
ASSUMES FLAT VORTEX SHEET
FLAT WING PLUS FLAT CANARD
FLAT WING PLUS FLAT CANARD, OPT.
-0.10
-0.20

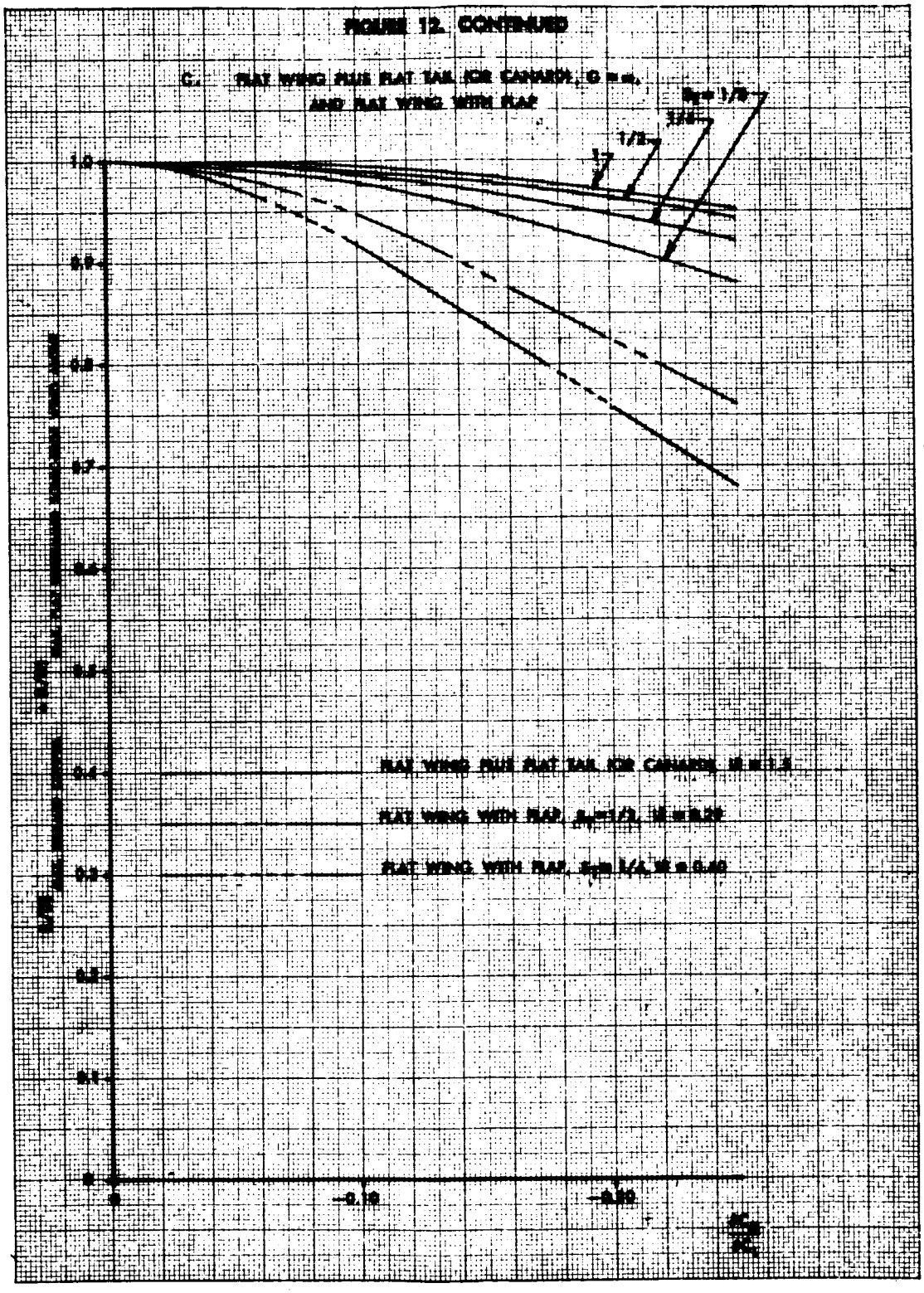
FIGURE 12. CONTINUED
C. FLAT WING PLUS FLAT TAB (OR CANARD), $\delta_e = 0$, AND FLAT WING WITH FLAP
$\delta_f = 1/3$
1/2
1/3
1/4
1.0
0.8
0.6
0.4
0.2
0
-0.10
-0.20
FLAT WING PLUS FLAT TAB (OR CANARD), $\delta_e = 1.5$
FLAT WING WITH FLAP, $\delta_f = 1/3$, $\delta_e = 0.29$
FLAT WING WITH FLAP, $\delta_f = 1/4$, $\delta_e = 0.40$

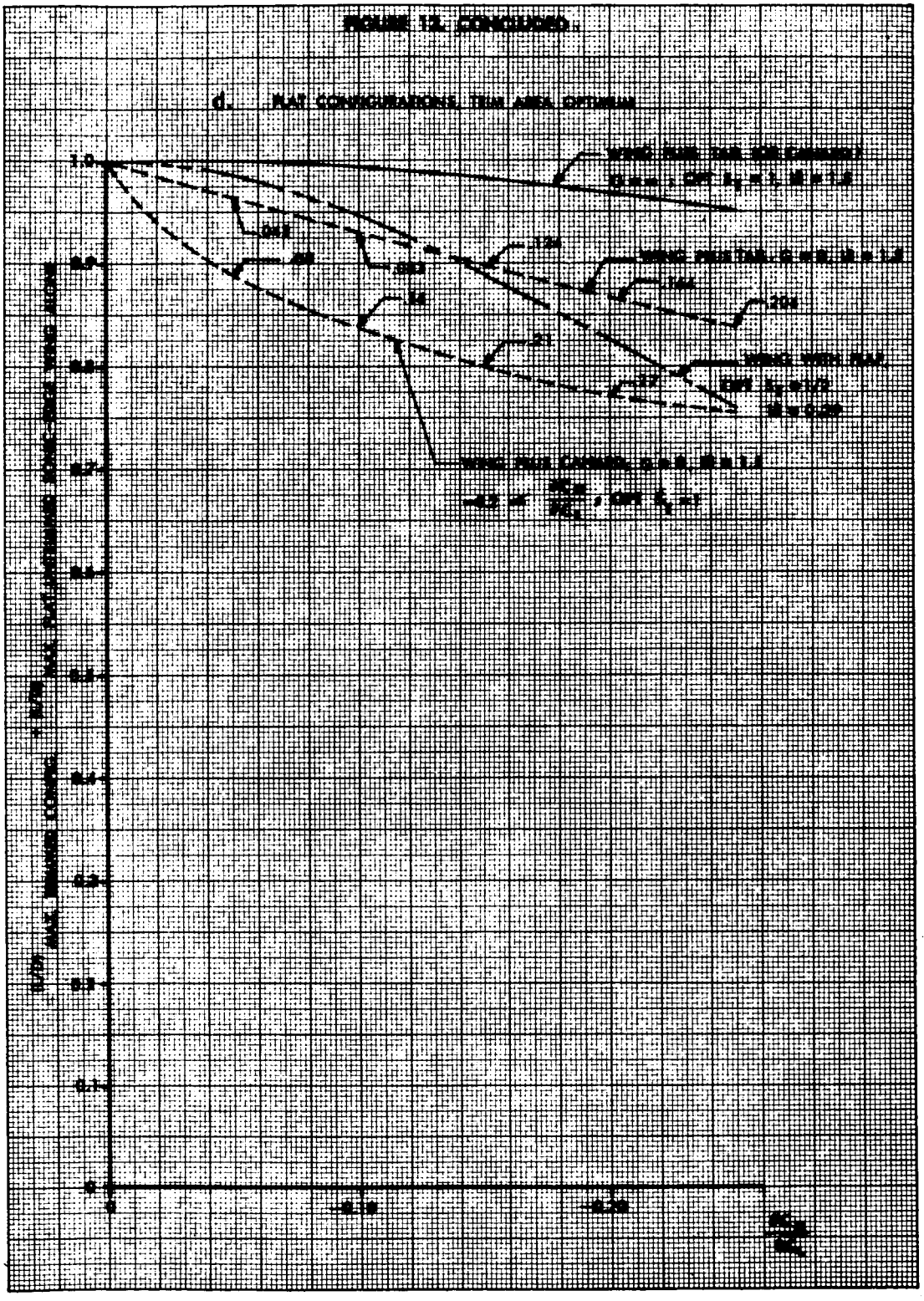
FIGURE 12. CONCLUDED.
d. MAT CONFIGURATIONS, TRIM AREA, OPTIMUM
1.0
0.9
0.8
0.7
0.6
0.5
0.4
0.3
0.2
0.1
0
-0.10
-0.20